ANALYSIS OF FLOW CHARACTERISTICS OF SLURRY TRANSPORTATION SYSTEM

A thesis submitted in the partial fulfilment of the requirements for the Degree of

DOCTOR OF PHILOSOPHY

By

MANI KANWAR SINGH

Registration Number: 951202004

Under the supervision of

Dr. DWARIKANATH RATHA
Associate Professor
Department of Civil Engineering
Thapar University

Dr. SATISH KUMAR
Assistant Professor
Department of Mechanical Engineering
Thapar University

DEPARTMENT OF CIVIL ENGINEERING

THAPAR UNIVERSITY,
PATIALA 147004, INDIA.

May 2017

THESIS CERTIFICATE

This is to certify that the thesis entitled **"Analysis of Flow Characteristics of Slurry Transportation System"** submitted by **Mr. Mani Kanwar Singh,** in the partial fulfillment of the requirements for the award of the Degree of **Doctor of Philosophy** in the Department of Civil Engineering, **Thapar University, Patiala (INDIA)** is a bonafide record of research work carried out by him under our supervision and guidance. The contents of this thesis, in full or in parts, have not been submitted to any other Institute or University for the award of any degree or diploma.

(Dwarikanath Ratha)
Associate Professor
Department of Civil Engineering
Thapar University, Patiala,
Punjab, INDIA

(Supervisor)

(Satish Kumar)
Assistant Professor
Department of Mechanical Engineering
Thapar University, Patiala,
Punjab, INDIA

(Supervisor)

DECLARATION

I, **Mani Kanwar Singh,** hereby declare that the thesis, entitled, **"Analysis of Flow Characteristics of Slurry Transportation System"** submitted to the **Thapar University,** in partial fulfillment of the requirements for the award of the Degree of Doctor of Philosophy in Civil Engineering is a record of original and independent research work done by me during the period 2013-2017, under the supervision and guidance of **Dr. Dwarikanath Ratha,** Associate Professor, Department of Civil Engineering, Thapar University and **Dr. Satish Kumar,** Assistant Professor, Department of Mechanical Engineering, Thapar University. The work contained in this thesis has not been previously submitted to meet the requirements for a degree or diploma at this or any other higher education institution.

(Mani Kanwar Singh)

Registration No: 951202004

ACKNOWLEDGEMENTS

Words are often less to revels anyone's deep regards. With an understanding that work like this can never be the outcome of a single person. I take this opportunity to express my profound sense of gratitude and respect to all those who helped me through the duration of this work.

This work would not have been possible without the encouragement and able guidance of the supervisors Dr. Dwarikanath Ratha and Dr. Satish Kumar. Their enthusiasm and optimism made this experience both rewarding and enjoyable. Most of the novel ideas and solutions in this work are the result of our numerous stimulating discussions. Their feedback and editorial comments were also invaluable for the writing of this thesis. I would like to express my gratitude to my supervisors Dr. Dwarikanath Ratha and Dr. Satish Kumar for their useful comments, remarks and engagement through the learning stages of this doctorate work. Throughout the long journey of Ph.D. with lot of ups and down during the research, supervisors thought of taking up the research activity with an inspiration and motivation helped me to stay focused on this particular subject. The trust made by supervisors helps me to stand in difficult conditions also.

I am extremely thankful to the Head of the department, Director and Dean Research & Sponsored Projects, Thapar University for extending the opportunity to undertake this doctoral research. I would like to express my appreciation and thanks to the Dr. Shruti Sharma, Ph.D. program coordinator, and my Doctoral committee members, Dr. Rajeev Mehta, Dr. Sarbjit Singh and Dr. Richa Babbar for their useful comments and suggestions showered during the interim research evaluations and presentations.

I would like to acknowledge the financial support from DST-SERB, Government of India for the fabrication of pilot plant test loop to carry out the doctoral studies. I would also like to thank Mr. Raj Kishore for their help during fabrication of pilot plant test loop is so appreciable which cannot be expressed in words. I am very much thankful to SAI Labs, Thapar University Patiala, Punjab and CSIR-Indian Institute of Toxicology Research, Lucknow, Uttar Pradesh, India for providing the facilities of characterization.

Grateful acknowledgement is made to my friends Mr. Maninder Singh, Mr. Rajan Verma, Mr. Gurprit Singh, Mr. Jashanpreet Singh, Mr. Jatinderpal Singh, and Mr. Kaushal Kumar. I am also thankful to all the teaching staff members of both civil and mechanical department for their invaluable cooperation and help during the entire tenure of my studies in the department and for their constant help throughout this doctoral research.

This research was never finished without the affection and co-operation of my daughter Mehreen Kaur Sarao. As I was not give her time during their toddlerhood but she understands me at every point without any complaining. During the research work, I had spent days, weeks and months for complete the objectives. This was only possible due to the support of my wife and other family members. Words cannot express how grateful I am to my wife Ms. Harkirat Kaur and my parents Sardarni Malkeet Kaur and Sardar Satinder Singh Sarao. I desire to express my deep appreciation to my parent in laws. As I am far apart from them but my in-laws Sardarni Rajveer Kaur and Sardar Raghuvir Singh Sandhu blessings are always with me. It is power of parents' blessings, which has given me the resolution, self-confidence and enthusiasm for hard work.

Last but not least, I would like to thank God for all good deeds. Without the blessings of God, nothing would be possible.

(Mani Kanwar Singh)

ABSTRACT

Coal is a major source of energy. In India, about 70% electricity generation is produced by combustion of pulverized coal in thermal power plants. The major challenge throughout the world is the efficient utilization of a fuel in power generation. The concentrated coal-water slurry contains 60–70% coal powder that is used as a liquid fuel for the replacement of oil as a fuel. The maximum concentration of slurry with appreciable viscosity increases the efficiency of transportation of the coal-water slurry in pipelines for fuel generation.

Combustion of coal in power plants generates a huge quantity of inorganic residues like bottom ash and fly ash, which have numerous ecological problems. Generally the coal ash is being transported hydraulically to ash pond through slurry pipelines at low solid concentrations, which is extremely uneconomical.

The efficient and economical transportation of coal water slurry as well as coal ash slurry is a major challenge. The parameters, which have significant effect on the slurry transportation system, are slurry concentrations and slurry rheology. The economy of slurry transportation is achieved by transporting higher concentration of slurry having minimum viscosity so that the power required for transportation will be minimum. So the understanding of impact of these parameters on slurry transportation is necessary for efficient designing of slurry transportation system. The present study is concerned with the analysis of impact of slurry rheology and slurry concentration on slurry transportation in a pipeline.

The coal samples are collected directly from the coalmines of Makum coalfield of Dibrugarh district of Assam for the present study. The coal samples are prepared by crushing with laboratory-size ball mill to the different fractional sizes required for experiments. The Makum field coal is also used for power generation in Guru Nanak Dev thermal power plant, Bathinda, Punjab, India. The fly ash and bottom ash produced during the power generation are collected from Guru Nanak Dev thermal power plant for the present study.

The various bench scale tests like particle size distribution, static settled concentration, specific gravity and potential of hydrogen value are performed to study the physiochemical properties of coal. The morphology of coal and coal ash samples is

determined by scanning electron microscopy **(**SEM). The leaching test of heavy metals from fly ash and bottom ash is investigated in order to predict the environmental effect from the ash disposal system. From the leaching test, it is also observed that the leached concentration of the tracing elements in the fly ash is more compared with the bottom ash at the same liquid to solid ratio.

The rheological characteristics of coal water and fly ash–water slurries have been studied to facilitate their conveying at higher concentrations. The rheological experiments of coal-water slurry are conducted in the solid concentration range of 30-60% (by weight). The apparent viscosity and shear stress are measured at shear rate ranging from 0–600 s^{-1}. The rheological behavior of coal water slurry is conducted for both unimodal and bimodal particle size distribution of coal and It is observed that with 30% addition of coarse size coal particle with finer coal particles for a slurry concentration shows the minimum apparent viscosity. Similarly the rheology of fly ash slurry is investigated with and without addition of bottom ash in the overall concentration range of 30-60% (by weight) and the maximum apparent viscosity reduction of fly ash slurry is found with 20% addition of bottom ash whereas marginal reduction in apparent viscosity is observed with 10 and 30% addition of bottom ash.

The present study is also concerned with determination of the pressure drop characteristics during the transportation of coal slurry as well as coal ash slurry by both experimentally and numerically. The experimental results show that the pressure drop is increased with increase in solid concentration. It is also found that the slurry prepared by adding the 30% of coarser particles of coal in finer particles significantly reduces the pressure drop as the viscosity is significantly reduced. Similarly the experimentation is also performed to investigate the effect of addition of bottom ash particles on pressure drop characteristics of fly ash slurry and it is found that the maximum reduction in pressure drop is observed with 20% addition of bottom ash. The numerical simulation is made using FLUENT software and it is found that the results obtained using SST k-ω turbulence model is in good agreements with the experimental data. Taguchi method is used to identify the various influencing parameters, which have significant effect on pressure drop during the transportation of slurry in pipeline. Flow velocity is found most significant parameter followed by addition of additive composition and solid concentration.

TABLE OF CONTENTS

LIST OF FIGURES

LIST OF TABLES

NOMENCLATURE

English Symbol	Description	Unit
W_R	Weight of solid particle retained	Grams
W_T	Total weight of solid particles	Grams
X_i	Mean diameter of the two successive sieve	Dimensionless
$C_{w\,max}$	Static settled concentration	% by weight
W_s	Weight of solids in the settled mass	Grams
W_w	Weight of water present in the settled mass	Grams
C_w	Solid Concentration	% by weight
W_b	Weight of beaker	Grams
W_{bs}	Weight of beaker and solid	Grams
W_{bw}	Weight of beaker and water	Grams
W_{bsw}	Weight of beaker, solid and water	Grams
V	Velocity	ms^{-1}
y_i	Pressure drop observations	mWc/100m
N	Total observations	Dimensionless
S/N	Signal to noise	Decibels(dB)
A	Weight of empty capsule/crucible	Grams
B	Weight of sample & crucible before drying	Grams
C	Weight of sample & crucible after drying	Grams
D	Weight of capsule and residue after ignition	Grams

Greek Symbol	Description	Units
S_m	Mass addition in the continuous phase	kg
u_i'	Fluctuating component	Dimensionless
$\bar{u}_i$	Time-averaged component	Dimensionless
ε	Dissipation rate is denoted.	m^2s^{-3}
k	Turbulence kinetic energy	Kgm^2s^{-2}
Ω	Turbulent frequency	Hz
τ	Shear stress	Pa
τ_y	Yield stress	Pa

Greek Symbol	Description	
η	Coefficient of rigidity	Dimensionless
α_c	Solid Concentration of continuum phase	% by weight
α_b	Solid Concentration of bulk solid phase	% by weight
ρ_c	Density of continuum	kgm^{-3}
ρ_b	Density of solid	kgm^{-3}
$\vec{v}_b$	Velocity of bulk solid	ms^{-1}
$\vec{v}_c$	Velocity of continuum	ms^{-1}
C_{vm}	Virtual mass force coefficient	Dimensionless
K_{bc}	Inter-phase drag coefficient	Dimensionless
C_l	Lift coefficient	Dimensionless
∇P	Static pressure gradient	$Pa.m^{-1}$
∇P_b	Solid pressure gradient	$Pa.m^{-1}$
$g_{o,ss}$	Distribution function	Dimensionless
P_b	Solid pressure	Pa
$\overline{\overline{\tau_{tc}}}$	Reynolds stress tensor	Dimensionless
$\overline{\overline{\tau_b}}$	Viscous stress tensors for bulk solid	Dimensionless
$\overline{\overline{\tau_c}}$	Stress tensor for continuum	Dimensionless
$\vec{v}_b^{tr}$	Transpose velocity vector for bulk solid	Dimensionless
$\vec{\vartheta}_c^{tr}$	Transpose velocity vector for continuum	Dimensionless
$\overline{\overline{I}}$	Identity tensor	Dimensionless
$\mu_{t,c}$	Turbulent viscosity	Pa.s
k_c	Turbulent kinetic energy	$Kg.m^2s^{-2}$
μ_c	Shear viscosity of continuum	Pa.s
$\vec{U}_c$	Phase weighted velocity	ms^{-1}
$\vec{U}_c^{tr}$	Transpose phase weighted velocity	ms^{-1}
λ_b	Bulk viscosity of the bulk solid	Pa.s
μ_b	Shear viscosity of solid	Pa.s
μ_c	Molecular viscosity of fluid	m^2s-1
e_{bb}	Coefficient of restitutions	Dimensionless
θ_b	Granular temperature	°C
d_p	Particle diameter	µm
G	Gravity	m^2s^{-1}

Metal/Compound name	Description
Al	Aluminium
C	Carbon
Co	Cobalt
Cr	Chromium
Cu	Copper
H	Hydrogen
Hg	Mercury
Iron	Fe
Mg	Magnesium
Mn	Manganese
Mo	Molybdenum
N	Nitrogen
Ni	Nickel
O	Oxygen
Pb	Lead
Si	Silicon
Zn	Zinc
Al_2O_3	Aluminium oxide
CO_2	Carbon-dioxide
CaO	Calcium oxide
FeO	Iron oxide
MgO	Magnesium oxide
SiO_2	Silicon oxide
TiO_2	Titanium oxide

LIST OF ABBREVIATIONS

Abbreviations	Description
APHA	American public health organization
EDS	Energy dispersive spectroscopy
CFD	Computational fluid dynamics
ESP	Electrostatic precipitators
GCI	Grid convergence index
LAN	Local area network
pH	Potential of hydrogen
PSD	Particle size distribution
RNG	Renormalization group
SEM	Scanning electron microscope
SST	Shear stress transport
TCLP	Toxicity characteristic leaching procedure
VOF	Volume of fraction method
VFD	Virtual frequency drive

CHAPTER 1
INTRODUCTION

This chapter gives the brief introduction about the background, motivation and objectives behind the research work in the fields of slurry transportation system, an overview about the identified problem and its applications. A brief summary of thesis structure in the form of chapters abstract are summarized at the end of the chapter.

1.1 BACKGROUND

Slurry transportation system is used to transport bulk solid materials with the help of carrier fluid for either short or long distances like mineral transportation in processing plants, transportation of coal, transportation of fly ash and bottom ash to dyke area in thermal power plants etc. Solid transportation through slurry pipeline has been also accepted by the different chemical and mining industries. Pipeline transportation is very popular due to its economy, reliability, convenient, low maintenance and availability throughout the year. The transportation of slurry through a pipeline is also extremely safe and leads to minimum environmental pollution (Kumar et al. 2014). It can also be laid over the difficult territory to reach the remote areas enriched by minerals like mountains, across water bodies and under the deep-sea else which are not accessible by conventional transportation mode like roadways and railways. Some additional features make pipeline transportation more attractive are reduction in traffic congestion, air and noise pollution and accidents. Under optimum operating conditions slurry transportation through pipeline is energy efficient and environment friendly.

Some of the researchers (Link et al. 1974; Aude et al. 1974; Aude et al. 1975) analyzed that long distance slurry pipelines are most economical as compared to other modes of transportation. The economical features of slurry pipeline i.e. the operating cost reduces with the increase in distance and volume of transportation, highly reliable and efficient, simple in construction and installation, lower manpower for operation and maintenances leads to encourage the huge applications of slurry pipeline (Kumar et al. 2014). However, the transportation through slurry pipeline has some limitations as listed as under:

- Very high initial capital cost.

- Single purpose utility.
- Requires large quantity of carrier fluid i.e. water or other liquid which may not be readily available every time at all places.
- Needs higher quality control for the efficient operation of pipeline.

1.2 PROBLEM IDENTIFICATION

Presently, major challenge throughout the world is the efficient utilization of a fuel in power generation. Numerous kinds of techniques are used to utilize the fuel in the solid form (pulverized coal), liquid form (petroleum) and gaseous form (compressed natural gas). Efficient fuel utilization for power generation at the best economic level has become the most important scientific challenge in the world. Universal oil crisis has forced scientists to study oil replacement with coal as an energy source and extensive studies have been started predominantly on coal liquefaction, gasification and combustion. A potential substitute to conventional fuel used in furnace is coal-water slurry (CWS) in atomized form which is a combination of water and fine powdered coal. Recently, coal-water slurry fuel has received maximum attention in its process development.

Coal-water slurry facilities have been fabricated in China, Japan, Russia, Canada, Australia, Italy, United States and Sweden. Out of these countries, China and Japan are most active countries and build several slurry pipeline facilities and boiler using coal-water slurry. In addition to these present studies, research on coal-water mixture preparation and its utilization has received considerable attention for its usage as a source of energy. The efficient utilization of coal-water slurry is possible only when the slurry suspension is prepared in such a way that permits the maximum concentration of coal and maintaining its viscosity at a minimum level. Additionally, it will be suitable for storage and transport through pipelines.

Combustion of coal in power plants generates a huge quantity of inorganic residues like bottom ash and fly ash which has low values for its utilization and have numerous ecological problems associated with their deposition (Blissett and Rowson, 2012; Kumar et al. 2013; Kumar et al. 2014).With the increasing demand of coal consumption in power generation generates large amount of fly and bottom ash as a by-product of coal combustion. Approximately 170 million tons per annum of fly ash is produced from

approximately 290 million tons of coal. This large volume of fly ash would occupy huge land area (presently about 65,000 acres of valuable land is occupied by ash ponds in India) and will pose a serious threat to the environment.

Presently, coal ash is being transported hydraulically to ash pond through slurry pipelines at low solid concentrations in power plants. Due to this the ash disposal pipeline operation is extremely uneconomical as the water quantity requirement is large and power consumption increases for pumping of water. Further, bottom ash particles are coarser than fly ash particles. So, coal ash transportation at low concentration also necessitates higher flow velocity and develops highly skewed concentration profile across the pipe cross-section. Studies carried out by researchers (Ghalot et al. 1992; Gandhi et al. 1998; Seshadri et al. 2008; Chandel et al. 2009; Kumar et al. 2014) reveals that different solid materials transportation at higher concentration in slurry pipeline shows reduced skewness in concentration profile and flow velocity. Authors (Seshadri et al. 2008; Kumar et al. 2014) concluded that coal ash transportation at higher concentrations is likely leads to the following additional advantages.

- The considerable decrease in water requirement leads to faster drying & settling of ash.
- The direct disposal of slurry on land may contaminate the groundwater through infiltration if the high percentage of water is present in slurry. The presence of low percentage of water in slurry has very less probability in contamination of groundwater unless the groundwater table is near to the land surface.
- Air pollution is also reduced due to retention of fly ash binding characteristics that gets washed away when slurry transportation is done at low concentration.
- The recirculation of water from the ash ponds can be avoided.

Pressure drop prediction for slurry pipelines is different from single-phase pipe flow because the existence of solid phase leading to extreme change in flow behavior. Many of the researchers (Durand, 1953; Babcock, 1971; Carleton et al. 1978; Darby and Melson, 1981; Chhabra and Richardson, 1983; Gahlot et al. 1992; Verma et al. 2006; Rabinovich and Kalman, 2011; Senapati et al. 2015) performed the experimental studies to calculate the pressure drop of slurry suspension in horizontal pipelines. The evaluation of pressure

drop with experimental correlations is found complex and time consuming. Some work has already been performed on the pressure drop for slurry flow in pipes by using pilot plant tests (Kaushal and Tomita, 2002; Seshadri et al. 2008; Kumar et al. 2014). The pipeline simulation provides the flow characteristics inside the pipe and helps to optimize the design parameters which further lead to cost and time reduction. Many investigators (Chen et al. 2009; Rawat et al. 2016) have performed the numerical simulation to investigate the pressure drop characteristics in slurry pipeline for the flow of solid-liquid flow. Single phase and multiphase approaches are introduced in literature to predict the pressure drop for different solid-liquid suspension.

1.2.1 Basic components of slurry transportation system

The basic components of slurry transportation system broadly classified into three sub systems as shown in the schematic diagram Figure 1.1. The three different sub systems are as under:

1. Slurry preparation facility
2. Main pipeline and pumping stations
3. Terminal utilization facilities

The first sub system is slurry preparation facility in which the solid particles are reduced to the appropriate size with the help of crushing and grinding to permit their transportation through slurry pipeline. The solid mixed with the carrier fluid in appropriate proportion up to the optimum level before the pumping of slurry.

The second sub system consists of a main pipeline and pumping stations depending over the distance of transportation. The total pumping facilities requirement is provided from either single or multiple pumping facilities along the length of slurry pipeline. Sometimes supplementary facilities like intermediate storage tank, corrosion and product quality control may be provided on lower level as compared to the initial level in the systems where intermediate pumping is required.

The third sub system is terminal utilization facilities. Storage tanks are provided for the receiving of slurry. The various operations like dewatering, filtration and drying also performed as per end utilization of the solid particles.

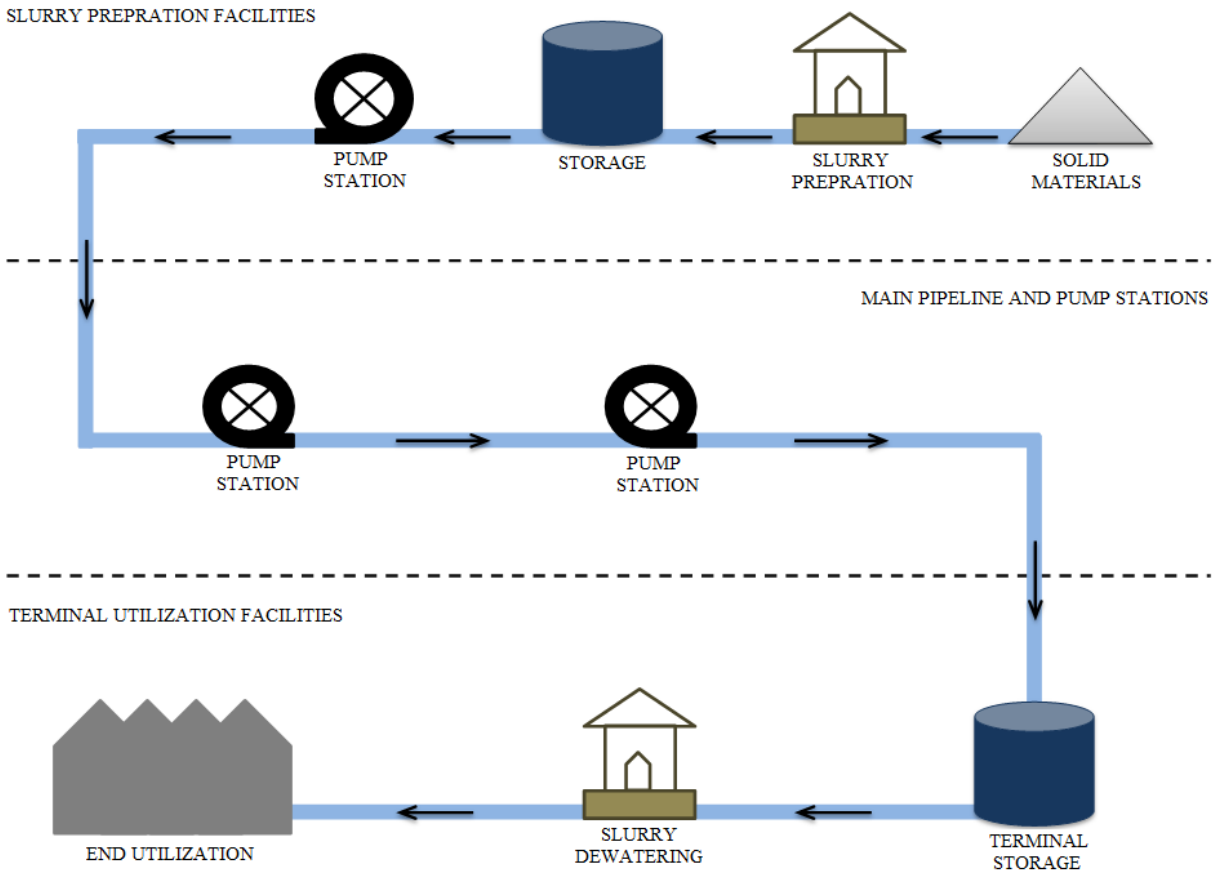

Figure 1.1: Basic slurry transportation system

The basic slurry transportation system design comprises the design of all the three subsystems. The design technology of the first and third sub system are properly well developed and understood whereas the design of the main slurry pipeline and pump facilities depends on the various parameters and still significant technology input is required for an optimal design.

1.2.2 Design of slurry transportation system

The parameters involved in the design of slurry transportation pipeline are categorized into three categories are hydraulic, corrosion and erosion(Seshadri, 1982; Gupta et al. 1995).Hydraulic parameters study shows that carrier fluid, optimum particle size distribution, optimum solid concentration, rheology of the slurry, specific gravity of the solids and material properties are very important factors affecting the design of slurry pipeline for higher solid concentrations i.e. solid concentration, C_w is greater than 50% (by weight). The hydraulic design of the piping system depends on the power requirements for

pumping which influence with solid concentration, particle size distribution, particle shape, viscosity and yield stress of the slurry (Kumar et al. 2014; Singh et al. 2016).

At present, universal correlations are not available to predict the flow behaviour of all possible slurries of various solids that can be transported hydraulically. Thus, the design has to be largely based on the data obtained from various tests as well as on the accumulated experience. Presently, solid materials like coal ash are being transported by slurry pipelines at solid concentrations which lie between 10 to 20% (by weight) making the whole system highly inefficient in terms of energy consumption as well as economy. The other associated problem with these pipelines is the excessive and uneven wear due to higher transportation velocity and the existence of highly skewed concentration profile. During the slurry flow at higher solid concentrations it becomes homogeneous and hence the slurry flow at lower velocities through the slurry pipeline results in laminar flow (Wasp et al., 1968).The numerical simulation provides information about the flow characteristics of the fluid in the slurry pipeline and thus provides information to designer for optimization of the slurry pipeline which reduces the cost and time for fabricating and testing of the slurry pipeline.

Many researchers (Ling et al. 2003; Krampa-Morlu et al. 2004; Mandal et al. 2005; Lin and Ebadian, 2008; Kaushal et al. 2012; Rawat et al. 2016) have studied the flow characteristics of pipeline using commercial CFD code. Pressure and velocity distribution inside the pipeline at different conditions have been predicted by using simulation studies.

1.3 OBJECTIVES AND SCOPE OF STUDY

1.3.1 Objectives

The main aim behind the present investigation is to analyze the flow characteristics of slurry transportation system. The specific objectives to meet the aim are the following:

1. To investigate the physio-chemical properties of coal, coal ash and rheological behaviour of coal and coal ash slurry at different solid concentrations.
2. To investigate the pressure drop characteristics for the flow of coal and coal ash water slurry in slurry pipeline.

3. To optimize the various influencing parameters of pressure drop for the flow of coal and coal ash water slurry in slurry pipeline.

1.3.2 Scope of the study

The investigation is undertaken with coal procured from Makum coal field, Dibrugarh, Assam and the coal ash samples are collected from the Guru Nanak Dev Thermal Power Plant, Bathinda, Punjab. The following studies in addition to others are undertaken for coal and coal ash samples:

- Physical characterization such as:
    - ✓ Particle size distribution
    - ✓ Static settled concentration
    - ✓ pH
    - ✓ Specific gravity
    - ✓ Proximate and ultimate analysis
- Mineralogical Characterization such as:
    - ✓ Scanning Electron Microscopy (SEM)
    - ✓ Energy-Dispersive X-Ray Spectroscopy (EDX)
- Leaching Characteristics
- Rheological Characteristics
- Pressure drop characteristics:
    - ✓ Experimentation
    - ✓ Numerical Simulation
- Optimization using Taguchi approach

1.4 METHODOLOGY

The various physical, chemical and mineral properties are investigated. The rheological characteristics of slurry suspensions are evaluated at different solid concentrations. The pressure drop in pipeline is also determined at different solid concentrations and flow velocities. The methodology adopted is shown in Figure 1.2.

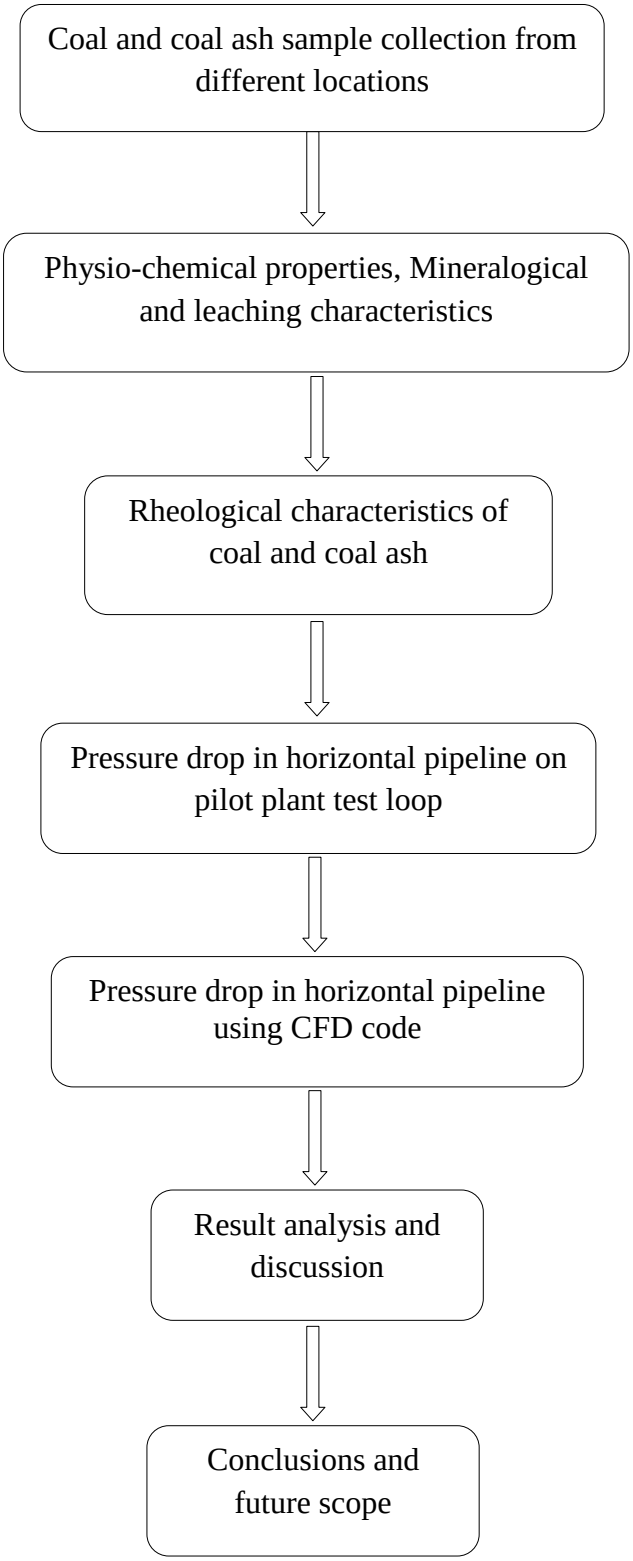

Figure 1.2: Flow chart of methodology

The aim and objectives are achieved by:

- The sample collection of coal and coal ash is from Makum coal field, Assam and Guru Nanak Dev Thermal power plant respectively.
- The physical, chemical and mineralogical properties of the collected samples.
- The rheological behaviour study of coal and coal ash slurry samples at different solid concentrations.
- The pressure drop characteristics for transportation of coal slurry as well as coal ash slurry in horizontal pipeline at different velocities and solid concentrations using pilot plant test loop.
- The numerical investigation of pressure drop characteristics of two phase solid-liquid flow at different concentrations and velocities using computational fluid dynamics code FLUENT.
- Optimization of various influencing parameters for pressure drop during transportation of slurry using Taguchi approach.

1.5 ORAGANISATION OF THESIS

The goal and particular objectives have been addressed with the different designed and planned methods. The investigations carried out in details and their results are described in different sections. A brief description of the layout of the thesis is presented in the following paragraphs.

- **Chapter 1-** Introduces the problem with specific objectives and presented the detailed methodology adopted to achieve these goals.
- **Chapter 2 -** The detailed literature review on the rheological behavior of coal water slurry as well as coal ash slurry, pressure drop of slurry during transportation in pipeline and numerical simulation of solid- liquid flow in pipeline are presented in this chapter.
- **Chapter 3** - The physical, chemical and mineralogical characterization of coal and coal ash are carried out in this chapter. This section also discusses about sample preparation, testing procedures, equipment details and their specifications.
- **Chapter 4 –** In this chapter the rheological characteristics of coal and coal ash slurry having various concentrations are carried out with the help of rheometer.

- **Chapter 5**-This section deals with the experimental set up of pilot plant test loop and the experimental determination of pressure drop during the transportation of coal and coal ash slurry having various concentrations and velocity.
- **Chapter 6** - This section deals with the numerical determination of pressure drop during the transportation of coal and coal ash slurry having various concentrations and velocity using FLUENT software. The results obtained from numerical model are also validated with the experimental results.
- **Chapter 7**- This chapter discusses the Taguchi method which is used to identify the various influencing parameters which have significant effect on pressure drop during the transportation of slurry in pipeline.
- **Chapter 8**- It deals with summarized observations and important conclusions drawn from experimental and numerical studies. Recommendations for future research work have been also presented.

CHAPTER 2
LITERATURE REVIEW

2.1 INTRODUCTION

Coal is a major source of energy for thermal power plants in India. Indian coals are having higher ash content ranges between 34 - 39 % while 10 -15% ash content is present in imported coal (Kumar et al. 2000; Chandel et al. 2009). During coal combustion bottom ash, fly ash, slag and desulfurization by-products of flue gas are produced as inorganic residues in the thermal power plants [2-5]. The thermal power plant ash disposal system can be sub divided into three sub-systems namely slurry transportation facility, pipeline and pumps, and terminal facility as discussed in the previous chapter. The slurry transportation system performance is dependent on the operating parameters. The rheological behaviour of slurry suspension play very vital role in effective operation of slurry transportation system. Presently, slurry transportation systems are operating on low concentrations for disposal of coal ash from thermal power plant to ash pond. This data give emphasis to investigate slurry transportation system for the flow of solid-liquid mixture at high concentration. Attempts have been made to study analyse the slurry transportation system for higher concentrations. A critical review of significant work carried out in this field has been presented in this chapter to give an understanding into the present state of knowledge.

2.2 RHEOLOGICAL BEHAVIOUR OF COAL ASH SLURRY

The rheology is defined as the study of deformation and flow of matter under the action of shear forces. The solid-liquid slurry flow behaviour in slurry pipeline depends upon the rheological characteristics of the slurry suspension. The rheological characteristics of the slurry suspension play a very important role in slurry transportation system design. On the basis of the rheological data of suspension, head loss can be calculated for solid-liquid mixture flow. The rheological behaviour of slurry suspensions depends upon various parameters like nature of slurry suspension, flow velocity, solid concentration, yield stress etc. Several techniques were used to reduce the frictional losses by reducing rheological characteristics. The present literature review focuses on techniques in which rheological characteristics of slurry suspension are directly affected. Various types of chemical

compounds were used as additives to improve the characteristics of slurry suspension. The most necessary characteristics of additives are lesser viscosity and more stability. Following discussions describes the rheological characteristics of slurry suspensions with and without additives.

Many investigators (Sive and lazaurus, 1987; Mishra et al. 1998; Verma et al. 2006; Senapati et al. 2005; Kumar et al. 2013) have studied the rheological behaviour of slurry suspensions of different materials. However no particular correlation is available for the prediction of different parameters affecting the rheological behaviour of a solid-liquid suspension. The rheological characteristics of the slurry suspension play a very important role in slurry transportation system design. On the basis of the rheological data of suspension, head loss can be calculated on the basis of flow rate-pressure drop relationship of the pipeline for solid–liquid mixture flow. Many investigators (Roscoe, 1952; Williams, 1953; Einstein, 1956; Rutgers, 1962; Moreland, 1963; Landel et al. 1965; Thomas, 1965; Krieger, 1968; Schrick et al. 1972 and Wilson, 1982; Naik et al. 2011) have studied the rheological behavior of the different slurries. Moreland (1963) studied the particle shape effect on the slurry rheology and found that the non-sphericity enhances the non-Newtonian behaviour of the slurry.

Thomas (1965) carried out a critical investigation on spherical particle for relative viscosity of solid suspension. The coefficient in the power in relationship was related to relative viscosity and solid volume fraction was determined using least squares procedure and a new expression for viscosity containing six terms was proposed. Gay et al. (1969) studied the rheological behaviour of slurries of different solids e.g. nickel, alumina, copper, and glass in suspending media such as liquid sodium, m-xylene and glycerin and found yield-pseudo plastic behaviour of slurry. They proposed a correlation, for the viscosity and yield stress of the slurry based on yield pseudo plastic model. However, Cheng (1980) observed that the viscosity of the suspension is independent of the particle size.

Darby et al. (1981) studied the non-Newtonian viscosity of methanol using methanol as perpetration of liquid solid suspension. They noticed that power law and Bingham plastic model can be used for apparent viscosity of slurry suspension. Lazarus and Sive (1984) carried out an experimental investigation to analyze the rheology of fly ash suspension

collected from South African power stations using a balanced beam viscometer. The rheology results indicated that the fly ash slurries may follow the Bingham plastic model.

Bunn and Chamber (1993) carried out an experimental investigation to analyze the rheology of fly ash suspension collected from Australian thermal power stations. The experiment was conduct with rotary viscometers and tube viscometers for rheological measurements of fly ash suspension at different concentrations varying by weightage from 60 to 80%. They also reported that fly ash suspension had shown non-Newtonian nature at higher concentration. Turian et al. (1992) found that the solid concentration of slurry impact on other properties like yield stress, viscosity and final settling concentration. Heywood et al. (1993) investigate the coal ash slurry rheological characterization at solid concentrations of 68 to 70 % (by weight). The rheological behaviour of coal ash suspension was predicted with the help of power law model. They found the exponent value of 'n' for model was as 0.46.

Ahmad et al. (1995) studied the rheology of two multi-sized particulate slurries namely iron ore and zinc tailings. They found that slurry rheology is a functioning solid concentration, chemical and physical properties of the solid suspensions. Biswas et al. (2000) investigated the rheology of coal ash slurry collected from different Indian thermal power plants. Results show that rheological and physical properties of vary over wide range from plant to plant.

Kumar et al. (2000) investigated the rheological properties of bottom ash, fly ash and with addition of bottom ash as additive. They noticed that rheological characteristic of fly ash suspension was improved with addition of bottom ash.

Parida et al. (1995) had carried out an investigation on rheological and flow characteristics of fly ash collected from Talcher Thermal Power Station, Orissa. They used power law model to predict the nature of slurry. They found that the nature of slurry become non-Newtonian beyond 50% solid concentration. The characteristic curve of power law was fitted as pseudo-plastic non-Newtonian.

Ward et al. (1999) had carried out an experimental study on the hydraulic transportation of fly ash slurry with and without addition of stabilizing additive. They found that slurry

viscosity increases with addition of stabilizing additive and recommended the use of dispersing additive to prevent the settling of fine coal ash (fly ash) particles.

Li et al. (2002) carried out an experimental investigation to analyze the rheology and sedimentation stability of fly ash suspension by addition of different additives. The fly ash was taken from the Matsuura Power Station on Kyushu Island (Japan) and slurry was prepared by mixing it with deionized water in concentration of 68% (by weight). They used four different additives namely carboxym, ethyl cellulose, rhamsan and xanthan gums and concentration of additives was varied up to 0.3% (by weight). The apparent viscosities of fly ash slurries were measured with the help of rheometer (Iwamoto Seisakusho Co., Ltd. Model IR-200). The temperature of the test samples was maintained at 298 K. They found that the additives were effective in terms of increasing stability of fly ash slurry and optimum concentration of additive found as 0.20 (by weight).

Verma et al. (2006) performed the experimental study on impact of particle size distribution on rheological behaviour of coal ash slurry suspension at higher concentrations. The experimentation was carried out by taking different size sample and each sample of different concentration. They noticed that fly ash more than 40% show non-Newtonian nature. Parida et al. (2006) performed an investigation on rheological characteristics of two different fly ash samples. Pseudo-plastic model was used to determine the pressure drop in pipeline for the flow of fly ash slurry. They found that higher concentration transportation of fly ash slurry in pipeline had drastically reduced the cost of transportation. Senapati et al. (2008) carried out an experimental investigation to analyze the rheology of coal ashes (fly and bottom ash) suspension with/without additive by using viscometer. They reported that fly ash slurry suspension show pseudo plastic nature and bottom ash slurry suspension viscosity can be determined with the help of power law model.

Seshadri et al. (2008) investigate the rheological behaviour of fly ash slurries of different range particle sizes ranges with and without additives at different solid concentrations. They used 0.1% (by weight) solid concentration of sodium-hexa-metaphosphate as additive and also calculated the pressure drop in a straight pipeline of 75 mm diameter. They found that the solid concentration and particle size distribution influence more to the

rheological characteristics of slurry of non-Newtonian as compared to the Newtonian nature.

Vlasak et al. (2009) observed the effect of addition of sodium hexametaphosphate as additive on rheology of fly ash suspension. They found that addition of sodium hexametaphosphate in small amount reduces viscosity of fly ash slurry. Chandel et al. (2009) carried out an experimental investigation to analyze the rheology of fly ash-water slurry with addition of additive. They used two different additives namely sodium-hexa-meta phosphate and Henko detergent and their ratio was kept constant i.e. 5:1. Bingham plastic model was used to predict flow behaviour of ash slurry at higher concentration. They reported that rheological properties of ash slurry is modified with addition of additive and also helps to lower pressure drop.

Bbranganca et al. (2009) reported that viscosity of coal ash suspension depends upon different factors as concentration, particle size, pH, and properties of liquid used for the slurry preparation. Senapati et al. (2010) carried out an experimental investigation to analyze the rheology of fly ash suspension at higher concentrations. Experiments were conducted by taking five sample of fly ash with volumetric concentration 0.32 to 0.4945. They found that viscosity of fly ash suspension is depends upon concentration and particle size.

Senapati et al. (2012) investigated rheological and leaching characteristics at higher solid concentrations of Indian ash samples. They used 0.2-0.6% of sodium silicate as additive. Bingham plastic model was used to study the flow behaviour of ash slurry at 50-60% (by weight) concentration. The addition of additive shows a positive effect, it helped in reducing the yield stress and viscosity. Pb, Zn and Cu shows higher concentration in the leachate as compared to Cd, Co and Ni. with the addition of sodium silicate the leaching of heavy metals was reduced. Senapati et al. (2013) have studied rheology behaviour of coal ash slurry suspension with HAAKE Rotational Viscometer. The investigation was conducted in the solid concentration range from 62 to 65 % (by weight). They found that dense slurry of fly ash suspension show pseudo plastic nature whereas fly and bottom ash mixture exhibits the non- Newtonian nature.

Kumar et al. (2013) performed an investigation on rheological characteristics of the bottom ash slurry. They used fly ash as an additive for bottom ash slurry at different ratios. They varied the solid concentration of fly ash slurry from 10-50% (by weight). Sodium bi-carbonate was used as an additive with proportion of 2-8% (by weight) at all solid concentrations of bottom ash slurry. They found that bottom ash slurry depicts the Newtonian nature upto 50% solid concentration. They also found that the relative viscosity of bottom ash slurry increase with the addition of fly ash whereas decreases with addition of sodium sodium bi-carbonate.

Pani et al. (2015) investigated the rheological behaviour of fly ash samples collected from Jindal Power Limited, Raigarh. The rheological investigation was performed at 50-60% solid concentrations range (by weight) using HAAKE Rotational Rheometer. They used Sodium silicate and ghadi detergent as additives and their weightage in slurry was varied from 0–0.6%. Results show that ash slurry exhibits Non- Newtonian behaviour and obtained data was fitted in Bingham Plastic model. They found that sodium silicate was more effective than ghadi detergent at 0.6% concentration (by weight).

Panda et al. (2014) investigate the rheological characteristics of fly ash and fly-bottom ash mixtures at high concentration with collected samples from thermal power plant of Talcher using Haake Rotational Viscometer. Addition of bottom ash in fly ash was carried on at 10 - 40%. The median particle size (d50) of fly ash and bottom ash samples were noted as 20 and 250 µm respectively. From the rheological study, it was found that the slurry of fly ash sample at 60% and above shows Bingham plastic fluid but after adding on bottom ash, the slurry shows yield pseudoplastic fluid. They also studied the procedure of calculating the friction factor for both types of fluid such as Bingham as well as pseudoplastic fluid.

Senapati et al. (2015) investigated the rheological behaviour of fly ash and the mixture of bottom and fly ash samples in concentration range from 60 to 67.5% using Haake Rotational Viscometer. Bottom ash added as an additive in the fly ash slurry ranging from 0-20 % (by weight). Particle median size (d50) of samples, namely fly and bottom ash was measured as 16.4 and 144µm respectively. From the rheological study, it was concluded that all the slurry samples exhibits pseudoplastic behaviour with concentration ranges from 60-67.5% (by weight). Fly ash slurry viscosity decreases with addition of bottom ash.

Assefa et al. (2015) investigated the rheological properties of high concentration slurry ranges from 50-70% (by weight). They proposed an empirical model for viscosity as a function of solid volume fraction, mean particle diameter and coefficient of uniformity and optimized using nonlinear least square method. The proposed model was validated with rheological data of (Chandel et al. 2009; Chandel et al. 2010; Biswas et al. 2000). They concluded that the proposed model shows close agreement with experimental data and able to predicted viscosity of multi-sized Bingham slurries at higher concentration.

Kumar et al. (2017) carried out\ an experimental investigation to analyze the rheology of bottom ash-water slurry with/without additives. They have taken Henko detergent and sodium sulfate as an additive. The weightage of additives in bottom ash suspension was varied in range of 0.2-0.6% and solid concentration of bottom ash suspension was taken in range of 10 to 60% (by weight). They found that the Reduction in apparent viscosity is highly noticeable by addition of sodium sulphate as compared to Henko detergent.

The investigators (Ahmad et al. 1995; Mishra et al. 2001; Maclnnes, 2002; Kumar et al. 2003; Seshadri et al. 2008; Verma et al. 2006; Parida et al. 2006; Senapati et al. 2010 ; Convery et al. 2010 and Kumar et al. 2013) found that fly ash slurry exhibit non-Newtonian nature above 40% solid concentration (by weight). They also observed that the yield stress and value of the Bingham plastic viscosity of fly ash slurry suspension increases at higher rate with increase in solid concentrations.

From the above literature studies it is found that small quantity of additives in slurry suspension are capable to improve the rheological characteristics of the slurry suspension. However, the proper additive agent selection is dependent upon the type of slurry to be transported through slurry transportation system. In order to design an efficient ash disposal system, selection of proper additive and its percentage addition plays a vital role to achieve better rheological characteristics.

2.3 RHEOLOGICAL BEHAVIOUR OF COAL WATER SLURRY

In addition to these existing extensive studies, research on coal water slurry preparation and utilization processes have received much attention due to the use of coal as an energy

source. The knowledge of rheology of slurry is very much vital particularly for the dense phase in slurry pipeline. Several studies are reported by researchers on the rheological behaviour of coal-water slurry (Leong et al. 1987; Roh et al. 1995; Turian et al. 1992; Wang and Zeng, 1998; Aktas and Woodburn, 2000; slatter, 2000; Yong-gang et al. 2009; Yuchi et al. 2005; Chen et al. 2010). The rheological behaviour of the coal water slurry depends on a large number of parameters. Several investigators have studied the many aspects which affects the rheology of coal water slurry which is discussed following.

A number of studies have been conducted to investigate the effect of particle size on the rheology of coal-water slurry (Usui et al. 1986; Round and Hessari, 1987; Toda and Kuriyami, 1988; Yavuz and Kucukbayrak, 1998; Slatter, 2011; Senapati et al. 2008; Boylu et al. 2004).
Hasan et al. (1986) investigated the rheological behaviour of coal water slurry prepared from sub-bituminous coal. Rheological tests were conducted using Brookfield viscometer with particle size varying from 0.044 to 0.223 mm. They observed that at all concentrations, the coal water slurry showed pseudoplastic behaviour. The data was fitted to the Power law model and the parameters were calculated. They found that the coal water slurry prepared by hot water drying had better fluidity as compared to the slurry prepared from as received coal.

Gahlot et al. (1988) carried out an experimental investigation to analyze the rheology of zinc tailing and coal-water slurries. The experiment was carried out with original crosser particle and finer size particle of slurries suspension. They proposed methodology to determine the viscosity of coarser particles of zinc and coal water slurry suspension. Reddy et al. (1994) studied the rheology of oil-coal slurry suspension and investigate the effect of coal properties on slurry suspension. The experiment data was of particle size distribution fitted into Rosin-Rammler model. They reported that viscosity of coal oil suspension is decreases with increases moisture content of parent coal.

Roh et al. (1994) investigated the impacts of coal loading and particle size on the rheological behaviour of coal-water mixtures. Seven bituminous coals were used in the study with particle size distribution obtained by sieving for particle greater than 38 μm and coulter counter for particles less than 38 μm. Rheological measurements were conducted using Haake RV-12 viscometer. They found that all the slurries exhibited pseudoplastic

behaviour. The blending with coarse coal fraction was useful in reducing the viscosity and the static stability.

Logos and Nguyen (1996) studied the effect of particle size on the flow properties of South Australian coal water slurry. The coal used for the preparation of coal water slurry was a low rank Lochiel coal from South Australia. The particle size distribution was varied by introducing coarser fraction of coal with the finer fraction in different proportions. The rheological parameters were evaluated using concentric cylinder viscometer (HAAKE, Model RVI00). The solid loadings were in the range of 23 % to 50 % by weight. They found that the slurries prepared from only finer fraction i.e. under 45 μm were more viscous than the coal water slurries prepared from a mixture of coarse and fine particles with coarse particles varying from 208-279 μm. They found that coal water suspension upto 23% (by weight) showed Newtonian afterwards suspension becomes pseudo-plastic or shear thinning. It is also observed that addition of coarser coal fraction reduced the viscosity of the finer coal water slurry.

Nguyen et al. (1997) studied the effect of coarser particles on rheological properties of finer coal-water slurries. The rheological properties were measured at solid concentrations ranges from 23-50% (by weight) using HAAKE RV-100 viscometer. They found that the solid concentration affected the nature of the slurry up to 23% solid concentration shows Newtonian above concentration shows shear thinning with the presence of yield stress .They found that addition of a coarser coal particles without any other additive lowers the viscosity substantially.

Ghanta et al. (2002) investigated impact of particle size distribution, concentration and surface properties on rheology of coal and copper ore slurry. They found that as the particle size of coal increases viscosity of coal slurry suspension decreases, whereas in case of copper ore as particle size increases viscosity also increases. They also observed that addition of coarse particle of ash in finer particle improve its rheology.

Mishra et al. (2002) studied the rheological properties of coal-water slurry of Indian coal. They evaluated the impact of various factors like temperature, pH, ash content, and solid concentrations on the rheology of coal-water slurry. Rheological measurements were made using HAAKE rotational viscometer RV30. The temperature is maintained constant by

using thermostatic bath. They found that the coal water slurry exhibited pseudoplastic behaviour with increase in shear rate. The apparent viscosity increased as the ash content of coal increased and decreased, as pH value was increased.

Lorenzi et al. (2002) investigated the influence of finer /coarse coal ratios on the rheological behaviour of coal-water slurry at different solid concentrations. They have taken the surfactant as copolymer of ethylene and propylene oxides with a concentration of 0.7% (by weight). The xanthan gum with a concentration of 0.05% (by weight) was used as a thickener to prevent particles settling. The rheological measurements were obtained from HAAKE VT 550 rheometer. They found that the optimum fine/coarse particle ratio was 55 % of fine coal with a minimum viscosity and also concluded that due to addition of surfactant air gets entrapped which causes change in the viscosity of the slurry.

Tiwari et al. (2003) performed an experimental investigation on coal-water slurry with the addition of anionic additives. The samples were obtained coal from Makum field of Assam called Ledo coal and from North Karanpura field of Jharkhand called Sirka coal. Naphthalene based and naphthalene-toluene based additives were added in the coal. The rheological properties of CWS were measured by a HAAKE RV-12 Roto viscometer. They found that with naphthalene based as an additive, the maximum coal loading was found as 70 % and with naphthalene-toluene based as additive the maximum loading was found around 69 %. The optimum concentration of additives for high coal was found as 0.8 % for naphthalene based and 0.9 % for naphthalene-toluene based.

Boylu et al. (2004) studied the effect of coal volume fraction, particle size distribution, and rank on the rheological properties of coal-water slurry. Experiments were conducted using two Turkish lignites coals and Sibria bituminous coal. The coal samples were prepared by mixing of different coal particles sizes to obtain mean particle diameter d50 of (19, 35, 50μm). The rheological experiments were performed on RVD2-Broolfield rotating viscometer. The measurements were performed in shear rate range of 100 s^{-1}. The pH value and temperature of slurry were kept constant at 7.0 and 25±2 0C respectively. The found the viscosity of coal –water slurry is the function of volume fraction, particle size and rank of coal.

Yuchi et al. (2005) performed the rheology experimentation of Chinese coal-water suspension with solid loading. They used Sodium naphthalene sulfonate formaldehyde as surfactant. The NXS-11 rotation viscometer was used to measure the rheological characteristics of coal-water slurry in the shear rate range of 3.18-113.5 s^{-1} at constant temperature of 25^{o}C. They found that suspension ability of slurry decreased with an increase of solid loading. The rheological behaviour of coal-water slurry is not dependent upon the rank of coal, most of middle rank coal having high carbon content of 82-85% shows dilatant fluid behaviour and some of other rank coal show shear thinning behaviour.

Gurses A et al. (2006) carried out an investigation on rheology of coal-water slurry with the influence of various parameters like solid concentration, pH value, temperature and additives. They performed the experimentation with the help of rotating type viscometer (Model: RV8-Brookfield). Ammonium Bromide (CTAB), Borrosperse NA-3A surfactants were used as additives. They found that viscosity of coal-water mixture increases at low speed whereas decrease at high speed with increase in temperature.. From the experimentation they found that CTAB are more effective additives upto 50% concentration (by weight) as compared to Borrosperse NA-3A surfactants.

Das (2008) investigated the rheological characteristics of coal-water slurry suspension with natural additive. The experimentation was carried out to impact various factor namely as ash content, temperature, pH, and concentration of saponin on rheology of coal-water slurry. They varied the concentration of coal-water slurry in range of 55-64 and additive was varied from 0.4–1.2 % (by weight). They reported that 0.8 % concentration of additive give maximum improvement in rheological properties of coal slurry.

Mosa et al. (2008) carried out an experimental investigation to analyze the effect of additives on rheology of coal-water slurry. They used three different additives namely sodium tri-polyphosphate, sodium carbonate and sulphonic acid. The concentration of additives was varied by weightage of 0.5 to 1.5%. Results show that apparent viscosity and flowablity of coal-water slurry reduces with an increase in weightage of additives.

Tian-ye et al. (2008) studied the effect of coal blending on the rheoloy of coal water slurry at three different types of coal samples collected from Daliuta (DLT), Linhuan (LH) and Yongcheng (YH). Largest size of coal was found as 300μm and about 75%

particles are finer than 74μm. Naphthalene sulfuric acid-formaldehyde condensate was used as dispersant. LH and YH coal was mixed with the DLT with the weight percentage of 10-40%. It was observed that addition of coal with high rank can improve the slurry ability and rheology of the low rank coal.

Senapati et al. (2008) investigated the rheology of coal-water suspension with natural additive by using HAAKE RV 30 rotational viscometer. They varied the concentration of coal-water slurry in range of 55-63.7. The additive was varied in the range of 0.4–1.2 % (by weight). They found that coal-water slurry suspension with addition of additive show Bingham plastic nature. Apparent viscosity of coal-water slurry reduces with an increase of proportion of additives.

Sahoo et al. (2010) compared the rheological characteristics of microwave treated high ash Indian coals with untreated coal. Coal samples were treated in the microwave at 900W for different time periods of 30, 60, 90 and 120 seconds. The rheological characteristics of coal samples investigated before and after treatment. Results shows that all slurry samples show pseudo plastic flow nature and viscosity of treated coal samples is lower than untreated. Treated coal samples exhibits better rheological properties as compared to untreated.

Zhou et al. (2010) investigated the rheological characteristics of concentrated coal-water slurry by applying the Herschel-Bulkley model. The rheograms were obtained from HAAKE rheometer in the shear rate range of 0-200 s^{-1}. The slurry was dispersed with lignin-based dispersant (MSL). The different coal water slurry samples were prepared at 64% solid concentration with 0.7- and 1.5% dispersant (by weight). They found that with 0.7% dispersant, the slurry showed shear-thinning characteristic and for 1.5% dispersant it showed shear-thickening characteristic. During experimentation, it was also found that with the increase in solid concentration the behaviour of coal-water slurry shifts to pseudoplastic behaviour whereas shifts to dilatant behaviour with the increase in dispersant dosage.

Buranasrisak et al. (2012) carried out experimentation to study the impact of particle size on the rheology of coal-water mixture. Naphthalene sulfonate formaldehyde (NSF) and Na-CMC were used as the dispersing agent and stabilizer in coal water slurries. The

viscosities of coal water slurries were measured using MV-2000 series II Cannon® Rotary viscometer at different solid loadings ranges between 60- 65 % by weight. They observed that maximum coal loading was possible when coal water slurry was made from bimodal particle size distribution.

Shao et al. (2012) studied the rheological behaviour and stability of coal alcohol fermentation wastewater slurries. The rheological properties were measured with the help of a rotary viscometer (NXS-4C). Measurements were performed at temperature of 25° ± 1°C. The solid concentrations of coal slurries ranging between 45-65% (by weight) with the shear rate variation of 0-100 s^{-1}. From the experimental results it was found that slurries of coal maize and cassava alcohol fermentation wastewater show pseudoplastic behaviour and high apparent viscosity due to the presence carboxlic groups and lower pH values. Tcoal-water slurry shows better stability as compared to coal maize and cassava alcohol fermentation wastewater slurries.

Singh et al. (2016) studied the effect of particles size, temperature of slurry and concentration on rheological behaviour of coal- water slurry. The solid concentration of slurry was taken in the range of 30- 60% (by weight). The rheological study was carried on for both kinds of particle size distribution such as unimodal and bimodal distribution of particles. From the rheological study, it was concluded that as concentration of solid increases, the apparent viscosity also increases. The pseudoplastic behaviour of slurry was observed at high concentrations. However, in the case of bimodal slurry, the apparent viscosity of fine particles slurry suspension is decreases with addition of coarse particulate.

The rigorous literature review depicts that there is a definite dearth of information regarding the rheological behavior of coal-water slurry of Indian coal with high-ash content. There is very little work carried out to determine the optimum concentration of additive required for maximum reduction in apparent viscosity of coal-water slurry. Better understanding of the rheological properties of coal-water slurry is essential for design and optimization of coal slurry transportation and combustion system.

2.4 INVESTIGATION OF PRESSURE DROP CHARACTERISTICS OF SOLID LIQUID FLOW IN SLURRY PIPELINE

A considerable research work has been done in past to predict the pressure drop for the flow of solid-liquid slurry flow through pipeline. The precise knowledge of above mentioned parameters provides a great help in selection of slurry pipeline and hence improves the power consumption. Various factors affect pressure drop have been investigated by numerous researchers. In the present study, prior to the research work an extensive review of the published works is carried out in the field of solid-liquid slurry transport with an emphasis on effect of various parameters.

Lazarus and Sive (1984) had carried out an investigation on pressure drop characteristics of fly ash slurry from South African power stations. The d50 of the fly ash samples was found as 17 microns and specific gravity of the sample was found as 2.3. Experiments were conducted for solids concentrations range of 10-30% (by volume). The rheology results indicated that the fly ash slurries tested would be described by Bingham plastic model. Pipeline loop tests were also conducted in a test pipe of 140 mm internal diameter at solids concentration of 10% to 30% (by volume). They found that the head loss of slurry in pipeline shows good agreements with predicted data.

Heywood et al. (1993) investigated the flow characteristics of coal-ash slurries at high concentration. The flow investigations were carried out on 8 km long pipelines of 150 and 200 mm diameter. The solid concentration of slurry was taken in the range of 68-70 %(by weight). They found that power law exponent becomes constant around 0.46 for coal ash slurries. The specific power consumption (SPC) was also computed at different slurry concentrations and the results indicated that the SPC increases with increase in slurry concentration.

Kumar et al. (2000) investigate the both rheological and pressure drop characteristics of bottom ash, fly ash and mixture of fly and bottom ash. From the experimentation results they conclude that the pressure drop with fly as slurries shows linear increase with increase in solid concentration whereas for bottom ash slurry the increase in pressure drop is not linear. The pressure drop in the case of coarser bottom ash slurry is lesser as compared to the finer fly ash slurry. The deposition velocity of fly and bottom ash mixture

is nearer to fly ash slurry whereas the value of pressure drop is much closer to the bottom ash.

Kaushal and Tomita (2002) evaluated the pressure drop of homogeneous slurry of zinc tailing slurry using wasp model at solid concentration of 10 to 40% (by weight). They observed that the predicted pressure drop showed reasonably agreements with the experimental data for straight pipe of 2-D channel. They found that solids concentration profiles are the function of velocity of flow, particle size and efflux concentration of slurry. The pressure drop for the flow of slurry through rectangular duct (200 mm × 50 mm) shows less than r the circular pipe having diameter of 105 mm.

Lu and Zhang (2002) discussed the resistance properties of coal-water paste flowing through the pipeline. Different four steel tubes were considered with nominal diameter of 25, 32, 40, and 62 mm and length 5500mm. The screw pump with maximum 16 m^3/h flow rate was used for pumping the slurry. Coal water paste with different water content was prepared in range of 22.1-33.5% (by weight). Pressure drop was measured with the help of electric differential manometer. The experimental results show that the energy loss coefficient for the laminar flow of coal-water paste in pipeline was similar to Newtonian fluid flow through pipeline.

Gillies et al. (2004) studied the pressure drop of heterogeneous sand slurry flow at high velocities. The test loop used to conduct experiments was of 0.09 and 0.27 mm in median diameter and 0.103 m of length. They measured the pressure drop with the help of calibrated pressure transducers and velocities with the help of calibrated magnetic flux flow meter. They developed a correlation to predict the friction losses in the pipeline for flow of heterogeneous slurries.

Skudarnov et al. (2004) performed the pressure drop experimentation in pipeline for flow of double-species slurries consists of glass beads and water. The various combinations were taken for double-species glass beads. Pressure drop for double-species slurries were compared with individual components at similar volume fraction of solids. They also studied the mean particle size effect on the pressure drop of double- species slurry flowing in pipeline. It has been concluded that an increase in the solid mean particle diameter results in higher pressure gradients for low velocities but lower pressure drop for high

flow velocities and also the pressure gradient curve for double-species slurry is always between the curves for individual components.

Kaushal et al. (2005) conducted an experiment with glass beads of mean diameter of 440 and 125μm and mixture of both glass beads in equal mass fraction on horizontal pipeline with 54.9 mm diameter. The velocity of slurry varied from 0- 5 ms^{-1}at concentration of 50% (by volume). They observed that the pressure drop increases with increase in concentration. But rate of increase in pressure drop is relatively lesser at higher velocities. The rate of pressured drop increase lesser at low velocity whereas increase rapidly at high velocity.

Verma et al. (2006) evaluated the pressure drop for fly ash slurry in a 90^o horizontal bend at high solid concentrations of 50-65% (by weight). The data from the experiment has been analysed to obtain the relative pressure drop, bend loss coefficient. The pilot plant test loop was consisting of closed circuit of MS pipe with 53 m diameter and 30 m length. A circular mild steel pipe bend having 90^o turn angle and radius ratio of 5.6 was used to generate the pressure drop data experimentally. They concluded that the relative pressure increases in pipe bend with the increase in velocity and approaches towards constant value at high velocity. The bend loss coefficient shows a reducing trend with increase in velocity. The pressure loss coefficient for bends increases marginally with the increase in the velocity.

Chandel et al. (2009) carried out an experimental study on the effect of additives on rheological and pressure drop characteristics of fly ash slurry by using pilot plant test loop. The pilot plant test loop was consisting of 40 mm diameter straight pipeline of 50 m length. The concentration of ash slurry was kept high (above 60% by weight) and mixture of Henko detergent and sodium carbonate was used as an additive. The flow rate inside pipeline was measured by calibrated electromagnetic flow meter. The results obtained from experiments showed reasonable agreement with analytical results calculated from the algorithm given by Darby and Melson (1981). They also found that the pressure drop gets reduced with the addition of soap solution in high concentrations fly ash slurry.

Chandel et al. (2010) studied the rheological and pressure drop characteristics in pipeline for the flow of fly and bottom ash mixture. The pilot test loop consists of 42 mm diameter

pipe and 50 m long. The mixture was taken in the ratio of 4:1 for fly and bottom ash. The concentration of ash slurry was kept high (50-70% by weight). They analysed the effect of velocity at different solid concentrations on pressure drop in pipeline. Predicted result shows close agreement with experimental results and also concluded that with the increase in velocity, the pressure drop increases for the specific solid concentration.

Chen et al. (2010) carried out an experimental study on wall slip flow behavior of coal water slurries with the help of pilot scale slurry transportation system. The pilot plant test loop was consisting of 25, 32, 40 and 50 mm diameter straight pipeline of 2200 mm length. A screw pump was used to pump the slurry by adjusting the speed of rotation. They observed that decrease the wall slip velocity with increase in solid concentration, temperature and particle size.

Vlasak et al. (2011) performed the experimental study for pressure drop and flow behaviour of sand slurry, stone dust slurry and sand-stone dust slurry. The mean particle diameters of sand were0.20 and 1.40 mm whereas for stone dust were 8 and 33μm. The experiments are performed on pipe loop with 1.75 and 26.8 mm inner diameters. The solid concentration for sand slurry ranges from 6-40%, for stone dust slurry 26-48% and 45-51% for stony dust-sand slurry. They found that coarser sand slurry gives higher pressure drop than finer sand slurry and the difference in their pressure drop decreases with the increase in velocity. The polydispersed sand slurries reach nearly the same value of hydraulic gradient as the finer sand slurry. The data analysis shows the non-Newtonian behavior of highly concentrated sand slurry.

Pavel and Zdenek (2011) performed an investigation on flow behavior of high concentration slurries influenced by particle size distribution and concentration. By the experimental investigation, flow behaviour and pressure drop of dense complex slurries which contain sand of different particle size, mean diameter ranging (0.20 to 1.40 mm) and inner diameter ranging (17.5 to 26.8 mm). The solid concentration of sand, sand-dust and stony dust-sand slurry lied in range 6-40%, 26-48% and 45-51% respectively. It was found that the sand slurry with coarser particles have high gradient than sand slurry with fine particles. They found that flow resistance of fine-grained stony dust slurry was reduced by adding coarse-grained material.

Senapati et al. (2013) investigated the friction mechanism and homogeneity between particle-fluid and particle-particle interactions of high concentration solid-liquid slurry. They have taken coal ash samples of fly ash and bottom ash mixtures in the ratio (5:1) with median diameter ranges of 9-52µm. They observed that the solid liquid mixture at concentration ranges of 62.5-67.5% by weight behaves as pseudo- plastic. The experimental test has been carried out on a pipe loop of 50mm diameter having slurry velocity range of 0.9-2.8 m/s and two sample were tested at three different concentration 62.5, 65 and 67.5% (by weight) having particle diameter of 19 and 26 µm. They found that Head loss in the pipeline for the flow of fly ash slurry decreses with addition of bottom ash.

Kaushal et al. (2013a) predicted the concentration distribution of highly concentrated solid-liquid slurry through pipeline. The kaushal and Tomita's (2002a) model found to be satisfactory for all particle sizes with concentration up to 26% and flow velocity up to 3.5m/s in pipeline of diameter 105mm. A modified model considering the effect of particle grading and particle sizes was proposed by the author. The modified model tested with experimental data of two particle sizes of 125mm and 440mm. They employed a Pilot loop test 22m long recalculated pipe of diameter ranges of (53.2mm- 495mm). The Modified model was found to be satisfactory for narrow and broad particles by comparing the experimental data with Kaushal et al. (2005), Gillies and shook (1994) and Matousek (2009).

Kumar et al. (2017) performed an investigation on pressure drop characteristics bottom ash slurry with and without addition of additive. They have taken Henko detergent and sodium sulfate as an additive. The additive added in bottom ash suspension by weightage of 0.2, 0.4 and 0.6%. The solid concentration of bottom ash suspension was kept in range of 10-60%. They found that the 0.4% addition of additive in slurry results in maximum pressure drop due in the pipeline.

Literature review indicates that majority of research done in past is focused on low or moderate concentration of solid particles. Pressure drop is the most important parameters to be ascertained while designing a hydraulic transportation system. Pressure drop is dependents on large number of parameters like particle size distribution, solid loading, mixing of different sized particles etc (Kumar et al. 2003; Kaushal et al. 2005;Chandel et

al. 2009; Senapati et al. 2013). In the absence of any universal correlation for pressure drop prediction, head loss is generally estimated by carrying out pilot plant studies and the data collected are then scaled up for prototype pipelines.

2.5 NUMERICAL SIMULATION OF PRESSURE DROP CHARACTERISTICS OF SOLID LIQUID FLOW IN SLURRY PIPELINE

From literature review of experimental pressure drop investigations, it is clear that a wide research work has been done in past on experimental prediction of pressure drop for the flow of solid-liquid slurry flow through pipeline. In the 21^{th} century, a great progress is observed in use of high performance computers for the prediction of flow behaviour by using CFD tools and software packages. In this context, a comprehensive literature review is carried out on numerical simulation study of pressure drop characteristics.

Chen et al. (2009) investigated flow characteristic of coal water slurry in straight pipeline using CFD. They used Eulerian multiphase approach with RNG k-ε turbulent model to evaluate the coal water slurry flow. They validated the numerical simulation model for the pressure drop data with previous studies available in literature. They investigated the effect of influx velocity and grain composition on pressure drop characteristics. They performed the experimentation on pilot plant test loop to evaluate the slurry flow characteristics inside different horizontal pipes. Results show that numerically simulated data hold good agreement with experimental data.

Eesa et al. (2009) studied the flow characteristics of coarser particles in pipe by using commercial computational fluid dynamics (CFD) code ANSYS CFX. They used an Eulerian-Eulerian approach to simulate the flow of coarser particles inside pipeline and positron emission technique to track the solid particles and particle motion. They analyzed the flow characteristics for the influence of solid concentration, particle size and mixture velocity. The concentration of particles was varying from 5 to 40% (by volume) having particle size of 2 to 9 mm (mean value). The velocity of mixture was taken as 25 to 125 mm s^{-1}. They found the asymmetric velocity profile of large sized particles which tends to increase with increase in particle size. It was also found that solid concentration of slurry increased as the pressure drop also increases.

Ekambara et al. (2009) investigated the flow behaviour of solid-liquid suspension in a pipeline by using commercial CFD code ANSYS CFX with 3D transient hydrodynamic model. The diameter of pipeline was taken as 50-500 mm. They studied the effect of velocity, solid concentration (by volume), particle size and pipe diameter on pressure loss, concentration and velocity profiles. The solid concentration of suspension was ranging from 8 to 45% (by volume) with particle size range of 90-500 μm at velocity range of 1.5-5.5 ms^{-1}. Result data show that the particle size distribution was found asymmetric in both experimental and numerical analysis and increases with increase in particle size.

Lahiri et al. (2010) performed an investigation on solid-liquid flow in pipeline by using commercial CFD package. They used Eulerian-Eulerian model with standard kε turbulence scheme to predict the influence of particle drag coefficient on concentration profile. Experiments were performed with water and glass beads slurry having particle size range from 125 to 440 μm and velocity range from 1-5 ms^{-1}. The solid concentration for the experimentation was taken as 10-50% (by volume). Numerically predicted and experimentally calculated pressure drop was found in good agreement. Results show that the asymmetry of concentration profile increases with increase in particle size and decreases with increase in velocity. It was also found that pressure drop increases with increase in concentration at a particular velocity.

Hossain et al. (2011) investigated the flow behaviour of solid particles in a straight horizontal pipeline of four bends. Numerical simulations were carried out with the help of commercial CFD code FLUENT 6.2. They solved the multiphase phenomenon for the flow of different solids with varying particle size diameters. Mixture model was used to solve the governing equations. Results show that particle deposition is a function of particle diameter and flow velocity. It is also observed that deposition occurs along the circumference of the pipe. High magnitude of solid concentration was observed at bottom of pipeline near the bend upstream and at 60^{o} from the bottom of pipeline for bend downstream.

Kaushal et al. (2012) performed a numerical simulation investigation for higher concentration solid-liquid flow through pipeline using computational fluid dynamics code FLUENT. They used the 3 m long horizontal pipeline of 54.9 mm diameter. Experiments were performed with glass beads having mean particle size of 125 μm and up to 5 m/s

flow velocity. The solid concentration was ranging from 0 to 50% (by volume). The pipeline mesh was discretized by using hexagonal cooper method. They used two different models namely Eulerian and mixture models to simulate the solid-liquid slurry flow for prediction of pressure drop and velocity distribution at different concentrations. They validated the numerical simulation models by comparing their model with the experimental data of Kaushal and Tomita (2007). Numerical simulation results show reasonable agreement with experimental results. They also found that the mixture model was failed to predict the accurate results of pressure drop due to existence of higher error at higher concentrations.

Mazumder et al. (2012) analyzed the effect of elbow radius on the pressure drop by using computational fluid dynamics (CFD). They performed the numerical simulation for the flow of air-water passing through four different 90 degree elbows. The elbow diameter was taken as 12.7 and 6.35 mm. The r/D ratio of elbow is varying from 1.5-3. The velocity of air was varying from 45.72 to 15.24 ms^{-1} whereas 0.1-10 ms^{-1} for water. The pipeline mesh was discretized by using hexahedral method. They predicted the results in terms of pressure drop with Empirical models such as Chisholm model and Azzi-Friedel model. Numerical model showed close results with both empirical model and experimental data.

Bandyopadhyay et al. (2013) analyzed the flow behavior inside pipe elbow by using computational fluid dynamics (CFD) code FLUENT. They employed Elurian-Elurian approach to simulate the flow inside pipeline. Results show that magnitude of pressure was found largest at extrados wall and least at center of pipe curvature. Pressure drop was found higher in 135^{o} elbow as compare to 45^{o} elbow. Cimzmadia et al. (2013) predicted the friction factor in straight pipe line for Bingham plastic fluid and the power law fluid using experiment and simulation. The solution contains 0.13, 0.05 and 99.82% of carbopol 971, NaOH and water respectively. The experimental setup consists of pipe diameter 20mm and length of pipe 298 mm long. Computational fluid dynamics approach has been used to validate the experimental data. CFD code ICEM has been used to develop the geometry which consists of 32000 elements and length of pipe was 10m. SST Turbulence model was used to simulate the flow. They analyzed the Headstrom number for Bingham fluid at different viscosity and keeping the other parameter constant like pipe diameter, density and yield stress. They observed that as there is increment in the yield stress in the Bingham plastic fluid the laminar segment shifter towards right with increase in

Headstrom number in the moody chart i.e. as the friction factor increases the laminar-transition appear at higher Reynolds number.

Kaushal et al. (2013b) numerically simulated the slurry flow in pipe bend. They used Eulerian multiphase approach to evaluate the silica-sand slurry flow. The pipeline mesh was discretized by using hexagonal cooper type non-uniform method. They employed the finite difference techniques to solve the volumetric governing equations. The diameter of pipe bend was taken as 53 mm with 148.4 mm radius of curvature for experimentation and simulation. The particles of silica sand have the median particle size of 450 μm. The geometric standard deviation σ_g for the particle used in the present study is found as 1.15. Simulation was done with various concentrations ranging from 0-16% (by volume) with velocity ranges from 1.7-3.6 ms^{-1}. They found that the value of bend loss coefficient retards with increase in flow velocity whereas increases with decrease in efflux concentration. They also observed that volume fraction distribution is more uniform at higher velocities.

Nabil et al. (2013) performed a numerical simulation study of solid-liquid slurry flow in a pipeline. They used CFD code FLUENT to simulate the slurry flow by employing Eulerian-Eulerian scheme and k-ε model. They used square pipeline of dimension 26.8×26.8 mm. The pipeline mesh was discretized by using tetrahedral method. They used different particle size diameter (0.2, 0.7 and 1.4 mm) of water-sand slurry with solid concentration ranges of 5-30% (by volume) flowing at different velocities ranges 0.5–5 m/s. They discretized the governing equations by utilizing first order upwind approach to solve the turbulent kinetic energy, momentum equation, volume fraction, and turbulent dissipation rate. Numerical simulated results were very close to the experimental data for medium and coarse slurry flow at low concentration (5-10%) and fails for the flow of coarser slurry at higher concentration.

Gopaliya and Kushal (2014) studied the effect of particle size of solid on solid-liquid flow in horizontal pipe using Computational fluid dynamics code GAMBIT and FLUENT 6.3. They have taken the mixture of water and sand as a solid material. The mixture solid concentration varied from 15-45% with four grain sizes (0.18mm, 0.29mm, 0.55mm, and 2.4mm) and velocity ranges of 1.8-3.1 m/s. The geometry consist of pipe diameter 53.2mm with 2.7m long horizontal pipe was created in GAMBIT to simulate the slurry

flow. There are 357120 hexahedral volume mesh cell generated. They have adopted a pipe wall roughness of 0.2mm and convergence criterion 10^{-3}. Pressure drop calculated over the last one meter of pipeline. The pressure drop increases with in concentration and velocity of all grain sizes. The particle velocity found to higher at the central core of the pipe region.

Wu et al. (2015) studied the pressure drop characteristics of solid-liquid flow in pipe line using computational fluid dynamics code COMSOL Multiphysics. They have taken coal mixture of coal gangue, cement, fly ash as a solid material. The mixture solid concentration varied from 78-79.5% concentration (by weight) at different flow rate (60, 70, 80 and 90 m^3/h). They employed a test loop pipeline system of 120 mm diameter with 35 m total length to investigate the flow behaviour of slurry in pipline. They observed that the fluid solid-liquid mixture behaves as a Bingham Fluid at high solid concentration. CFD Model was carried out to compare the outcomes of simulated results with loop test. They observed that the total pressure drop and partial pressure drop increase with increasing the slurry flow rate leads to increase the Darcy friction factor (fD) and the frictional resistance loss. At a given volumetric flow, pressure drop decreases with increases in inner diameter of pipe. The obtained results have shown a good agreement between model simulation and the loop test.

Rawat et al. (2016) carried out a numerical simulation of finer coal ash slurry at higher concentration using CFD code FLUENT. They used SST (Shear Stress Transport) k-ω model to solve the pressure drop of coal ash slurry inside pipeline. They validated the numerical simulation model by comparing the experimental data. Rheological data showed the non-Newtonian behaviour of slurry at higher concentrations. They found that pressure drop is a function of flow velocity. The pressure drop decrease in pipeline with increase in velocity.

Literature review reveals that commercial CFD tools are successful in prediction of pressure drop characteristics for the design of slurry transportation pipeline. Based on the literature review, it can be clearly seen that the performance of a slurry pipeline has been predicted using numerical techniques and limited studies have been carried out on pressure drop characteristics of slurry pipeline for the complex flow of coal-water slurry.

2.6 GAP IN KNOWLEDGE

Based on literature review, following gaps in present research on the flow characteristics of the solid - liquid slurry suspension in the pipeline are observed.

- The physical and chemical properties of coal changes widely throughout the world. The properties of the coal used in different industries as well as same type of industry located at different place will also vary. Since the properties of coal are changing, the rheological behavior of coal slurry will also change which have a great impact on transport of slurry in a pipe. So it is necessary to know the rheological behavior of slurry prepared from all different types of coals used in various industries. From the literature review it was found that a very limited number of studies have been done on the rheological behavior of slurry prepared from various type coals available in India.
- The slurry transportation also occurs through various transitions of pipes such as sudden expansion, bends etc. in a pipeline. The pressure drop characteristics also changes when the different geometrical parameter of pipe line changes.
- From the literature review it was found that very few investigations has been carried out to study the effect of different geometrical parameters on pressure drop characteristics in the slurry transportation system in pipeline.

CHAPTER 3
PHYSICAL CHEMICAL AND MINERALOGICAL CHARACTERISTICS OF COAL AND COAL ASH

3.1 INTRODUCTION

The coal-water slurry suspensions with high solid concentration have a comprehensive application in energy production. The thermal power plants utilize the pulverized coal produced by ball mills that converts the larger size of coal particles into a micron range of size. During the coal cleaning process, highly concentrated suspension of coal-water slurries are produced and transported to power plants for its utilization. The proper utilization of coal-water slurry in engineering applications is only possible after the investigation of its properties. The behaviour of coal-water slurry is non-Newtonian in nature at higher solid concentrations and its characterization is determined through various bench scale tests like particle size distribution, proximate and ultimate analysis, pH, specific gravity and static settled concentration.

The thermal power plant produces fly and bottom ash as coal combustion by-products which are disposed to ash pond. The efficient and economical transportation of coal ash in the thermal power plant is a major challenge. The particle size, shape, specific gravity, static settled concentration, pH value and morphology of coal ash play a major role to determine the flow characteristics of coal ash slurry in pipeline.

The literature presented in previous chapter also reveals that slurry flow behaviour depends upon the various parameters like particle size distribution, static settled concentration, specific gravity, pH value. The physical, chemical and mineralogical characteristics study is necessary to establish the flow characteristics of the coal and coal ash slurry in pipeline and its design. So the various bench scale tests are performed to determine physiochemical characteristics of the coal. Also various materials characterizations tests of the coal are performed and presented along with their results in this chapter.

3.2 BENCH SCALE TESTS

The materials selected for the study of physical, chemical and mineralogical properties are coal and coal ash. The coal samples are collected directly from the coal mines of Makum coal field of Dibrugarh district of Assam. The coal samples are prepared by crushing with laboratory-size ball mill to the different fractional sizes required for experiments. The Makum field coal is also used for power generation in Guru Nanak Dev thermal power plant, Bathinda, Punjab, India. The fly ash and bottom ash produced during the power generation are collected from Guru Nanak Dev thermal power plant for the present study. The fly and bottom ash are collected directly from electrostatic precipitators (ESPs) and hoppers respectively installed at thermal power plant.

The various bench scale tests like particle size distribution, static settled concentration, specific gravity and potential of hydrogen value are performed to study the physiochemical properties. The morphology of coal and coal ash samples is determined by scanning electron microscopy **(**SEM).

3.2.1 Particle size distribution (PSD)

The particle size distribution represents the percentage of particles present in a particular particle size range. The particle size distribution affects the static settling and viscosity of the slurry which contributes in variation of pressure drop during slurry transportation through pipeline. In the present study, particle size distribution of coal and coal ash samples is determined by sieve analysis method.

The coal and coal ash sample with known weight of solids are taken and dried properly in an oven. The dried sample is sieved through a set of British standard sieves (1700, 1000, 710, 500, 355, 250, 150, 106, 75 and 53 μm). The percentage of coal and coal ash retained on each particular sieve is collected and the weight of retained coal and coal ash samples are measured. The retained percentage for every sieve is calculated by using equation 3.1.

$$\text{Retained Sample} = \frac{W_R}{W_T} \times 100 \tag{3.1}$$

Where, W_R = Weight of solid particle retained (grams) and W_T = Total weight of solid particles (grams).

The sieve analysis data for coal and coal ash samples are plotted between particle size and percentage finer to understand the particle size gradation present in the sample. The weighted mean diameter of different coal and coal ash samples is calculated using the equation 3.2.

$$d_{wm} = \frac{\sum W_R X_i}{\sum W_i} \tag{3.2}$$

Where, W_R is the weight retained on sieve (grams) and X_i is the mean diameter of the two successive sizes of sieves.

The collected coal sample from the Makum coal field is first crushed with the help of jaw crusher to particle size below 5cm and these crushed particles are further processed with the help of ball mill to obtain finer particle size less than 500 µm. The pulverized coal sample is dried in electric oven to remove moisture from the coal. The coal sample is passed through the British Standard sieves. The particle size distribution of coal sample is shown in Figure 3.1 and tabulated in Table 3.1. About 38.39% particles are finer than 75 µm in which 34.21% particles lies in range of 53-75 µm particle size. About 20.36% particles are coarser than 150 µm in which 14.92% particle lies in range of 106-150 µm and only 6.21% particle lies in range of 150-250 µm.

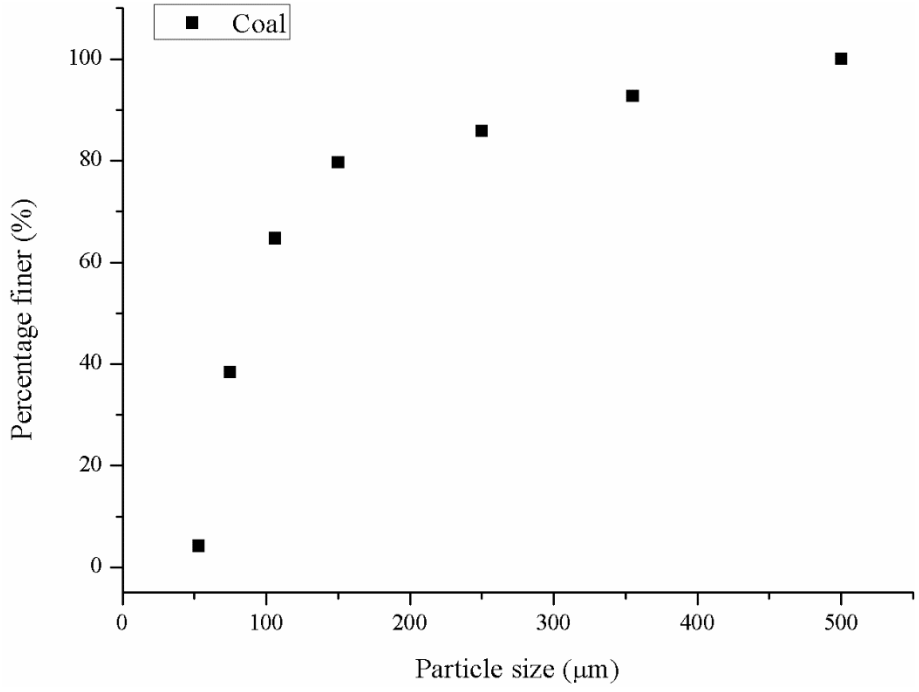

Figure 3.1: Particle size distribution of coal sample

Table 3.1: Particle size distribution of coal

Particle size (μm)	1700	1000	710	500	355	250	150	106	75	53
Coal (% Finer)	-	-	-	100	92.68	85.85	79.64	64.72	38.39	4.18

Similarly, particle size distribution analysis is performed for fly and bottom ash. The particle size distribution of both coal ash samples- fly and bottom ash are shown in Figure 3.2-3.3 and tabulated in Table 3.2. The largest particle sizes of fly and bottom ash are determined as 355 and 1000 μm respectively. In bottom ash, more than 73.50% particles are coarser than 150 μm and only 15.40% particles are finer than 75 μm whereas in the fly ash 73% particles are finer than 75 μm. It also shows that the fly ash is finer than the bottom ash. The weighted mean diameters of coal, fly and bottom ash is determined by using equation 3.2 and calculated as 130.31, 59.76 and 203.99 μm respectively.

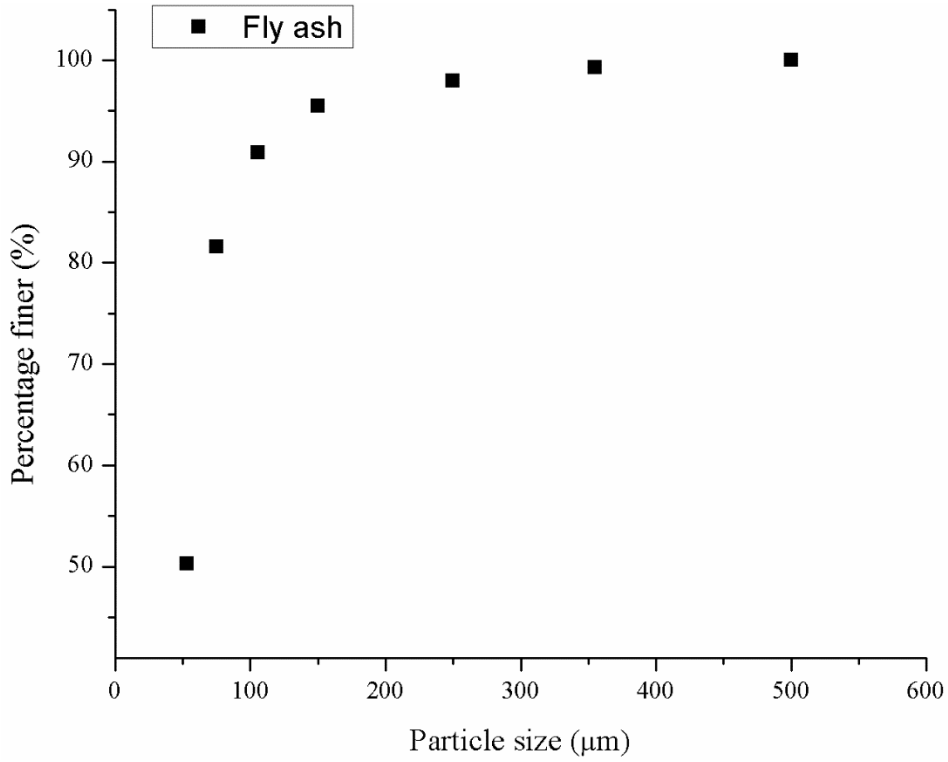

Figure 3.2: Particle size distribution of fly ash sample

Table 3.2: Particle size distribution of fly and bottom ash

Particle size (μm)	1700	1000	710	500	355	250	150	106	75	53
Bottom ash (% Finer)	100	96.80	95.04	91.54	89.04	80.64	73.50	36.00	15.40	6.16
Fly ash (% Finer)	-	-	-	100	99.26	97.96	95.46	90.83	81.59	50.25

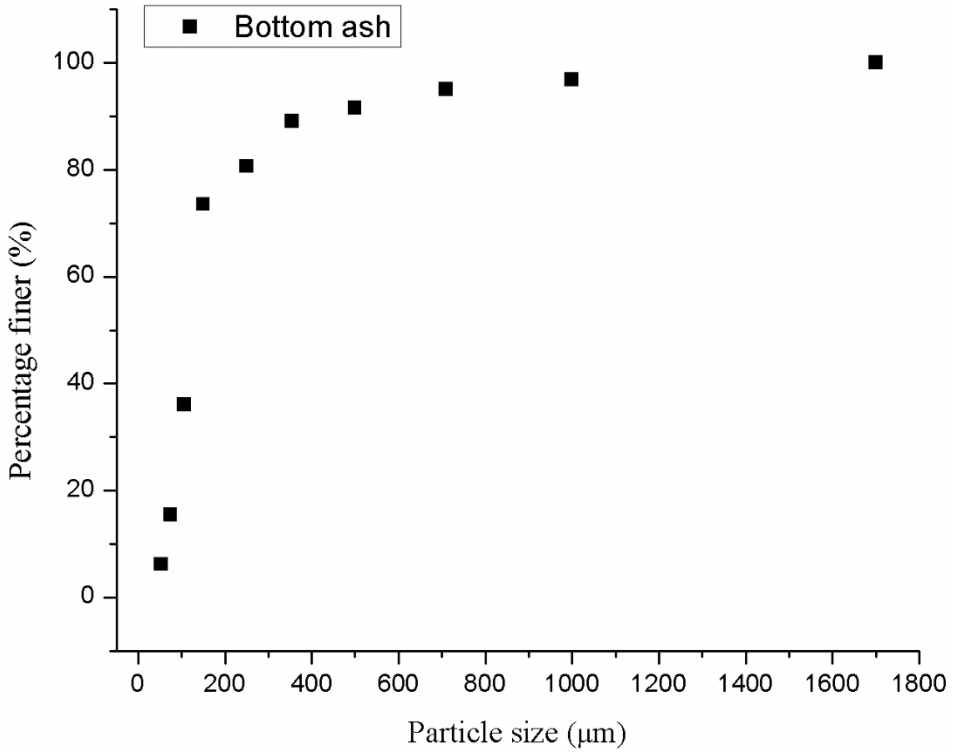

Figure 3.3: Particle size distribution of bottom ash sample

3.2.2 Static settled concentration

Static settled concentration is an important parameter for the transportation of slurry through pipeline. During the slurry transportation, specific energy consumption increases as the solid concentration of slurry suspension approaches maximum static-settled concentration. The maximum value of static settled solid concentration for coal, fly and bottom ash samples is determined by the gravitational method and its value depends on the various parameters like particle size distribution, particle shape, specific gravity and viscosity of slurry suspension etc. The static settled concentration of coal, fly and bottom ash slurry suspension is measured for initial solid concentration ranges 30-50% (by weight). It is carried out by using 500 ml graduated glass cylinder of 50 mm diameter as

per prescribed standards. The slurry is prepared at a specific initial mixture solid concentration and allowed to settle down in a graduated cylinder. Thus, interface reading are taken for various intervals till no further settlement of solid particles occurs. This analysis is performed till the solid particles cease to settle and the maximum settled concentration is measured. Equation 3.3 is used to determine the maximum settled concentrations at different solid concentrations.

$$C_{w\,max} = \frac{W_s}{(W_w + W_s)} \tag{3.3}$$

Where $C_{w\,max}$ = Static settled concentration (%), W_s = weight of solids in the settled mass (grams) and W_w = weight of water present in the settled mass (grams).

The experiments are carried out for coal particle size ranges varying as 53-75, 106-150 and 150-250 μm. The static-settled concentration for different particle size ranges of coal are tabulated in Table 3.3.The maximum value of static-settled concentration of coal particle size ranges from 53-75, 106-150 and 150-250 μm is found as 65.81, 64.22 and 63.21% respectively with initial solid concentration of 30% (by weight). Similar type of trend is observed with 40 and 50% initial solid concentrations (by weight). It is also observed that finer particles shows maximum static settled concentration as compared to the coarser particles. Settling is almost negligible after 10 hours for 53–75 μm coal whereas after 5 hours for 150–250 μm coal. The settlement is completely ceased after 16 hours for all the solid concentrations of coal-water slurries.

Similar experiments are also carried out for both fly and bottom ash. The value of static settled concentration is measured with time variation which is summarized in Table 3.4.The maximum static settled concentration of fly and bottom ash slurries are found as 60.12 and 54.35% with initial solid concentration of 30% (by weight). With 40 and 50% initial solid concentration, the value of maximum static settled concentration of fly ash is measured as 62.91 and 64.41% whereas for bottom ash is found as 56.79 and 58.75% respectively. The coarser irregular shape of bottom ash particles leads to lower static settled concentration whereas the fine spherical shape of fly ash particles leads to higher static settled concentration (Biswas et al. 2000, Kumar et al. 2016). In present study, the settlement is completely ceased after 8 hours for all the solid concentrations in fly and bottom ash.

Table 3.3: Maximum static-settled concentration for different sizes of coal particles at various concentrations

Time (min)	Initial concentration of suspension (Cw)								
	30%			**40%**			**50%**		
	Particle size (μm)								
	53-75	**106-150**	**150-255**	**53-75**	**106-150**	**150-255**	**53- 75**	**106-150**	**150-255**
0	30.03	29.91	30.03	40.03	40.03	39.98	50.05	50.05	50.07
1	30.26	30.25	30.14	40.85	40.61	40.39	50.48	50.33	50.41
2	30.96	30.72	30.61	41.09	40.97	40.95	50.77	50.63	50.58
3	31.82	31.57	31.32	41.82	41.71	41.66	51.52	51.37	51.27
4	32.87	32.33	32.07	42.46	42.59	42.39	52.29	52.14	51.98
5	33.69	33.14	32.86	43.11	42.85	42.69	52.93	52.76	52.71
10	34.87	34.42	34.12	44.48	44.48	44.11	53.56	53.74	53.65
20	36.79	36.13	35.81	45.64	45.65	45.12	54.57	54.24	54.43
30	38.93	38.19	37.65	50.05	49.87	48.97	58.21	58.01	57.35
60	57.33	56.12	55.35	60.68	60.15	59.68	64.42	64.18	63.95
120	60.81	60.35	59.91	62.31	62.58	61.84	66.12	65.87	65.06
180	61.75	61.28	60.81	63.43	63.14	62.81	67.41	67.41	66.81
240	63.21	63.21	62.22	64.61	64.61	64.51	68.18	67.66	67.42
360	63.86	63.59	62.60	66.24	65.36	64.30	69.10	68.31	67.82
480	64.23	63.72	62.71	66.76	65.82	64.85	69.54	68.72	68.01
720	65.05	64.11	63.06	66.94	66.02	65.00	69.86	68.90	68.34
960	65.81	64.22	63.21	67.00	66.13	65.11	70.00	69.00	68.42

Table 3.4: Maximum static-settled concentration for fly and bottom ash at various concentrations

Time (min)	Initial concentration of suspension (C_w)					
	30%		40%		50%	
	Fly ash	Bottom ash	Fly ash	Bottom ash	Fly ash	Bottom ash
0	30.31	30.18	40.16	40.06	50.33	50.16
1	30.66	30.42	40.75	40.41	50.77	50.31
2	31.02	30.53	41.47	40.75	51.21	50.59
3	32.01	30.89	42.87	41.36	51.97	51.34
4	33.21	31.62	44.08	42.48	52.92	51.64
5	34.34	32.13	45.08	43.55	53.56	52.26
10	36.37	33.61	47.05	44.81	54.22	53.05
20	39.41	35.39	48.35	45.97	55.61	54.03
30	43.48	37.19	50.81	47.22	57.24	55.75
60	51.27	47.03	58.44	52.54	60.83	56.66
120	56.72	52.24	60.98	55.01	62.56	57.21
180	58.37	53.28	61.52	55.66	63.24	57.78
240	59.67	53.64	62.34	56.34	63.94	58.36
360	59.99	54.18	62.78	56.69	64.29	58.62
480	60.12	54.35	62.91	56.79	64.41	58.75

3.2.3 Specific gravity

Specific gravity is the ratio of slurry density with respect to density of water as a standard reference. The specific gravity of solid materials is a significant parameter which decides the settled concentration of the solid-liquid suspension.

The specific gravity of coal and coal ash is determined by using standard pycnometer method. Initially, a 50 ml beaker is taken and dried in oven for 1 hour preceded by cleaning with clear tap water. The weight of beaker (W_b) is measured after taking it out from oven. Beaker is filled with 30 grams of oven dried sample and weight of beaker with sample (W_{bs}) is measured using weighing machine. The distilled water is poured in beaker and stir for 5 minutes to ensure the proper mixing. The weight of beaker along with slurry sample (W_{bsw}) is weighted again after 1 hour. The sample is removed from the beaker and properly cleaned with tissue paper. The weight of beaker (W_{bw}) is measured again after filling it with distilled water up to same level. The correlation represented in equation 3.4 is used to calculate the specific gravity of coal and coal ash samples.

$$\text{Specific gravity} = \frac{(W_{bs}-W_b)}{\{(W_{bw}-W_{bsw}) + (W_{bs}-W_b)\}} \quad (3.4)$$

Where, W_b = Weight of beaker (grams), W_{bs} = Weight of beaker and solid(grams), W_{bw} = Weight of beaker and water (grams) and W_{bsw} = Weight of beaker, solid and water (grams)

The value of specific gravity for coal, fly ash and bottom ash are determined from the experiment as 1.45, 2.28 and 2.05 respectively.

3.2.4 Proximate and ultimate analysis

Proximate analysis helps to predict the behaviour of coal while handled and burned during energy generation. In present study, proximate analysis of coal sample is performed according to IS: 1350. The moisture content, ash content, volatile matter and fixed carbon in the coal sample is determined. The weight loss gives the free moisture present in the coal sample. Pulverized coal sample of 1 gram is taken in porcelain silica crucible. The crucible filled with coal is weighted with a high precision electronic weighing machine. After weighing, the crucible is placed inside oven. The sample is taken out at regular intervals and cooled upto room temperature and weighed until there is no change in weight of sample observed. The moisture content is calculated by using equation 3.5.

Inherent moisture content (%) = $\frac{(B-C)}{(B-A)} * 100$ (3.5)

Where, *A* is the weight of empty capsule/crucible (grams), *B* is the weight of sample & crucible before drying (grams) and *C* is the weight of sample & crucible after drying (grams).

For volatile matter, dried coal sample in crucible is placed in muffle furnace maintained at 950 ± 20 ºC for the escape of volatile material. The coal sample is heated for 10 minutes and taken out from the furnace and bring down to room temperature using cold iron plate. The final weight of crucible with contents is taken using weighing machine and volatile matter is calculated by using equation 3.6.

Volatile matter (%) = $\left[\frac{(B-C)}{(B-A)} * 100 - (moisture\ percentage)\right]$ (3.6)

For ash content, coal sample is again placed in muffle furnace and temperature is raised up to 700 ºC. The residue is moistened with a drop of alcohol. The ignition is continued for 15 minutes until the black particles disappear. Equation 3.7 is used to calculate the ash content in sample.

Ash content (%) = $\left[\frac{(\mathrm{D}-\mathrm{A})}{(\mathrm{B}-\mathrm{A})} * 100\right]$ (3.7)

In above equation, *D* represents the weight of capsule and residue after ignition (grams).
The non-volatile fixed carbon is the residue remained after expelling the volatile matter from coal sample. The fixed carbon of coal sample is thus calculated by using equation 3.8.

Fixed carbon (%) = 100 – [Moisture (%) + Ash (%) + Volatile matter (%)] (3.8)

The ultimate analysis is carried out to determine the amount of the principal chemical elements present in coal. Table 3.5 shows the results of proximate and ultimate analysis of coal sample.

Table 3.5: Proximate and ultimate analysis of coal sample

Proximate analysis		Ultimate analysis	
Parameters	Weight (%)	Elements	Weight (%)
Moisture content	3.52	C	44.375
Ash content	38.30	H	3.028
Volatile matter	16.60	N	1.05
Fixed Carbon	41.58	S	0.391
Mineral matter	42.13	O	51.16

3.2.5 Potential of hydrogen (pH)

The pH value of coal, fly and bottom ash samples at given solid concentration are determined by using digital pH meter. The pH meter electrode is moistened with distilled water. The calibration of pH meter is initially done by sinking electrode into the buffer solutions to ensure correct readings. Then, electrodes are cleaned with distilled water. The pH value is measured at solid concentrations of 30-60% (by weight) by the immersion of electrodes in the slurry suspension of samples. In present study, pH value of coal-water slurry is determined to examine their effect of loading of coal samples.

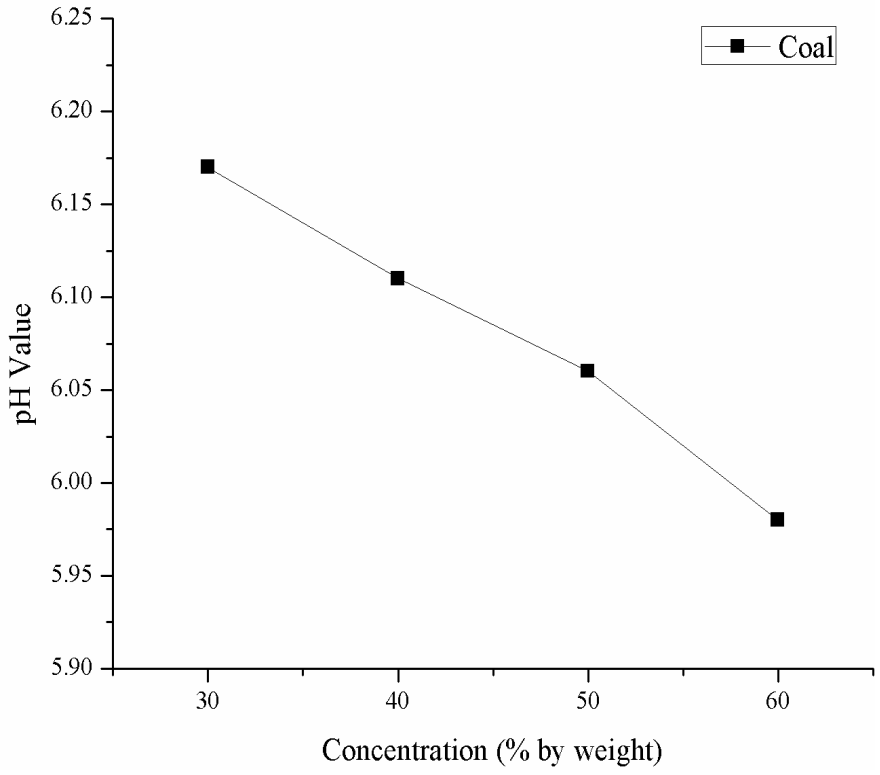

Figure 3.4: pH value of coal sample

The pH values of coal ash slurry at different solid concentrations lies in range 30-60% (by weight) are represented in Figure 3.4 and summarized in Table 3.6. The pH value of coal-water slurry sample for solid concentrations ranging from 30-60% lies in between 5.98-6.17. From the results it is concluded that solid concentration of coal has very little effect on pH value.

Table 3.6: pH values of coal at different solid concentrations

Solid concentration (by weight)	30%	40%	50%	60%
pH value	6.17	6.11	6.06	5.98

Fig 3.5 shows the variation of pH value of fly and bottom ash slurry sample with different solid concentrations ranging from 30-60%. The pH values of fly and bottom ash slurry are measured with variation of the solid concentration (by weight) in range 30-60% is Figure 3.5 and summarized in Table 3.7. The pH value of fly and bottom ash varies with the solid concentration in the range of 7.52-7.38 and 7.54–7.43 respectively. The non-reactive nature is depicted from the pH values of both samples. It can be concluded that the fly and bottom ash slurries solid concentration has negligible effect on pH value.

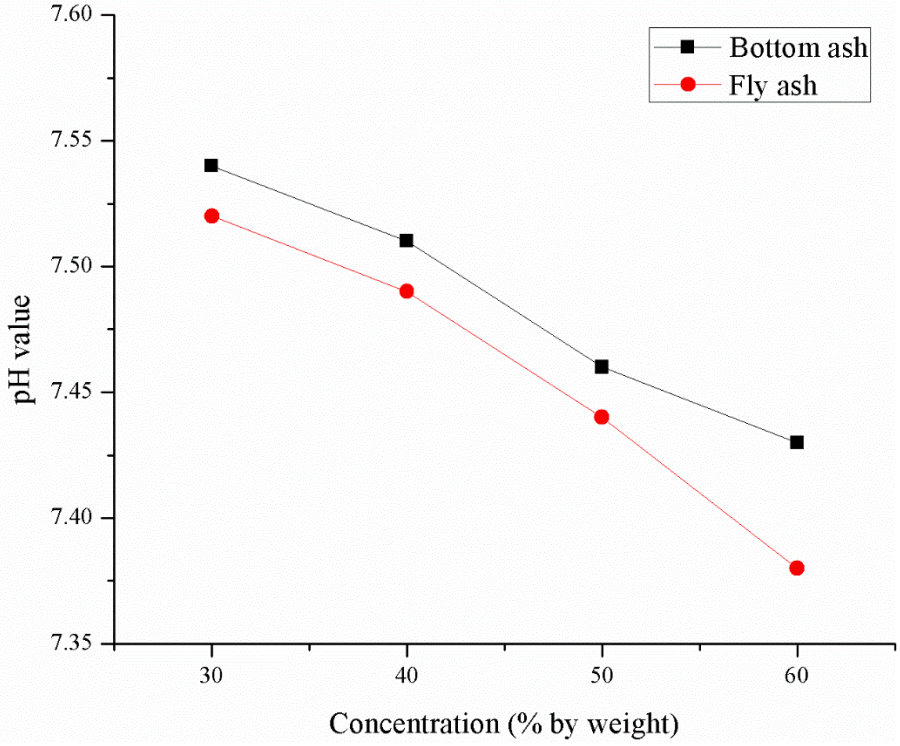

Figure 3.5: pH value of fly and bottom ash sample

Table 3.7: pH values of fly and bottom ash at different solid concentrations

Solid concentration (by weight)	30%	40%	50%	60%
pH value of fly ash	7.52	7.49	7.44	7.38
pH value of bottom ash	7.54	7.51	7.46	7.43

3.3 MINERALOGICAL CHARACTERISTICS

The mineralogical characteristics provide information about the structure, size and chemical composition of coal and coal ash samples which can be determined by scanning electron microscopy-energy dispersive X-ray spectroscope. Both morphology and chemical composition of sample are determined. The morphology defines the particle shape and size which provide the information for its end utilization. The chemical composition provides the information about different compounds present.

3.3.1 Scanning electron microscopy (SEM)

The scanning electron microscopy (SEM) technique provides the helpful information like particle size and structure through the high-resolution images. It is a type of electron microscope which gives the information of specimen by producing very high-resolution images of a sample surface up to the nanometer scale and produces image by scanning with help of electron beam. The high-energy electrons interact with the atoms of sample producing signals and provide information about surface topography and its composition. The SEM micrograph provides the 3-D appearance which is very beneficial for understanding about the surface structure. The morphology of coal, fly and bottom ash samples are analyzed by using JEOL, 6510LV model of scanning electron microscopy-energy dispersive X-ray spectroscope. The electrons interact with sample and generate various different signals that can be sensed and provides the surface topography.

The chemical composition gives information about the presence of different elements and their compounds in the sample. The chemical composition is determined with the help of energy dispersive X-ray spectroscope. This works on the basic principal of spectroscopy that there is unique atomic structure for every element and permitting a unique set of peaks on its electromagnetic emission spectrum. This method allows interaction between source of X-rays excitation and testing sample. High-energy X-rays beam strikes at the sample to

stimulate the X-rays emission from a specimen. The energy-dispersive spectrometer measures the different number and level of energy produced by striking of X-rays on the surface of sample. These differences in energies of X-rays measure the specimen elemental composition. The coinciding (overlapping) peaks on spectrum may decrease the accuracy of EDS spectrum and it also affected by the nature of sample.

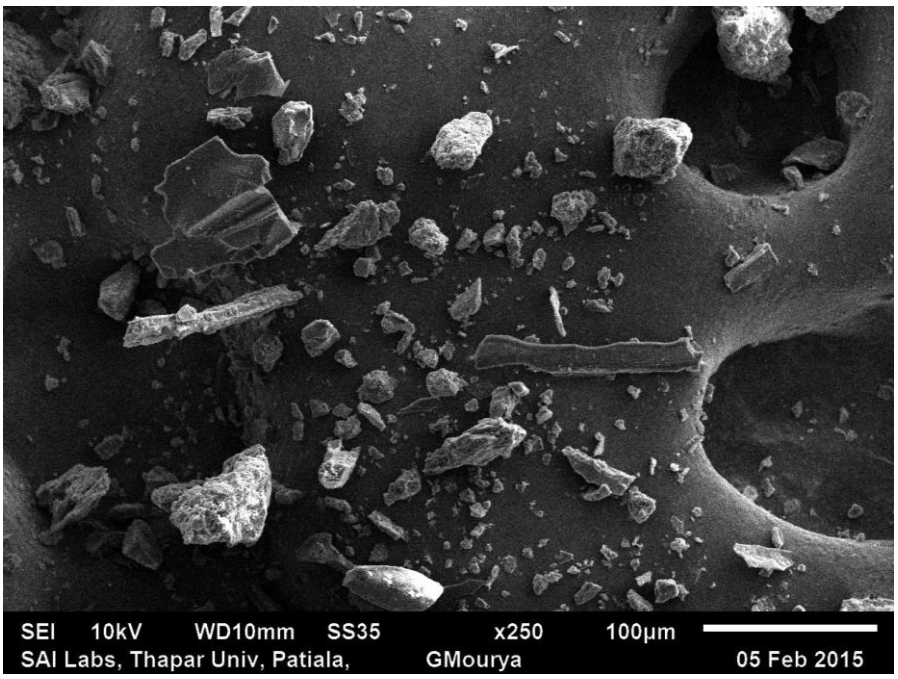

Figure 3.6: SEM image of coal sample

Figure 3.6 shows the SEM image of the coal sample at X250 magnification in which the irregular shape of coal particles is observed from the surface morphology. It is also found that the coal sample is amorphous in nature. This image analysis of SEM image is useful to estimate the porosity of coal. The detailed compositions of the elements are tabulated in Table 3.8. The elements carbon (C) and oxygen (O) are present in major proportion whereas aluminium (Al) and silicon (Si) are present in minor proportion. The elements such as C, Al & Si are present in the form of their oxide because of abundance presence of oxygen. The carbon-dioxide (CO_2) compound shows its maximum presence i.e. 99.03% whereas aluminium oxide (Al_2O_3) and silicon oxide (SiO_2) are present in minor proportions 0.46 and 0.56% respectively.

Table 3.8: EDX of coal sample

Elements	Carbon	Aluminium	Silicon	Oxygen
% (by weight)	27.03	0.24	0.24	72.49

The scanning electron micrographs (SEM) of fly and bottom ash at X500 magnification are represented in Figure 3.7-3.8. It is perceived that fly ash particles have smooth surfaces and a spherical morphology along with cenospheres (hollowspheres) and the particles are habitually found as agglomerates. The bottom ash particles are comparatively porous, coarser, and highly irregular in shape than the fly ash particles and which may be causing more drag for particle flow in slurry pipelines.

The chemical composition of both fly and bottom ash samples shows that in both the coal ash samples, the proportion of aluminium and silica oxides is higher in comparison to other elements including titanium, magnesium, iron and calcium. The compound compositions of both coal ash samples are tabulated in Table 3.9. The percentages of silica and aluminium oxides in fly and bottom ash samples are 32.85 & 45.27% and 51.21 & 37.46% respectively.

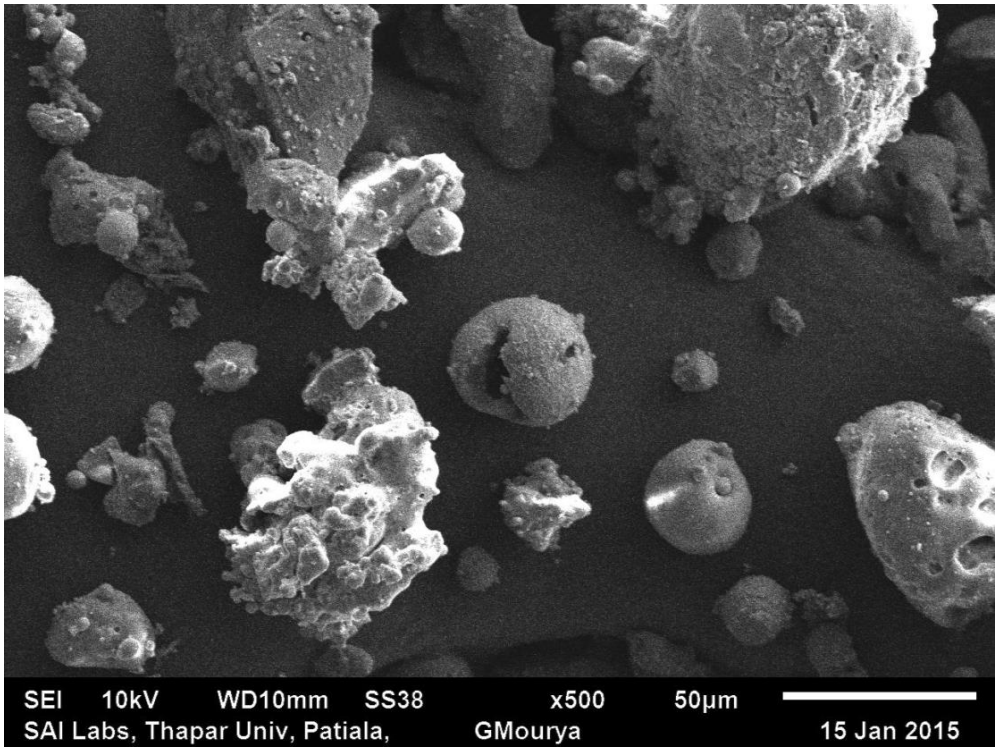

Figure 3.7: SEM image of fly ash sample

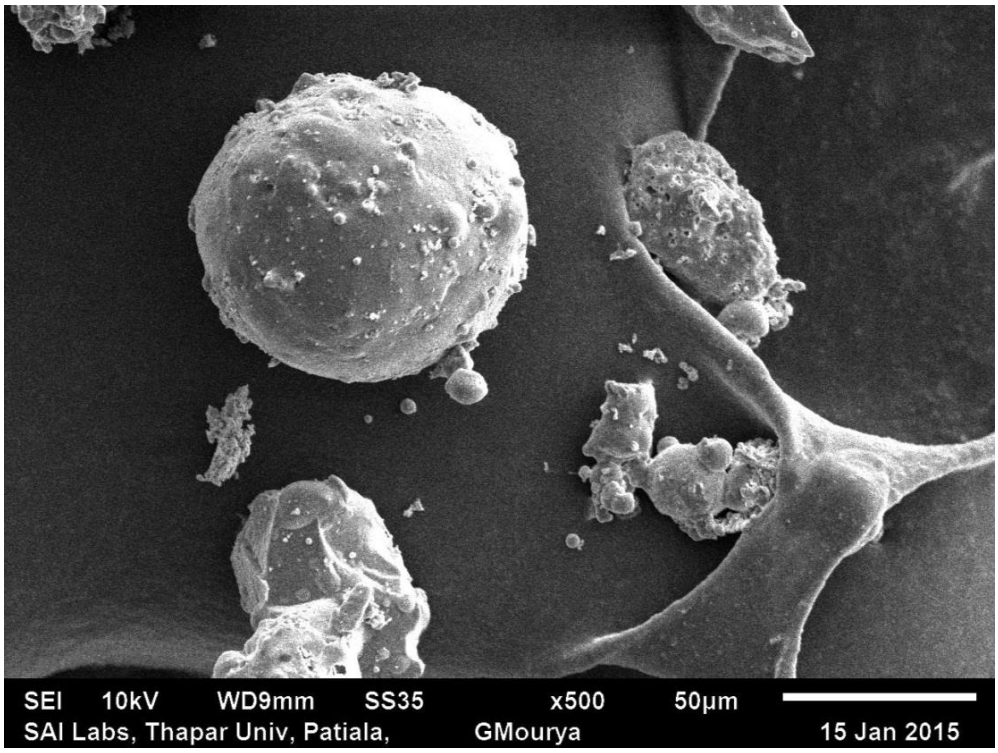

Figure 3.8: SEM image of bottom ash sample

Table 3.9: EDX of fly and bottom ash sample

Elemental Compounds	CO_2	MgO	Al_2O_3	SiO_2	CaO	FeO	TiO_2
Fly ash (% by weight)	15.34	-	32.85	45.27	1.72	2.97	1.85
Bottom ash (% by weight)	4.21	1.32	37.46	51.21	1.37	2.17	2.26

It is concluded that these particles have a high surface enrichment in Al/Si which indicates that these particles have a drag affect during the flow which is also the similar observation presented by (Kumar et al., 2013). The reasonable proportion of alumina and silica makes fly and bottom ash to be utilized as a raw material for synthetic alumino-silicate aggregates for refractory and ceramic applications (Tripathy and Mukherjee, 1997). The abundance presence of silica leads to increase in strength and CaO presence provides cementing properties during stowing. The unburned carbon is also present in very negligible amount. Hence, fly and bottom ash can also be utilized in coal mines as a stowing material (Nayak et al., 1999).

3.4 LEACHING CHARACTERISTICS

The transported ash slurry is generally disposed directly either in surface water or in the land. The tracing elements present in ash slurry infiltered through the soil and mix with ground water over a period of time. The production of the large amount of the toxic metal elements in ash disposal system of the thermal power plants can pose negative environmental effects on human health and on plants (Tripathy and Mukherjee 1997;Ugurlu 2004; Baba et al. 2010 and Blissett and Rowson 2012). So the present study conducted the leaching test of heavy metals from fly ash and bottom ash slurry in order to predict the environmental effect from the ash disposal system.

The leaching characteristics of the fly ash and bottom ash samples are determined using the toxicity characteristic leaching procedure (TCLP) method. The collected sample is dried at 120°C for 12 h duration and then cooled. Extraction fluid is prepared by diluting 5.7 ml glacial acetic acid with distilled water to a volume of 1liter. The pH value of the solution is maintained as 2.88 ± 0.05. The Remi orbital shaking lubricator (Model: RS 12 plus) is used for shaking of the solution. The mixture shaking operation is performed with the period of 24 h at 40 rpm in the temperature environment of 30°C. At the end of the leaching experiment, liquid is filtered through a 0.45-μm micropore membrane filter. The leaching experimentation is repeated with the variation of the L/S (liquid to solid) ratio of 40:1, 60:1, and 80:1. The final extracts are stored in a refrigerator at the temperature of 4°C until the tracing element determination. All the tracing elements are analyzed using atomic absorption spectrophotometer (AAS 4129, make- ECIL, India) following the standard methods (APHA, 1995).

The results of leaching tests for the bottom and fly ash sample are presented in Figures 3.9-3.10. The tracing elements like manganese (Mn), magnesium (Mg), chromium (Cr), zinc (Zn), copper (Cu), nickel (Ni), lead (Pb), iron (Fe), cobalt (Co), mercury (Hg), and molybdenum (Mo) are determined by the TCLP method. The L/S ratio is taken to be 20:1, 40:1, 60:1, and 80:1. The leaching test data of the bottom ash are shown in Figure 3.9. From Figure 3.9, it is observed that the leachate concentration of the tracing element increases with increase in the L/S ratio. The tracing element concentration of Mn, Mg, Cr, Zn, Cu, Ni, Pb, Fe, Co, Hg, and Mo increases from 112 to 135, 70 to 82, 55 to 63, 36 to

40, 33 to 36, 20 to 25, 7.50 to 9.50, 3.50 to 6, 0.22 to 0.40, and 1.50 to 1.57 mg/Kg, with the variation of L/S ratio from 20:1 to 80:1.

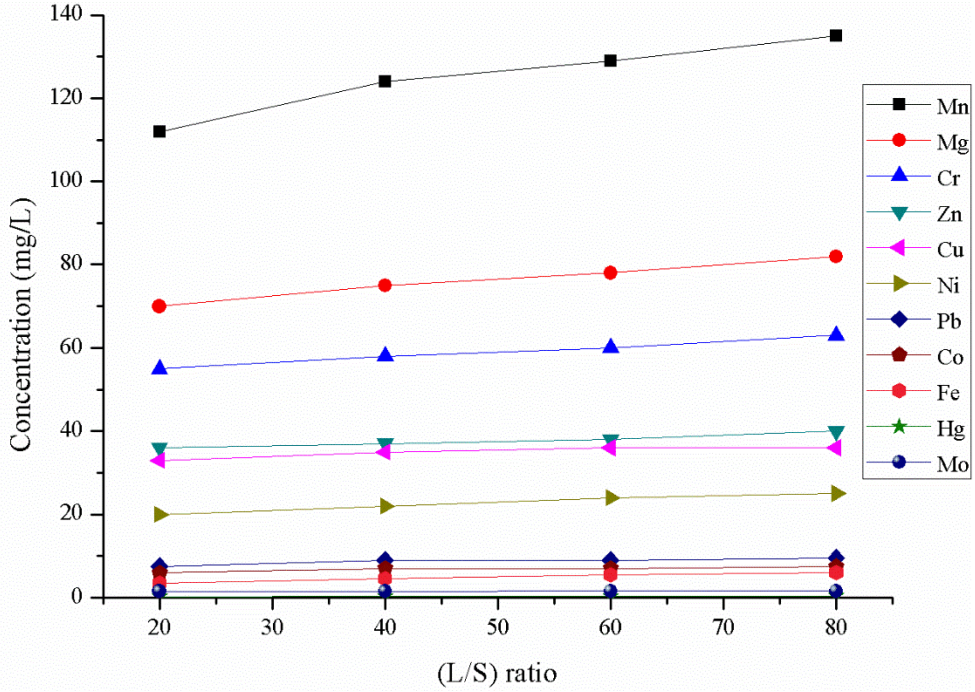

Figure 3.9: Concentration of different leached elements in bottom ash with variation of liquid to solid ratio

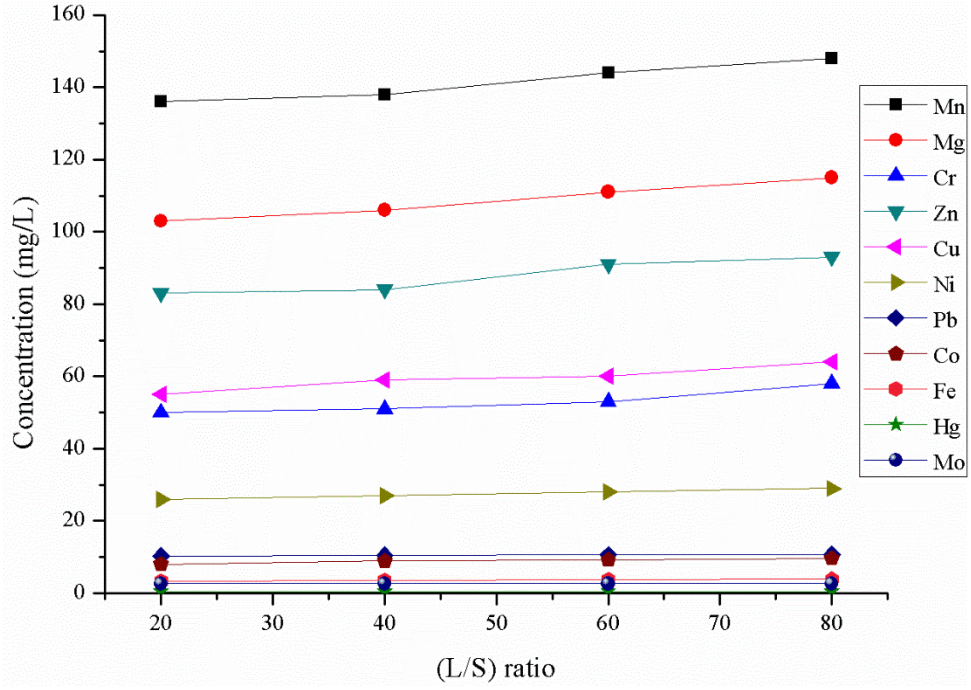

Figure 3.10: Concentration of different leached elements in fly ash with variation of liquid to solid ratio

The tracing element result data of fly ash are presented in Figure 3.10, which show the similar nature of leaching characteristics as bottom ash. In the fly ash, the tracing element concentration of Mn, Mg, Cr, Zn, Cu, Ni, Pb, Fe, Co, Hg, and Mo increases from 136 to 148, 103 to 115, 50 to 58, 83 to 93, 55 to 64, 26 to 29, 10.34 to 10.74, 8.00 to 9.96, 3.30 to 3.90, 0.50 to 0.56, and 2.61 to 2.68 mg/Kg, with the variation of L/S ratio from 20:1 to 80:1. From the leaching results of the fly and bottom ash data, it is observed that the tracing elements of Mn, Mg, Cr, Zn, Ni, Pb, Fe, and Cu are the most abundant elements while Hg, Mo, and Co are the least abundant elements, present in the range of 0.20–2.66 mg/kg. The element Mn shows the maximum leachibility, whereas Hg shows the minimum leachibility in both fly and bottom ash samples. Similar types of analysis results have been reported in the literature with coal ash of different thermal plants (Baba et al., 2010; Blissett and Rowson, 2012; Singh et al., 2012). It is also observed that the leached concentration of the tracing elements in the fly ash is more compared with the bottom ash at the same L/S. Minimum leachibility of the solution is observed with the L/S of 20:1, whereas maximum leachibility of the solution is observed with L/S of 80:1. Similar result has been reported by investigators (Praharaj et al., 2002; Baba et al., 2010).

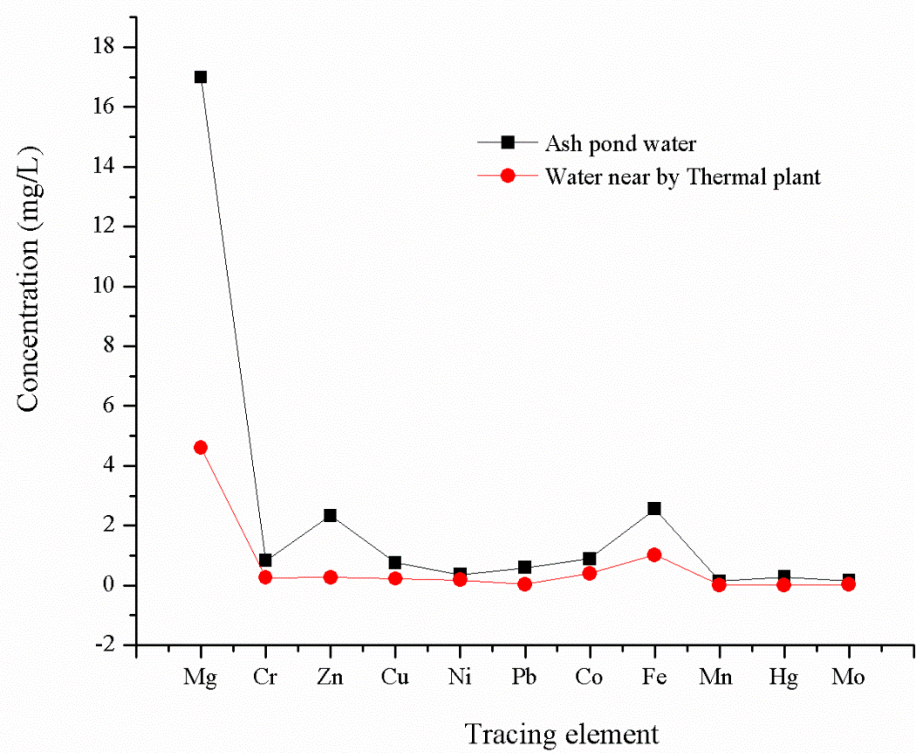

Figure 3.11: Concentration of different leached elements in groundwater sample

The effect of the leaching characteristics from the fly ash and bottom ash waste is determined in the water of an ash pond and the water of a village close to the thermal power plants, which is shown in Figure 3.11. Total 11 elements are traced in the collected water: Mg, Zn, Hg, Mo, Cu, and Co are under the prescribed limits of the drinking water (IS 10500, 2009) and Cr, Pb, Mn, Ni, and Fe crossed the standard limits.

These elements may cause many harmful effects on human health like heart attack, damage of the nervous systems, lung tumors, liver failure, etc. The leaching concentration of toxic elements can be controlled by replacing the conventional slurry ash disposal systems with a high-concentration slurry ash disposal system, where evaporation controls the production of leachate (Iyer and Scott, 2001). Using good-quality coal and temperature control during the combustion process also minimize the leaching concentration. Green technology should also be adopted for controlling the toxic heavy metals pollution due to the bottom ash disposal in and around thermal power plants.

3.5 CONDLUDING REMARKS

In the present chapter, the physio-chemical, mineralogical and leaching characteristics of coal and coal ash samples are studied. Based on the experimentation following conclusions are drawn:

- The particle size distribution of coal sample shows 38.39% particles are having their particle size less than 75 μm. Similarly in fly and bottom ash, 73 and 15.4% particles are finer than 75 μm respectively. The specific gravity of the coal, fly and bottom ash are determined as 1.45, 2.28 and 2.05 respectively.
- From SEM analysis, it is observed that coal sample shows the irregular shape of particles and amorphous in nature. Fly ash particles are smooth and spherical whereas bottom ash particles are coarser, and irregular in shape.
- From the leaching tests for the fly and bottom ash sample the tracing elements of Mn, Mg, Cr, Zn, Ni, Pb, Fe, and Cu are the most while Hg, Mo, and Co are the least abundant elements.
- Leached concentration of the tracing elements in the fly ash is more compared with the bottom ash at the same L/S. Minimum leachibility of the solution is observed with the L/S of 20:1, whereas maximum leachibility of the solution is observed with L/S of 80:1. .

CHAPTER 4
RHEOLOGICAL CHARACTERISTICS OF COAL AND COAL ASH SLURRY

4.1 INTRODUCTION

The flow behaviour of slurry in pipeline depends upon the rheological characteristics of the slurry suspension. In power plants, generally the coal water slurry is being transported in pipeline for fuel generation and the coal ash is being transported hydraulically to ash pond through slurry pipelines for their disposal. The maximum concentration of slurry with appreciable viscosity increases the efficiency of transportation of the slurry in pipelines. The energy required for transportation of slurry through pipeline highly depends upon the slurry viscosity. So the study of rheological behavior of coal-water slurry and fly ash slurry is necessary for their economical transportation through pipeline. So the present work is carried out to study the rheological behavior of coal water slurry and coal ash slurry at different concentration and also the study is extended to evaluate the effect of particle size, solid concentration, and unimodal and bimodal particle-size distribution on the rheology of both coal-water slurry and coal ash slurry. The details of the experiment and the apparatus used are described in the following section.

4.2 RHEOMETER

The Rheometer (Model:Rheolab Q-C, Make: Anton Paar Company Ltd, Germany) is used to determine the rheological characteristics (i.e. shear strain rate and shear stress relationship) of coal and coal ash slurry. The working principle of RheolabQ-C (Rheometer) is based on Searle principle and it consists of electronically commuted highly dynamic synchronous drive and highly precise encoder. The photographic diagram of Rheolab Q-C (Rheometer) is shown in Figure 4.1. The rheological properties are determined from the values of shear stress at different shear rates. Rheometer consists of bob and co-axial cylindrical cup measuring system. The slurry houses in between the rotating bob mounted on the vertical spindle and the stationary cylindrical cup is concentric with the bob. The shearing of slurry suspension takes place by rotation of the rotating bob. The detailed specifications of rheometer are tabulated in Table 4.1.

Table 4.1: Specifications of rheometer

Sr. No.	Components	Specifications
1	Motor type	Synchronous electric motor
2	Shear stress range	0.5 to 3 x 107, mPa
3	Shear rate range	0.01 to 4000, sec^{-1}
4	Speed range	0.01 to 1200, min^{-1}
5	Temperature range	-20 to 180, ^{o}C
6	Torque range	0.25 – 75, mN-m
7	Viscosity range	0.1 to 109, mPa-s

Figure 4.1: Rheolab Q-C (Rheometer)

4.2.1 Slurry sample preparation

The slurry sample of 100 ml is prepared by the mixing of required quantity of solids (i.e. coal and coal ash) in water to get the desired concentration of solids. The coal samples are prepared by crushing with laboratory-size ball mill to the different required fractional sizes 53-75, 106-150 and 150-250 µm whereas fly and bottom ash are collected directly from the Guru Nanak Dev thermal power plant, Bathinda (Punjab) for the experiments. The electronic pan balance with resolution of ±0.0001 gram is used for weighing of solids and slurry suspension is gently prepared with glass rod to avoid the attrition and spillage of particles. The bob and cup assemblies are fixed with locking device before experimentation. The slurry suspension is poured into stationary cylindrical cup upto the

definite mark on cylinder and again stirred with glass rod for 5-10 minutes to ensure homogenization of slurry. Meanwhile, bob is lowered into the stationary cylindrical cup and system is coupled to the rotating spindle by pushing down the flanged coupling. During the spindle rotation, slurry is subjected to shearing action in between the annular gap present between stationary cylindrical cup and bob, and hence shear stress is measured as a function of shear rate. The result output data is obtained with the help of Rheoplus software which is installed on a computer connected to the rheometer by LAN connection. Rheological tests are conducted in the shear rates range of 0-600 s^{-1} at constant temperature of 25 °C. Each experiment is performed at least three times to check the accuracy of rheological data.

4.3 RHEOLOGICAL CHARACTERISTICS OF COAL-WATER SLURRY

The rheological experiments of coal-water slurry are conducted in the solid concentration range of 30-60% (by weight). The apparent viscosity and shear stress are measured at shear rate ranging from 0–600 s^{-1}. In present study, two different cases are considered to investigate the rheological behaviour of coal-water slurry. In first case, the rheological characteristic of coal in particle size range of 53-75 μm is studied. In the second case, rheological behaviour of finer coal particles (53-75 μm) is evaluated with addition of coarser particles of coal in the range of 106-150 and 150-250 μm respectively.

4.3.1 Rheology of 53-75 μm sized coal-water slurry

The rheological experiments are conducted on coal samples of 53-75 μm particle size with solid concentrations of 30-60% (by weight). The variation of shear stress and apparent viscosity with shear rate at different solid concentrations (by weight) are shown in Figure 4.2-4.3. Rheological result data reveals that both shear stress and apparent viscosity are enormously affected with solid concentrations. As the solid concentration is increased, the apparent viscosity of the coal-water mixture is also increased. The increase in the apparent viscosity with solid concentration may be due to an increase in the particle-to-particle interactions with the increase in resistance between particles. The frictional force between particles becomes significant thus accompanying resistance is reflected with the increase in viscosity (Mishra et al. 2002).

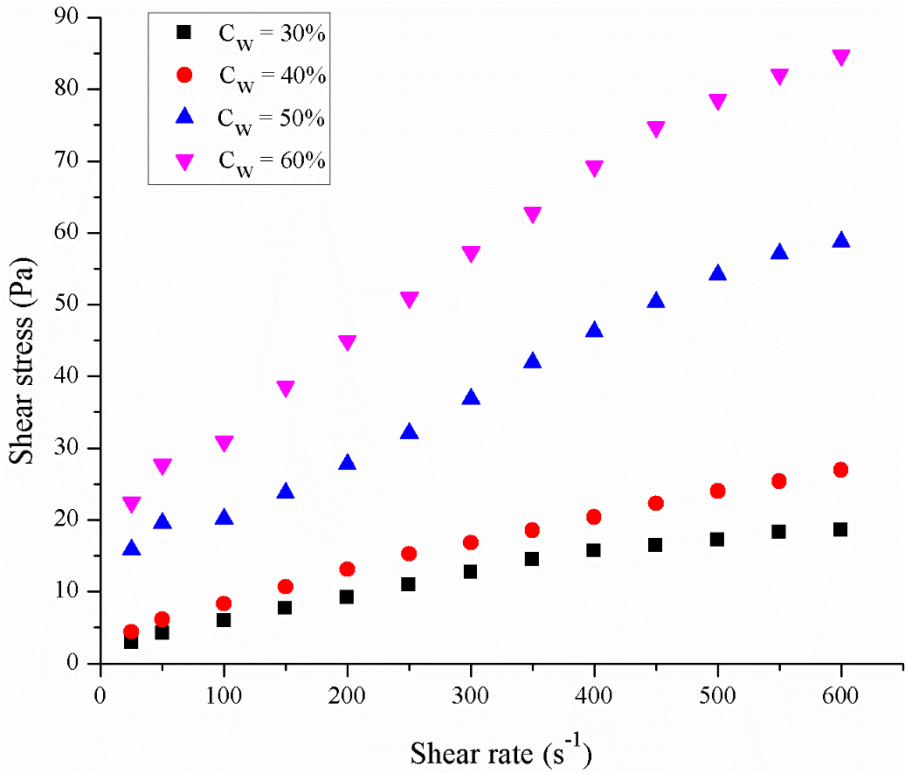

Figure 4.2: Shear stress-shear rate of of 53-75 µm sized coal-water slurry at different solid concentrations

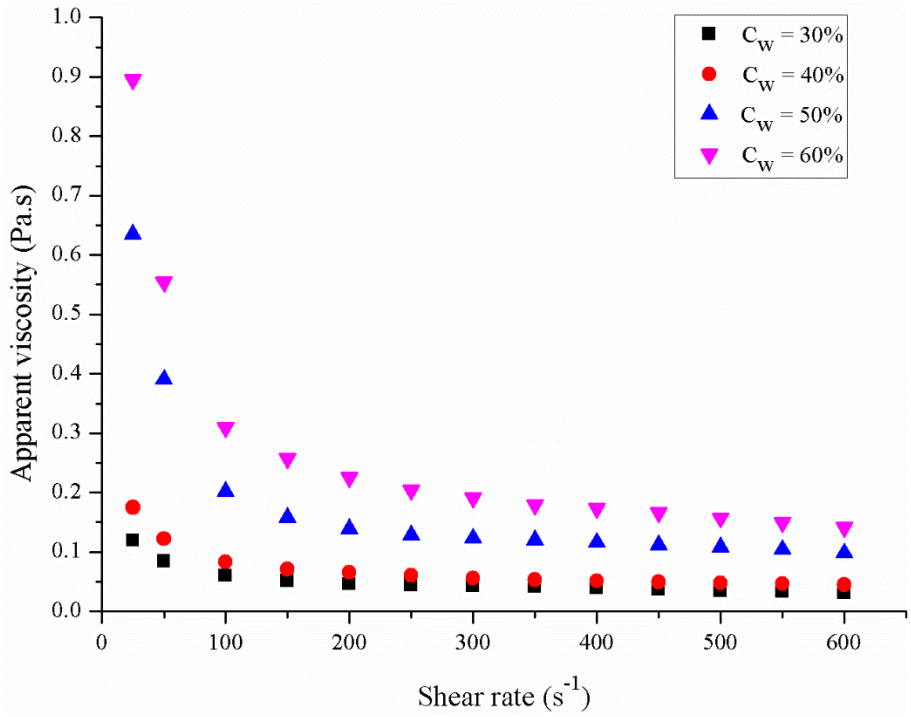

Figure 4.3: Apparent viscosity and shear rate of 53-75 µm sized coal-water slurry at different solid concentrations

The coal-water slurry shows Newtonian behaviour upto 30% solid concentration and beyond 30% solid concentration coal-water slurry shows pseudoplastic i.e. (shear thinning) behaviour. The apparent viscosity is independent with shear rate upto 30% solid concentration of coal-water slurry. Above the 30% solid concentration, apparent viscosity decreases with increase in shear rate due to shear thinning behaviour. Coal-water slurry with 40% solid concentration shows a decreasing trend in apparent viscosity upto the shear rate of 100 s^{-1} and afterwards marginal drop is observed with further increase in shear rate. The decreasing trend of apparent viscosity is observed upto 300 s^{-1} shear rate with 50 and 60% solid concentration of coal-water slurry

4.3.2 Effect of 106-150 μm sized coal addition on rheology of 53-75 μm sized coal-water slurry

The rheological experiments of 53-75 μm sized coal are also performed with blending of 106-150 μm sized coal particles to determine the rheology of bimodal distribution of coal-water slurry. The coal-water slurry sample is prepared by 20, 30 and 40% addition of 106-150 μm sized particles with 53-75 μm sized coal particles. Figure 4.4-4.7 shows the variation of apparent viscosity of bimodal slurry for different solid concentrations at three different shear rates of 100, 300 and 600 s^{-1}.

From Figure 4.4, the value of apparent viscosity for 53-75 μm sized coal with 20 and 30% addition of 106-150 μm sized coal are decreased as 34.4 and 20.7% respectively at 100 s^{-1} shear rate. Whereas 15.9% increase in value of apparent viscosity is observed with increasing the addition of 106-150 μm sized coal from 30% to 40%. At 300 s^{-1} shear rate, 39 and 16.4% decrease in apparent viscosity is found with 20 and 30% addition of 106-150 μm sized coal in 53-75 μm sized coal whereas 12.9% increase in apparent viscosity is observed by increasing the addition of 106-150 μm sized coal from 30 to 40%. The percentage reduction in apparent viscosity at 600 s^{-1} shear rate with 20 and 30% addition of 106-150 μm sized coal is 25.8 and 17.1% respectively whereas 15.5% increase in value of apparent viscosity is observed by increasing the addition of 106-150 μm sized coal from 30 to 40%. The value of apparent viscosity for 53-75 μm sized coal with 20, 30 and 40% addition of 106-150 μm sized coal for 40% solid concentration is shown in Figure 4.5. It is observed that 20, and 30% addition of 106-150 μm sized coal in 53-75 μm sized coal leads to 40 and 23% decrease in apparent viscosity whereas 12.7% increase is observed with further addition of 106-150 μm sized coal upto 40% , at 100 s^{-1} shear rate.

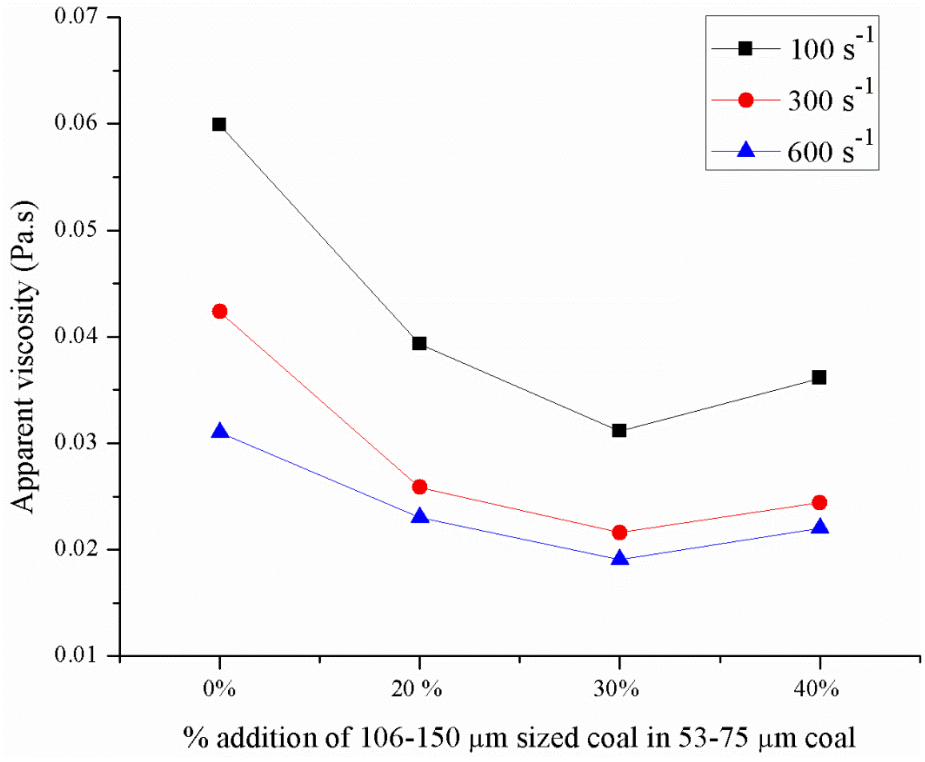

Figure 4.4: Apparent viscosity of 53-75 µm sized coal-water slurry with addition of 106-150 µm sized coal at 30% solid concentration

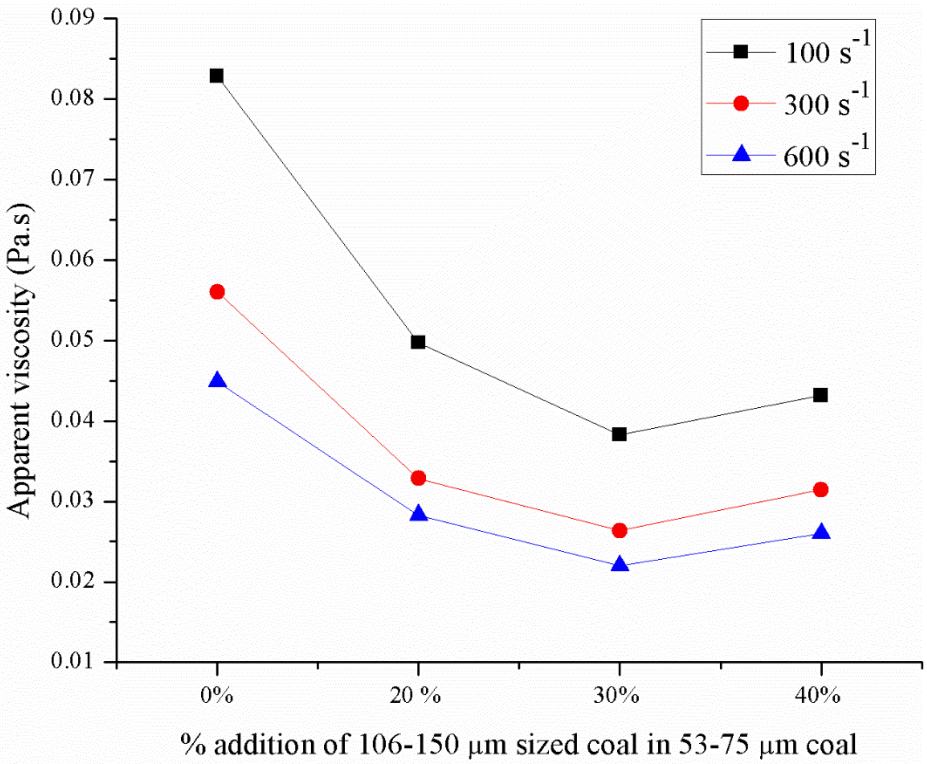

Figure 4.5: Apparent viscosity of 53-75 µm sized coal-water slurry with addition of 106-150 µm sized coal at 40% solid concentration

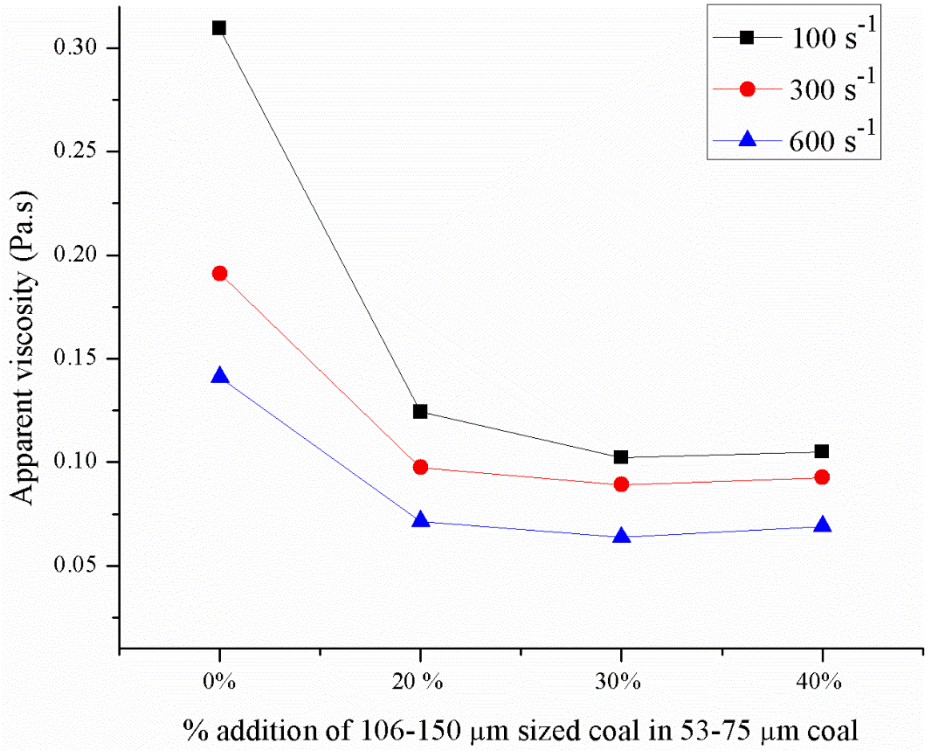

Figure 4.6: Apparent viscosity of 53-75 µm sized coal-water slurry with addition of 106-150 µm sized coal at 50% solid concentration

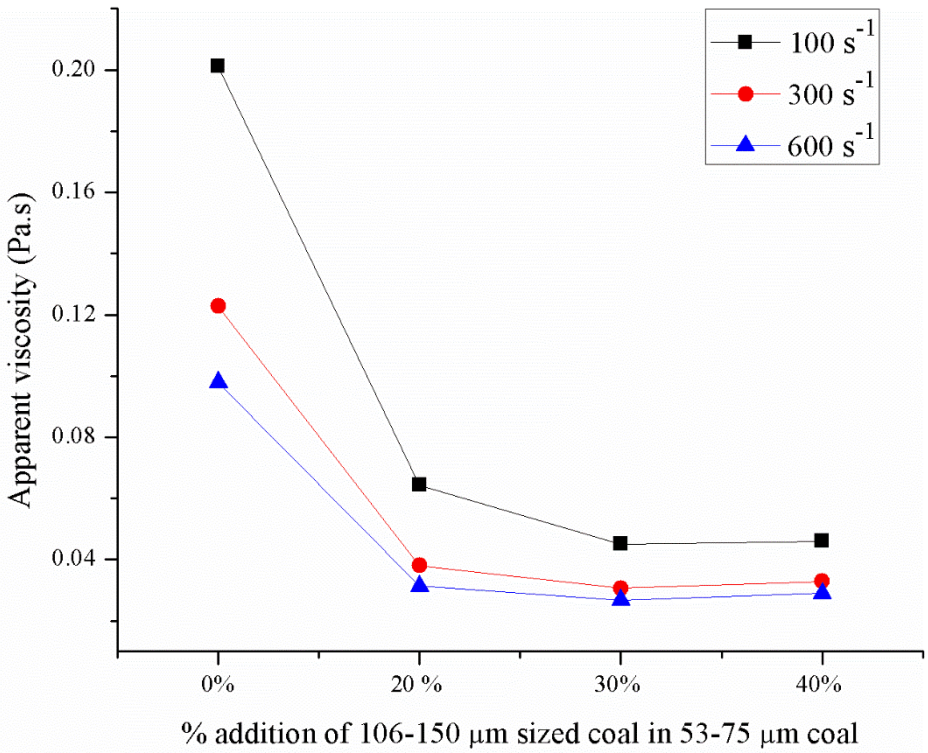

Figure 4.7: Apparent viscosity of 53-75 µm sized coal-water slurry with addition of 106-150 µm sized coal at 60% solid concentration

Similar trend of apparent viscosity is observed for 50 and 60% solid concentrations are represented in Figure 4.6-4.7. At 50% solid concentration, apparent viscosity is decreased by 68 and 29.8% with 20 and 30% addition of 106-150 μm sized coal. whereas 2.1% increase is observed with further addition of 106-150 μm sized coal upto 40%, at 100 s^{-1} shear rate. From Figure 4.7, the apparent viscosity with 20 and 30% addition of 106-150 μm sized coal is decresed by 59.8 and 17.8% whereas 2.7% increase is observed with 40% addition of 106-150 μm sized coal at 100 s^{-1} shear rate.

From Figures 4.4-4.7 it is concluded that the minimum apparent viscosity occurs at 100 s^{-1} shear rate for all solid concentrations ranges between 30-60% (by weight). The value of apparent viscosity for 53-75 μm sized coal-water slurry decreases upto 30% addition of 106-150 μm sized coal at all solid concentrations and further addition leads to increase.

4.3.3 Effect of 150-250 μm sized coal addition on rheology of 53-75 μm sized coal-water slurry

The rheological experiments are performed with bimodal-slurry sample prepared by mixing of 20, 30 and 40% of 150-250 μm sized coal particles in 53-75 μm sized coal-water slurry. The variation in the apparent viscosity of 53-75 μm sized coal with 20, 30 and 40% addition of 150-250 μm sized at 30% solid concentrations (by weight) is shown in Figure 4.8.

The apparent viscosity at 100 s^{-1} shear rate, is reduced by 40.9 and 8.5% with 20 and 30% addition of 150-250 μm sized coal respectively but the apparent viscosity increased by 9.2% with further addition of 150-250 μm sized coal upto 40%. However at 300 s^{-1} shear rate, 48.5 and 0.3% decrease in apparent viscosity is found with 20 and 30% addition of 150-250 μm sized coal respectively while 6.2% increase is observed with increase in the addition of 150-250 μm sized coal from 30 to 40%. The apparent viscosity at 600 s^{-1} shear rate is decreased by 35.4 and 10.1% with 20 and 30% addition of 150-250 μm sized coal respectively. The further 40% addition of 150-250 μm sized coal leads to 27.7% increase in value of apparent viscosity.

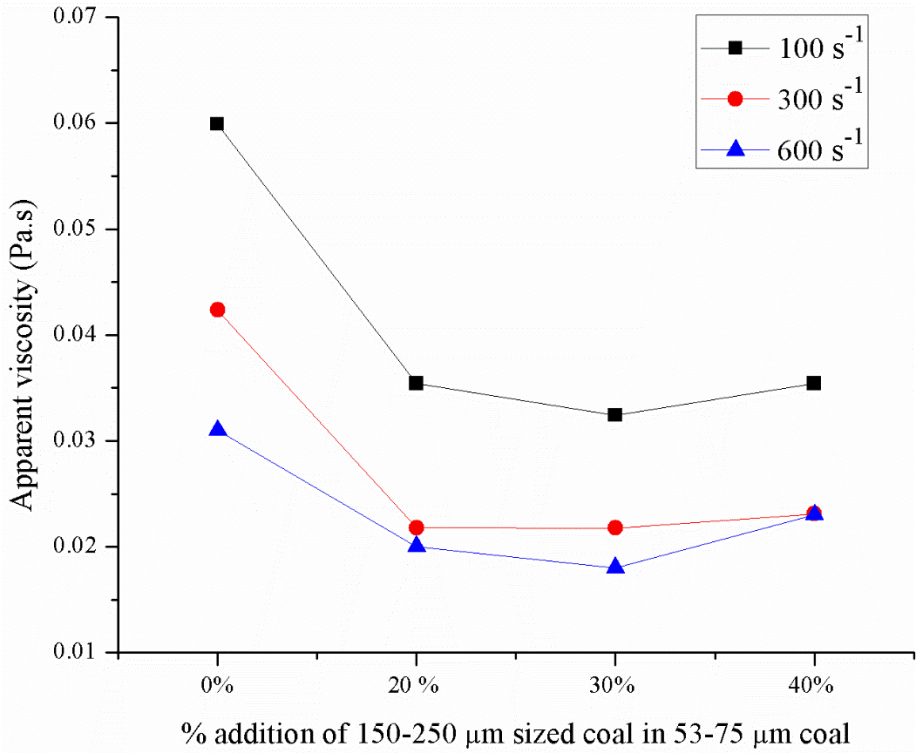

Figure 4.8: Apparent viscosity of 53-75 µm sized coal-water slurry with addition of 150-250 µm sized coal at 30% solid concentration

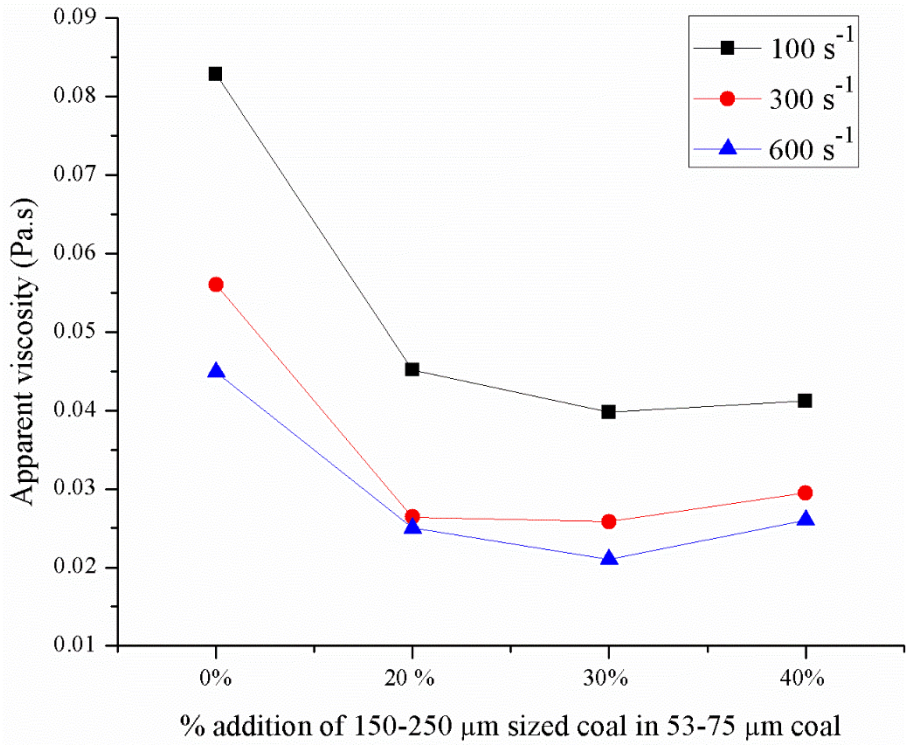

Figure 4.9: Apparent viscosity of 53-75 µm sized coal-water slurry with addition of 150-250 µm sized coal at 40% solid concentration

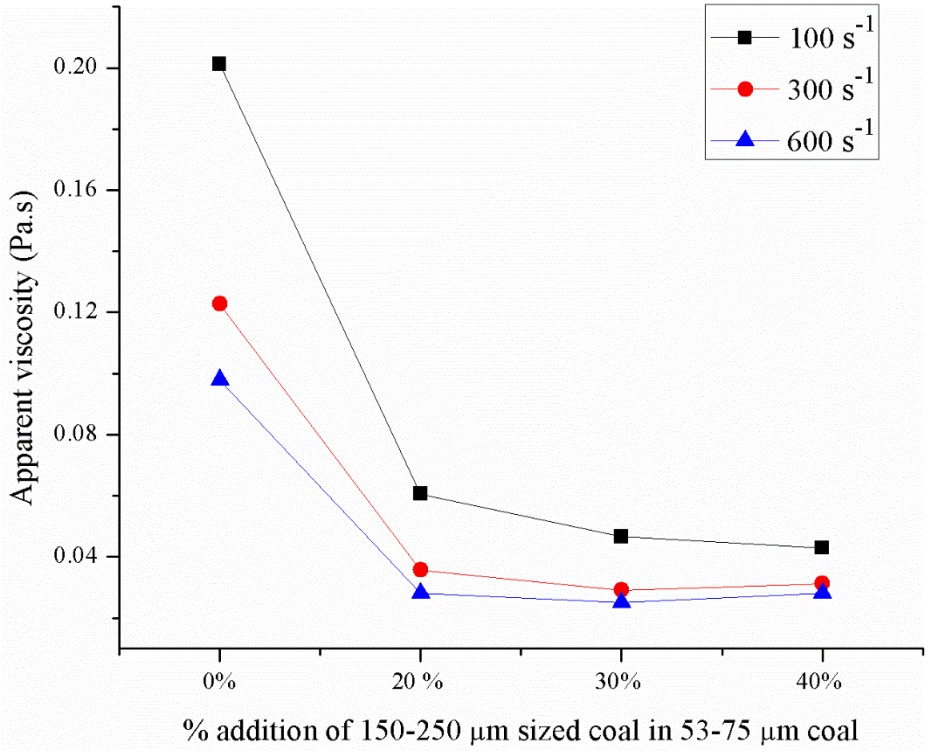

Figure 4.10: Apparent viscosity of 53-75 µm sized coal-water slurry with addition of 150-250 µm sized coal at 50% solid concentration

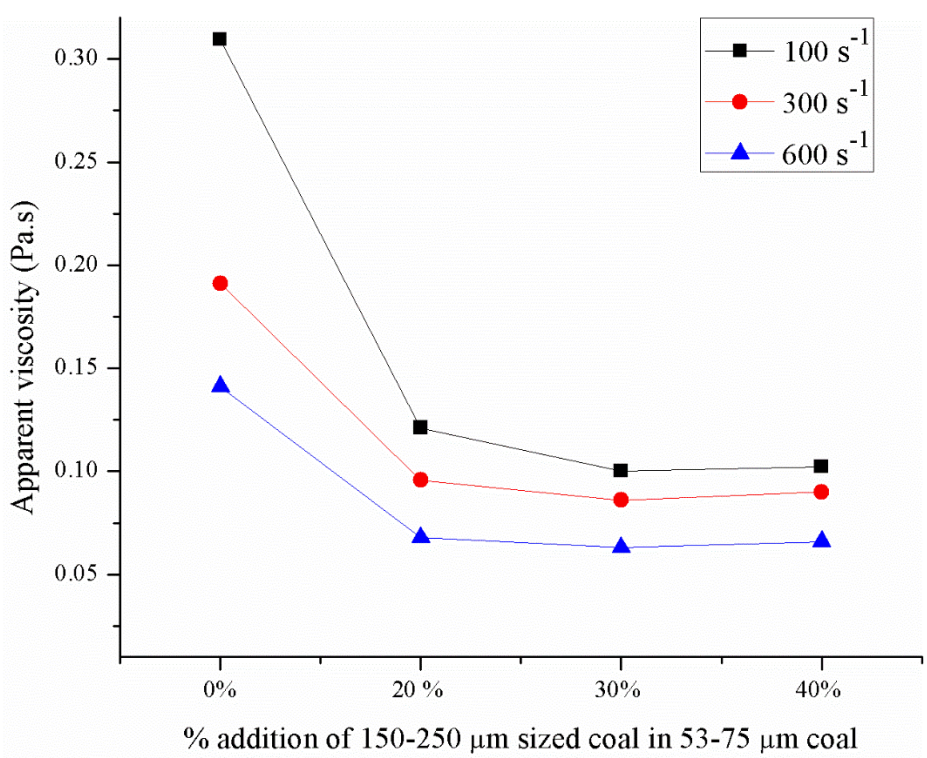

Figure 4.11: Apparent viscosity of 53-75 µm sized coal-water slurry with addition of 150-250 µm sized coal at 60% solid concentration

The apparent viscosity reduction of 53-75 μm sized coal-water slurry with addition of 150-250 μm sized coal at 40% solid concentration is presented in Figure 4.9. It is observed that at 100 s^{-1} shear rate 45.5 and 11.9% reduction is found in apparent viscosity with 20 and 30% addition respectively and 3.6% increase in apparent viscosity with 40% addition of 150- 250 μm sized coal.

Similar trend in apparent viscosity is observed for 50 and 60% solid concentrations are represented in Figure 4.10-4.11. The percentage reduction in apparent viscosity for 50% solid concentration at 100 s^{-1} shear rate with 20 and 30% addition are 69.9 and 23.1% respectively but further 40% addition of 150-250 μm sized coal leads to 2.9% increase in apparent viscosity. However 60.9 and 17.3% reduction is observed with 20 and 30% addition of 150-250 μm sized coal respectively at 60% solid concentration but 2.2% increase is found with further 40% addition of coarser coal particles.

From rheological experimental data, it is perceived that maximum reduction in apparent viscosity of 53-75 μm sized coal-water slurry is found with 30% addition of 150-250 μm sized coal for shear rate ranges between 100 s^{-1} - 600 s^{-1} at all solid concentrations (by weight). It is also observed that with addition of 150-250 μm sized coal shows more reduction in apparent viscosity of 53-75 μm sized coal-water slurry as compared to the 106-150 μm sized coal. The minimum value of apparent viscosity is achieved for transportation of coal-water slurry with 30% addition of 106-150 and 150-250 μm sized coal particles.

4.4 RHEOLOGICAL CHARACTERISTICS OF FLY ASH SLURRY

The rheological behaviour of fly ash slurry is also studied in order to transport the high solid concentration of fly ash slurry in a pipeline. The rheology of fly ash slurry is investigated with and without addition of bottom ash in the solid concentration range of 30-60% (by weight). Bottom ash is added as an additive with fly ash slurry in the percentage of 10, 20, and 30% (by weight). The experiments are conducted for shear rate varies from 0–600 s^{-1}.

4.4.1 Rheology of fly ash slurry

The rheological experiments are conducted on fly ash slurry at different solid concentrations namely 30, 40, 50 and 60% (by weight) to find the shear stress with shear rate. During the experimentation the temperature of slurry sample is maintained at 25 ºC with the help of thermostatically controlled water bath. The shear stress-shear rate of fly ash slurry with above mentioned solid concentrations is shown in Figure 4.12.

It is clearly seen from Figure 4.12 that shear stress increases with increase in strain rate for all fly ash slurry suspensions. It is also seen from Figure 4.12 that at higher concentration, the slurry requires certain value of yield stress to start deformation and further the shear stress and shear rate curve becomes straight line which is the flow behavior of the Bingham Fluid. Equation 4.1 is represented for Bingham fluid.

$$\tau = \tau_y + \eta \frac{du}{dy} \qquad (4.1)$$

Where, τ represents shear stress (Pascal),τ_y represents yield stress (Pascal) and η represents the coefficient of rigidity.

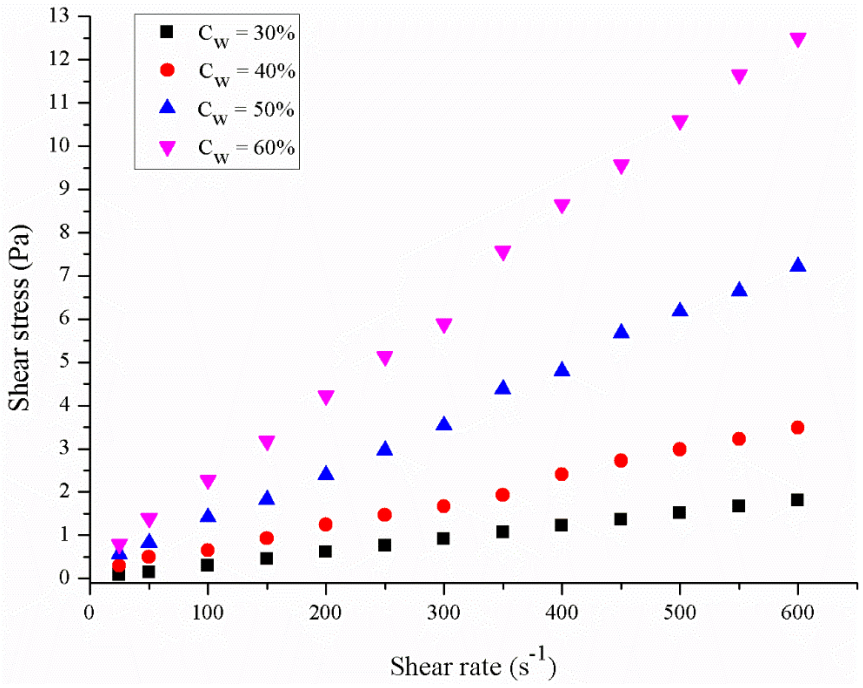

Figure 4.12: Shear stress-shear rate of fly ash slurry at different solid concentrations

The variation of the shear stress with shear rate for all solid concentration shows that all the data points fall in a straight-line equation. The slope of the straight line increases with the increase in solid concentration which shows that the value of yield stress increases. The yield stress value for fly ash upto 30% solid concentration (by weight) is zero which implies that fly ash shows Newtonian behaviour upto 30% whereas above 30% solid concentration yield value in non-zero which shows that fly ash slurry follows the Bingham fluid behaviour.

Figure 4.13 represents the apparent viscosity of fly ash slurry at different solid concentrations (by weight). Results show that apparent viscosity of slurry suspensions is the function of solid concentration. Higher shear stress value is needed to initiate shearing with the increase in slurry solid concentration due to the presence of relatively more numbers of solid particles. Similar observation is also observed by many researchers (Gandhi et al. 2001, Seshadri et al. 2008, Chandel et al. 2009, Naik et al. 2011, Senapati et al. 2010) with fly ash slurry suspension.

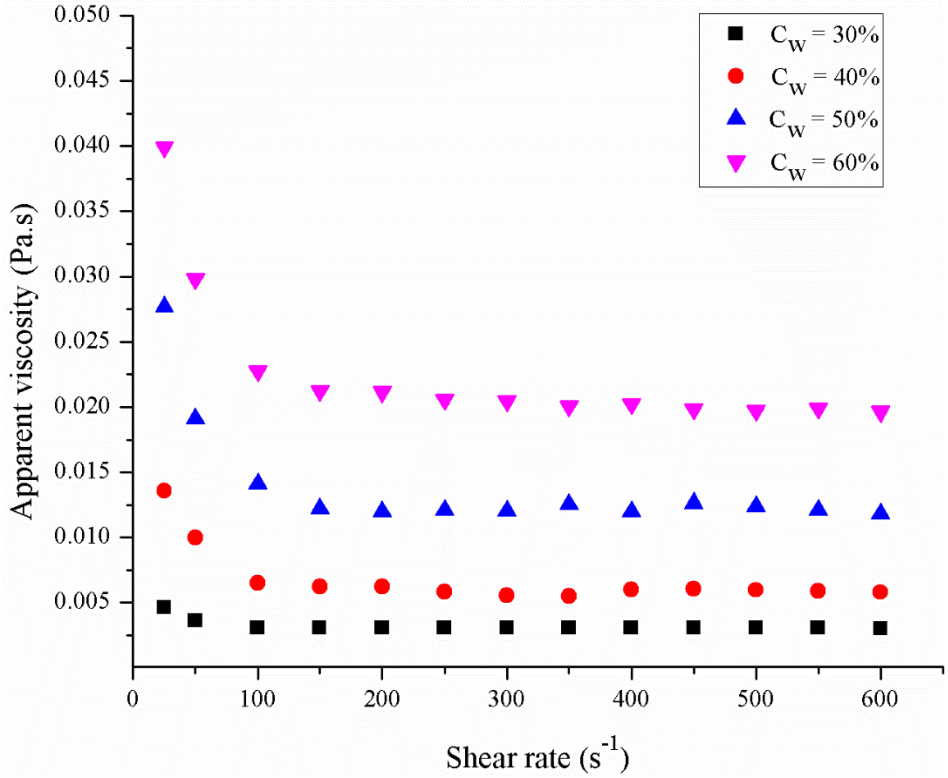

Figure 4.13: Apparent viscosity-shear rate of fly ash slurry at different solid concentrations

4.4.2 Effect of bottom ash addition on rheology of fly ash slurry

The previous section describes the rheological behaviour of fly ash slurry at different solid concentrations. Currently, fly and bottom ash is being transported hydraulically to ash pond through separate slurry pipelines at low solid concentrations in power plants. Due to this the ash disposal pipeline operation is extremely uneconomical as the water quantity requirement is large and power consumption increases for pumping of water. An attempt has been made to investigate the possibility of transportation of fly ash slurry with addition of bottom ash at higher solid concentrations in slurry pipeline. So the experiments have been carried out to determine the rheological behavior of the slurry sample of 30, 40, 50 and 60% concentration that is prepared by adding the bottom ash of 10, 20 and 30% with fly ash.

Shear stress-shear rate of fly ash slurry with 10, 20 and 30% addition of bottom ash at 30% solid concentration (by weight) is shown in Figure 4.14. From the Figure 4.14, it is observed that shear stress of fly ash slurry decreases with addition of bottom ash. At 100 s^{-1} shear rate, shear stress of fly ash slurry decreases as 1.65, 9.73 & 4.09% with addition of 10, 20 and 30% bottom ash whereas the decreasing rate of shear stress is 3.81, 9.63 & 4.89% respectively at shear rate of 300 s^{-1}. Similarly, the percentage reduction in shear stress at shear rate of 600 $s^{-1}$is 4.42, 9.65 and 4.41%, respectively.

From the results data, it is seen that reducing trend in shear stress of fly ash slurry pronounced more at high shear rate condition. Similar trend is observed for 40, 50 and 60% solid concentration (by weight) of fly ash slurry, as shown in Figure 4.15-4.17. At shear rate of 100 s^{-1}, shear stress is reduces as 6.60, 15.60 and 8.95% with 10, 20 & 30% addition of bottom ash for 40% solid concentration whereas 13.67, 18.54 & 7.85% for 50% solid concentration and 13.18, 11.23 & 8.89% for 60% solid concentration respectively.

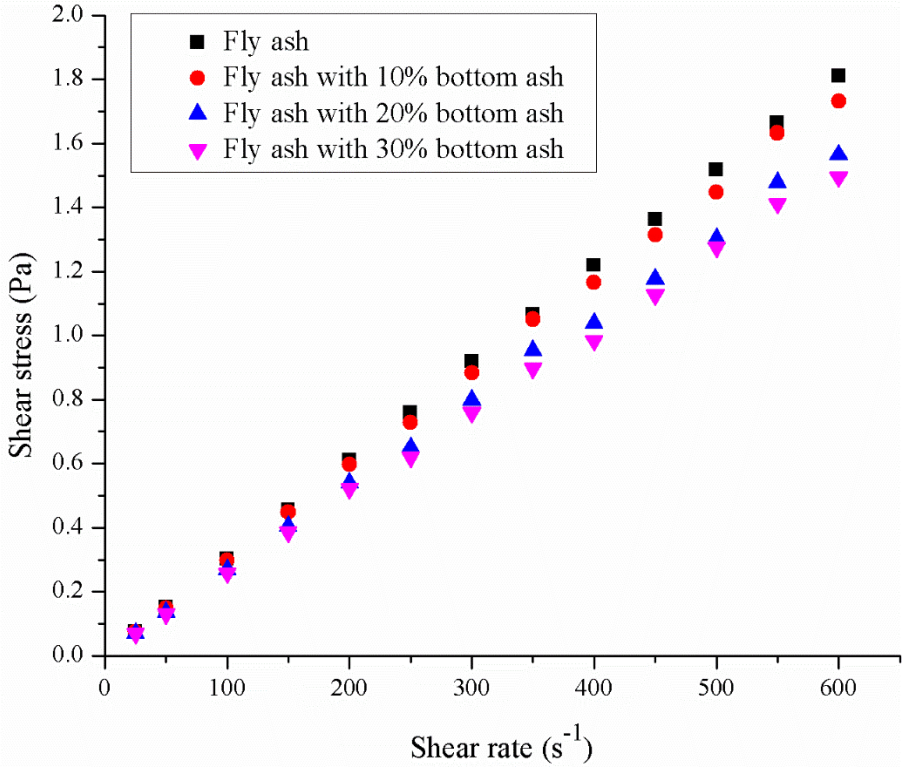

Figure 4.14: Shear stress-shear rate of fly ash slurry with addition of bottom ash at 30% solid concentration

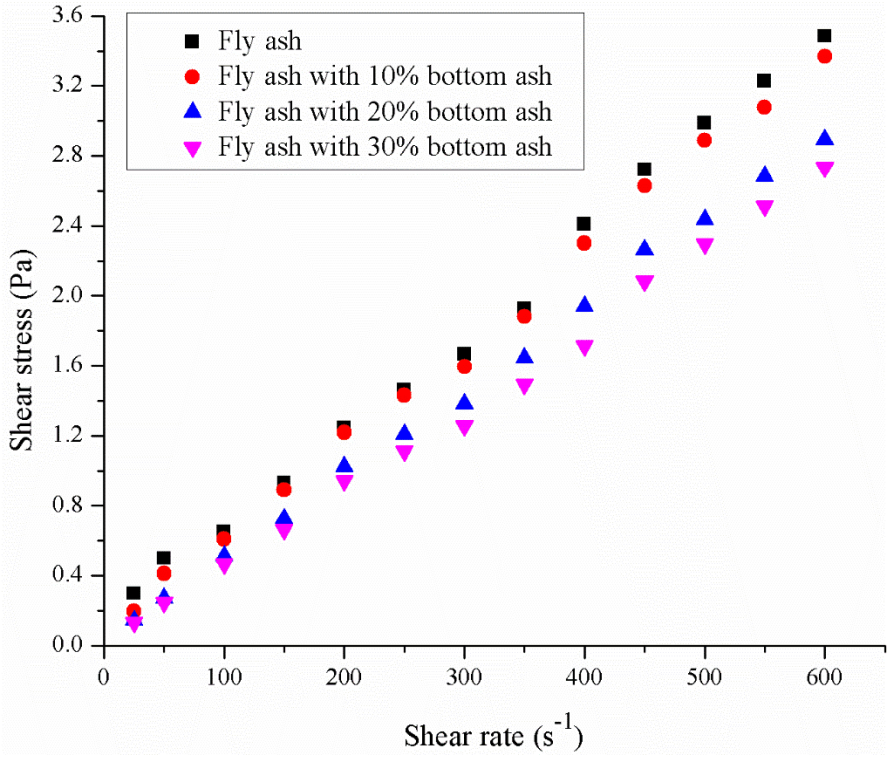

Figure 4.15: Shear stress-shear rate of fly ash slurry with addition of bottom ash at 40% solid concentration

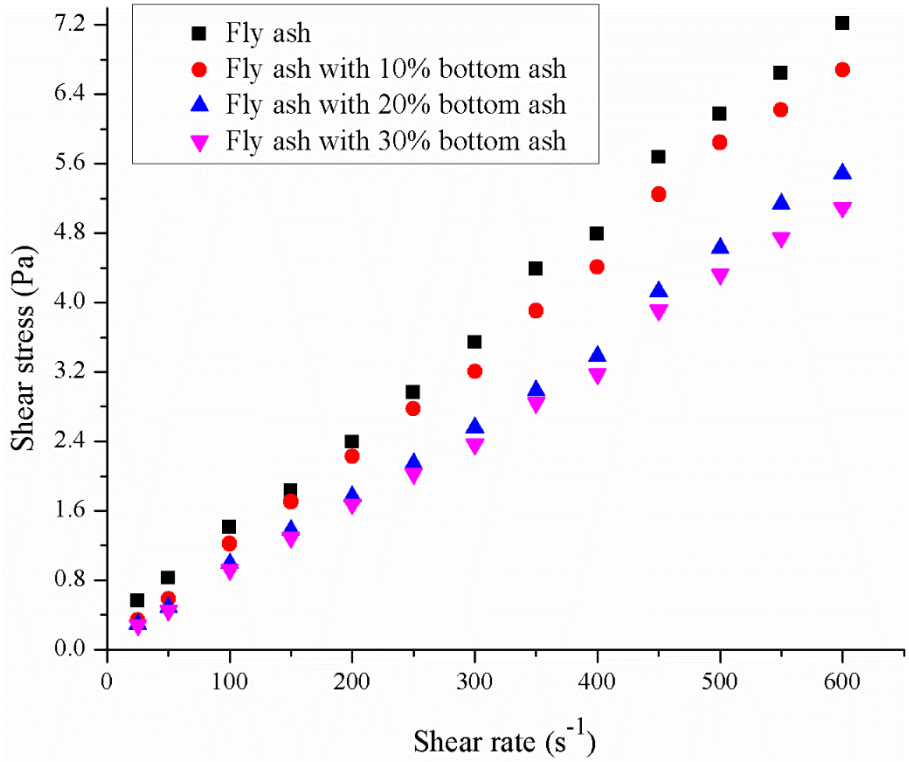

Figure 4.16: Shear stress-shear rate of fly ash slurry with addition of bottom ash at 50% solid concentration

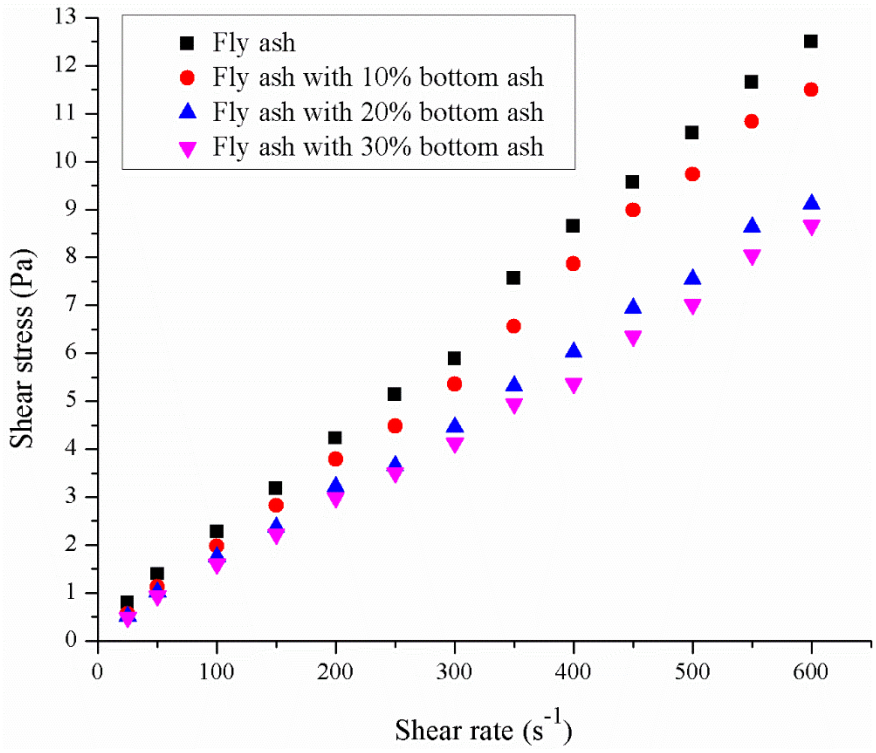

Figure 4.17: Shear stress-shear rate of fly ash slurry with addition of bottom ash at 60% solid concentration

Apparent viscosity of fly ash slurry suspension with 10, 20 and 30% addition of bottom ash at 30% solid concentration (by weight) is shown in Figure 4.18. Figure 4.18 indicates that apparent viscosity of fly ash slurry decreases with the addition of bottom ash. The presence of bottom ash coarser particle in fly ash finer particle suspension promotes particle dispersion and permits the reduction of surface tension as well as interparticulate forces of particles which resulting in reduction of Bingham viscosity (Chandel et al. 2009, Senapati et al. 2010, Kumar et al. 2014). At shear rate of 100 s^{-1}, the reduction in apparent viscosity is found as 1.65, 9.73 and 4.09% with 10, 20 and 30% addition of bottom ash respectively. However, 10, 20 and 30% addition of bottom ash in fly ash slurry leads to 3.81, 9.63 and 4.89% reduction in apparent viscosity at 300 s^{-1} shear rate whereas apparent viscosity decreases as 4.42, 9.65 and 4.41% at shear rate of 600 s^{-1}.

Similar trend of apparent viscosity is observed for 40, 50 and 60% solid concentrations (by weight), as shown in Figure 4.19-4.21. At shear rate of 100 s^{-1}, the percent reduction in apparent viscosity with 10, 20 and 30% addition of bottom ash is found as 6.60, 15.60 & 8.95% for 40% solid concentration, 60.33, 17.97 & 7.10% for 50% solid concentration and 8.01, 20.24 and 4.92% for 60% solid concentration respectively.

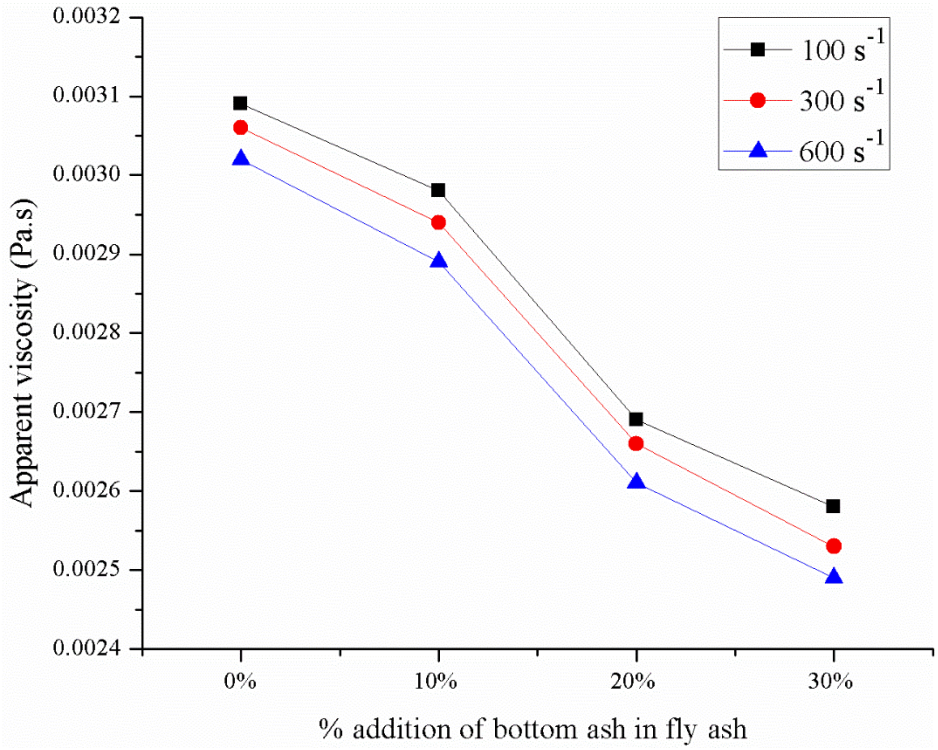

Figure 4.18: Apparent viscosity of fly ash slurry with addition of bottom ash at 30% solid concentration

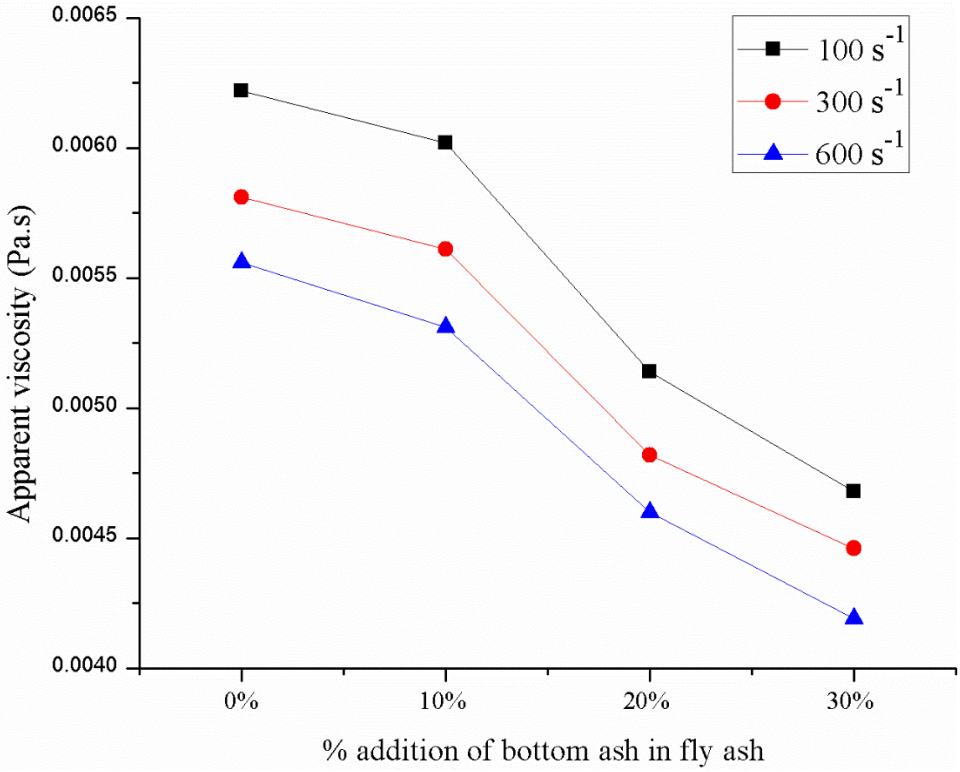

Figure 4.19: Apparent viscosity of fly ash slurry with addition of bottom ash at 40% solid concentration

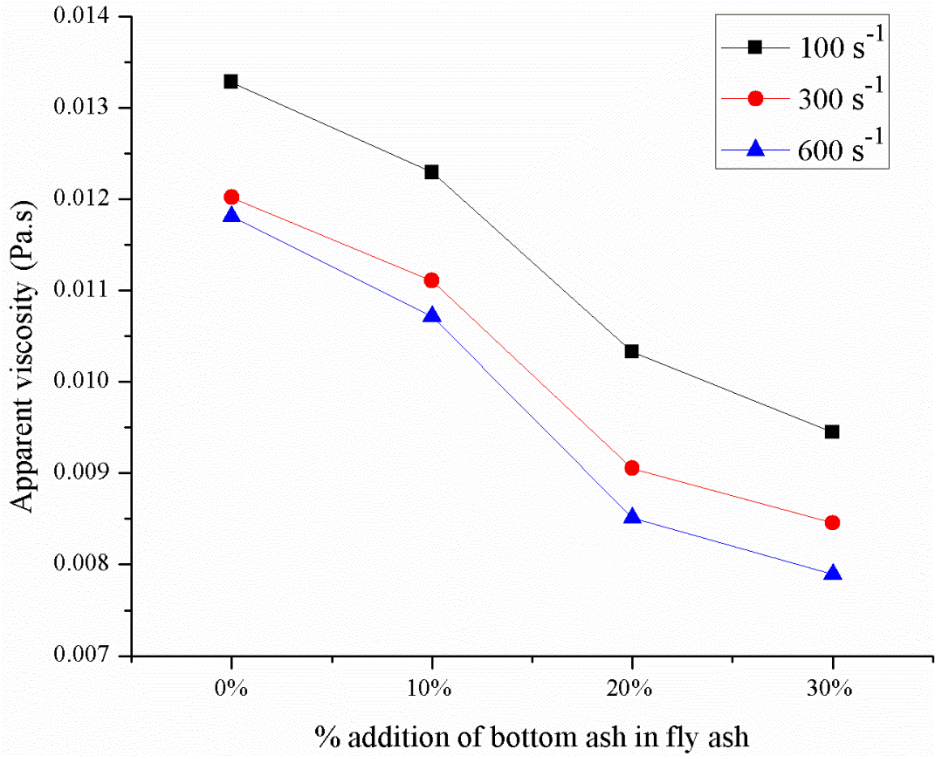

Figure 4.20: Apparent viscosity of fly ash slurry with addition of bottom ash at 50% solid concentration

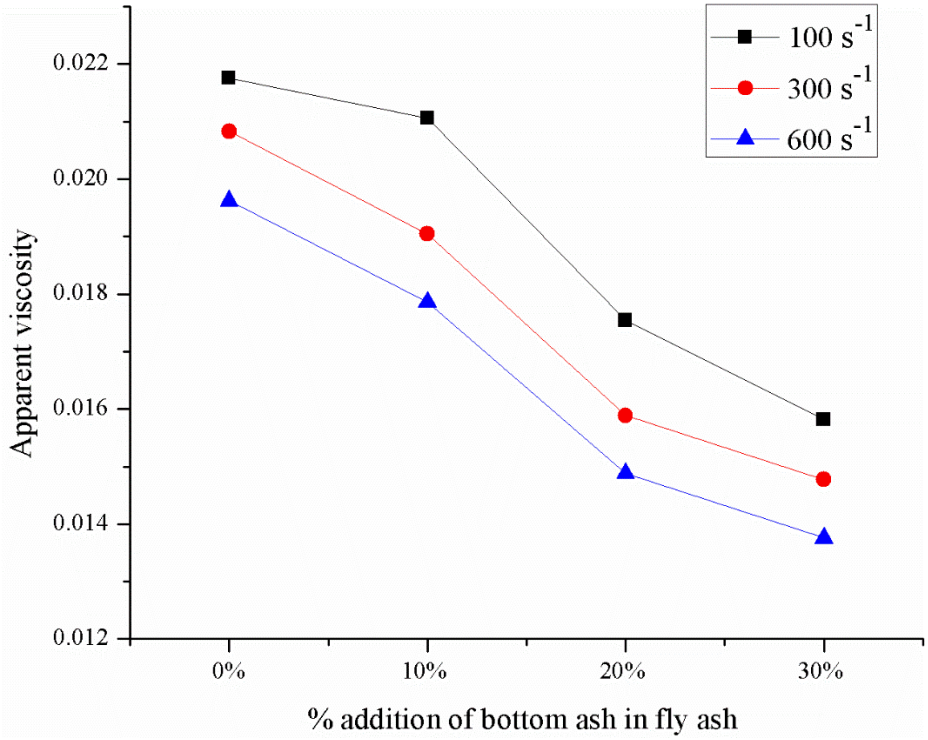

Figure 4.21: Apparent viscosity of fly ash slurry with addition of bottom ash at 60% solid concentration

From the analysis of experimental data, it is concluded that apparent viscosity of fly ash slurry suspension reduces with increase in percentage of bottom ash from 10 to 30%. The maximum apparent viscosity reduction of fly ash slurry is found with 20% addition of bottom ash whereas marginal reduction in apparent viscosity is observed with 10 and 30% addition of bottom ash. The reducing trend in apparent viscosity supports to minimize the energy consumption and pressure drop during the flow of slurry suspension in the pipeline.

4.5 CONCLUDING REMARKS

The rheological characteristics coal-water slurry and fly ash slurry are determined experimentally for different solid concentrations. Also the rheological characteristics of coal-water slurry have been determined by addition of coarser coal particles in finer coal particles. Similarly the rheological characteristics of fly ash slurry have been studied by addition of bottom ash in fly ash. Based on the rheological studies following conclusions are drawn :

- The coal-water slurry shows Newtonian behaviour upto 30% solid concentration and beyond 30% solid concentration coal-water slurry shows pseudoplastic i.e. (shear thinning) behaviour.
- Addition of 150-250 μm sized coal shows more reduction in apparent viscosity of 53-75 μm sized coal-water slurry as compared to the 106-150 μm sized coal. The minimum value of apparent viscosity is achieved for transportation of coal-water slurry with 30% addition of 106-150 and 150-250 μm sized coal particles.
- Fly ash shows Newtonian behaviour upto 30% whereas above 30% solid concentration yield value in non-zero which shows that fly ash slurry follows the Bingham fluid behaviour
- Apparent viscosity of fly ash slurry suspension reduces with increase in percentage of bottom ash from 10 to 30%. The maximum apparent viscosity reduction of fly ash slurry is found with 20% addition of bottom ash whereas marginal reduction in apparent viscosity is observed with 10 and 30% addition of bottom ash.

CHAPTER 5

PRESSURE DROP CHARACTERISTICS FOR THE FLOW OF COAL AND COAL ASH SLURRIES THROUGH PIPELINE

5.1 INTRODUCTION

The slurry transportation through pipeline at high solid concentration requires careful investigation. Design of high concentrated slurry disposal system is complex process as compared to the conventional disposal system. The slurry flow characteristics shows their dependence upon large number of parameters like particle size, solid concentrations, flow velocities, pressure drop etc. The design of slurry disposal system is generally limited to low solid concentration i.e. less than 40% (by weight) as based on technology available in middle of last century and its disposal at low concentration is highly uneconomical and not eco-friendly (Ghalot et al. 1992; Gandhi et al. 1998; Seshadri et al. 2008; Senapati et al. 2012; Kumar et al. 2014). The high concentration disposal system is new emerging way of slurry transportation. Generally, the designing of such pipelines involves the calculation of pressure drop which can be predicted by conducting rheological tests. However, the coarser particles present in slurry makes the rheological experiments quite insufficient because the study of slurry flow containing coarser particles is complex phenomenon. The literature review presented in Chapter 2 has highlighted the need to generate pressure drop data for the flow of multi-sized slurries at high concentrations.

The ashes produced in India usually have higher specific gravity and large content of non-combustible matter. Furthermore, they also differ widely in their chemical/mechanical properties as well as particle size distributions. In order to optimize the hydraulic design of pipeline made for high concentration slurry transportation, it is essential to study the physio-chemical and rheological characteristic of slurry which is described in Chapter 3 and 4 respectively and the basic studies using pilot plants test loop for generation of required data.

From literature (Verma et al. 2006; Seshadri et al. 2008; Chandel et al. 2009; Senapati et al. 2010), it is found that the pressure drop characteristics are needed to be studied for the flow of coal ash at higher solid concentrations. The thermal power plants are producing

very large quantity of coal ash and disposal of coal ash is a challenging task. The pressure drop and flow velocity are very important parameters for the slurry pipeline design. Literature study shows that small amount of additives able to reduce the pressure drop in pipeline (Chandel et al. 2009; Kumar et al. 2014; Senapati et al. 2015).

The objective of the present chapter is to investigate experimentally the pressure drop characteristics of coal-water slurry and coal ash slurry having various concentrations during their transportation through a pipeline. Also the effect on pressure drop by addition of coarser particles of 106-150 and 150-250 μm sized coal in finer particles of 53-75 μm sized coal-water slurry at different solid concentrations (by weight) are presented. Similarly the pressure drop of fly ash slurry is investigated with and without addition of bottom ash in the solid concentration range of 30-60% (by weight). In order to carry out the experiment, a pilot plant test loop of pipe with uniform cross section is fabricated at Mechanical Engineering Department, Thapar University, Patiala. The detailed experimentation of pressure drop with variation of different parameters is discussed in the following section.

5.2 CHARACTERIZATION OF COAL AND COAL ASH

Various bench scale tests are performed to determine the physio-chemical and mineral properties of coal & coal ash samples are presented in Chapter 3 and rheological properties of coal and coal ash study are already presented in Chapter 4.

5.3 EXPERIMENTAL SETUP

In present study, the pressure drop in horizontal slurry pipeline is investigated with the help of pilot plant test loop which is existing in Mechanical Engineering Department, Thapar University, Patiala. Experimental setup consists of a long pipeline with 50 mm diameter along with the other necessary equipments. Figure 5.1 shows the schematic diagram of pilot plant test loop. The photographic view of pilot plant test loop equipped with progressive slurry pump is shown in Figure 5.2. The main components of the test loop include slurry preparation tank, water measuring tank, stirrer, virtual frequency drive, progressive slurry pump, flow control valves, sampler, observation chamber and pipeline to facilitate the system operation. The measuring instruments used are electromagnetic flow meter, pressure transducers and data acquisition system. The test loop consists of an

approximately 60 meters long closed circuit of pipeline. The slurry preparation tank having maximum capacity of 1.37 m^3 with 1.9 m tank height and has 1.3 m × 1.3 m top cross section.

Slurry preparation tank is made up from 3 mm thick stainless steel sheet. A stirrer is made up by using a 30 mm pipe with rectangular plates welded around its periphery. Induction motor of 1 hp with 3 phase power supply is used to run the stirrer through gear box with 1:30 reduction ratio. The specifications of progressive slurry pump (Model: SDA4 S17000 CWWTRG, Make: SYNO Engineers Ltd. Kanpur) are mentioned in Table 5.1. The virtual frequency drive (VFD) is used to control the operating speed of progressive slurry pump. Water measuring tank is also used to measure the flow rate by monitoring the level of slurry suspension in tank over a known time interval. Water measuring tank also used to clean the pipeline after completion of experimentation. Both slurry preparation tank and water measuring tank are provided with drain valves for their proper cleaning. The data acquisition system is provided with data logger having 16 input ports which connects the pressure transducers and flow meters to store the experimental data. Experimental data from the data logger unit can be assessable to computer through internet by means of LAN (local area network) connectivity.

Table 5.1: Specifications of progressive slurry pump

Parameters	Value
Maximum flow rate	60 m^3/h
Maximum rpm	360 rpm
Input power	11.1 Kw
Temperature range	Up to 80 °C
pH Value	5-7.7

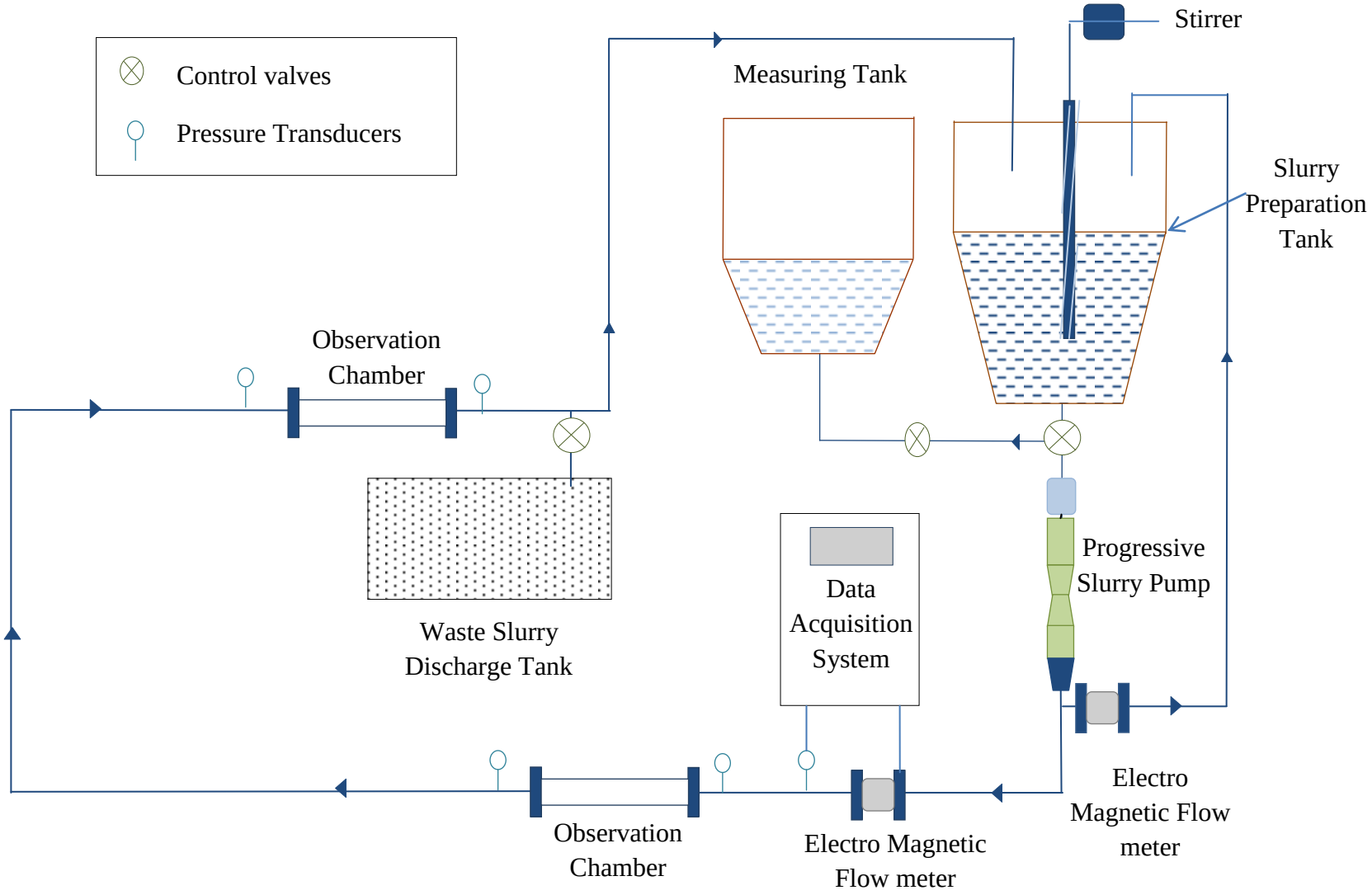

Figure 5.1: Schematics diagram of pilot plant test loop

Figure 5.2: Photographic view of pilot plant test loop

5.3.1 Instrumentation

Different instruments are used for the measurement of various operating parameters during the experimentation. The specifications and measuring procedures are explained as under.

5.3.1.1 Flow rate measurement

The mass flow rate in the test loop is measured by electromagnetic flow meter (Model- MM-50-1STS-TP68-2MP and Make- IOTA Flow Systems, India). The maximum pressure and temperature working range of electromagnetic flow meter are 40 bar and 60 ºC respectively. The measurements taken by electromagnetic flow meter follow the accuracy is ±0.5% deviation from main scale.

5.3.1.2 Pressure Measurement

Pressure in the slurry pipeline is measured with the help of Flush type pressure transducer (Model: S11; Make: WIKA Alexander Wiegand SE & Co., Germany). Pressure transducers are installed at pressure taps provided at different locations in test loop pipeline with fixed distances to measure the pressure. The accuracy of pressure transducers is ±0.25% of the main scale.

5.4 EXPERIMENTAL PROCEDURE

Experiments are conducted with the help of pilot plant test loop for the flow of coal and coal ash slurry. The slurry of required solid concentration is prepared in hopper shaped slurry preparation tank. A motor driven stirrer is provided on top of slurry preparation tank for uniform and proper mixing of slurry. It also prevents the settling of slurry suspension during the experimentation. Progressive slurry pump with maximum flow rate of 60 m^3/hr is driven by 3 phase squirrel cage induction motor (11 kW, 440 V and 21A) is used to transport the prepared slurry from the slurry preparation tank in close loop pipeline circuit. The slurry is discharge back to slurry preparation tank after circulation through the pipeline so that the continuous flow of slurry through the pipe line will be possible. The test loop pipeline is provided with a sampler, for slurry sample collection to monitor its density and solid concentration. The test loop pipeline is provided with flow control valves to change the flow rate over a wide range.

The flow meters (electromagnetic type) and pressure transducers are installed for measurement of discharge and pressure in the pipeline.. The monitoring of mass flow rate of slurry through the pipeline is done with the help of electro-magnetic flow meter (Make: IOTA Flow Systems, India) mounted horizontally on 50mm test loop pipeline. The pressure drop is measured by providing pressure taps over the fixed distance on the pipeline and pressure transducers are installed at pressure taps.

Subsequently, the slurry is prepared from coal, fly and bottom ash to measure the pressure drop in horizontal pipeline with different solid concentrations during transportation. The pressure drop measured from pilot-plant test loop is presented as a function of flow velocity in terms of mWc/100 m (meter of water column per 100 meter) of pipeline.

5.5 RANGE OF PARAMETERS

The experiments are performed on test loop to investigate the pressure drop characteristics in pipeline for 50-75 μm sized coal-water slurry with and without addition of 106-150 & 150-250 μm sized coal. The solid concentrations ranges from 30-60% (by weight) with flow velocities range of 2-5 ms^{-1}. The physio-chemical and mineralogical properties of the coal and coal ash have been already discussed in chapter 3 and rheological properties of coal-water slurry and fly ash slurry have also been discussed in chapter 4. Similarly, pressure drop characteristics of fly ash slurry are analysed subsequently with and without addition of bottom ash with above said parameters.

5.6 PRESSURE DROP CHARACTERISTICS OF COAL-WATER SLURRY

The pressure drop characteristics of coal-water slurry are investigated in the solid concentration of 29, 41, 51 and 61% (by weight). Pressure drop investigation is carried out with two different cases of coal-water slurry. In first case, the pressure drop characteristic of 53-75 μm sized coal-water slurry is studied whereas in second case, pressure drop characteristics of 53-75 μm sized coal-water slurry is evaluated with addition of 106-150 and 150-250 μm sized coal respectively.

5.6.1 Pressure drop characteristics of 53-75 µm sized coal-water slurry

Pressure measurements are taken for 53-75 µm sized coal-water slurry with solid concentrations of 29, 41, 51 and 61% (by weight) at different velocities ranging from 2-5 ms^{-1}. The variation of pressure drop with flow velocity at different solid concentration is shown in Figure 5.3. It is found from Figure 5.3 that the pressure drop characteristics of coal-water slurry increases with increase in solid concentration. The viscosity and slurry density of coal-water slurry increases with the increase in solid concentration which leads to increase in pressure drop in pipeline. Similar trend in pressure drop is observed by the various investigators (Verma et al. 2006; Seshadri et al. 2008; Chandel et al. 2009; Kumar et al. 2017).

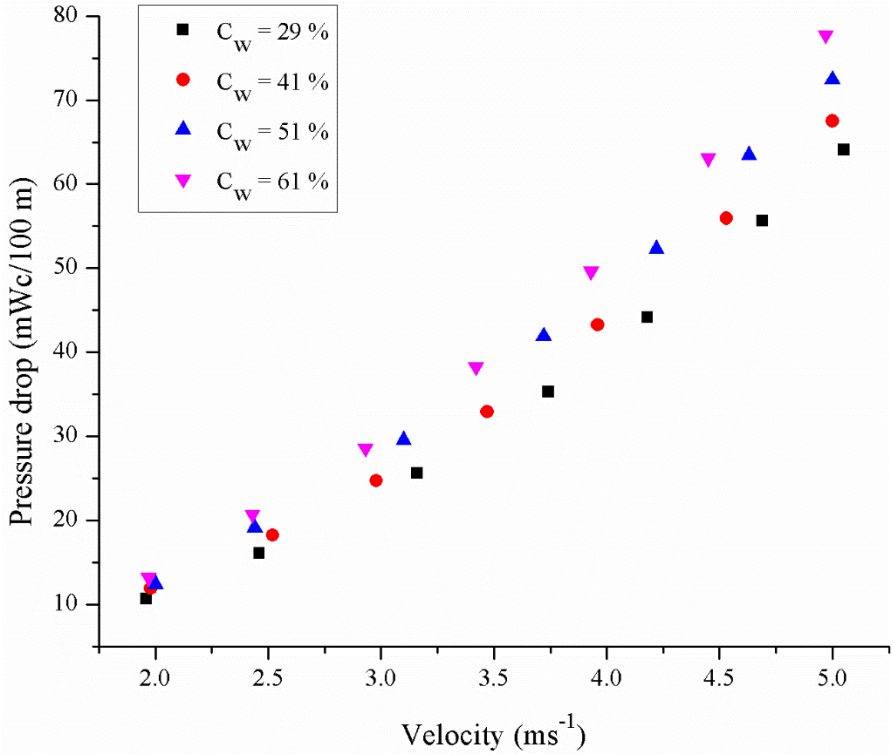

Figure 5.3: Pressure drop characteristics of 53-75 µm sized coal-water slurry

Maximum pressure drop is observed at solid concentration of 61% with 5 ms^{-1} flow velocity while with 2 ms^{-1} at 29% solid concentration shows minimum value of pressure drop. At 5 ms^{-1} flow velocity, the pressure drop increased by 6.75, 7.32 and 7.84% with the increase in solid concentration from 29-41, 41-51 and 51-61% (by weight) respectively. It is also observed that that pressure drop is the function of flow velocity. At 29% of solid concentration (by weight), pressure drop is increased by 112.60, 73.09 and

55.85% respectively with the increase in flow velocity from 2-3, 3-4 and 4-5 ms^{-1}. The similar trend is also reported by the researchers (Verma et al. 2006; Chandel et al. 2009).

5.6.2 Pressure drop characteristics of 53-75 µm sized coal-water slurry with addition of 106-150 µm sized coal

The pressure drop experimentation during the transport of coal-water slurry is also conducted to investigate the effect on pressure drop characteristics of coal-water slurry by blending 106-150 µm sized coal particles with 53-75 µm sized coal particles. The solid concentrations of 29, 41, 51 and 61% (by weight) is prepared by adding the 20, 30 and 40% of the 106-150 µm sized coal particles with remaining percentage of 53-75 µm sized coal particles. In this way there are three different cases for one solid concentration leads to total number of cases to twelve for which the experiment has been conducted. Figure 5.4-5.7 shows the effect of addition of 106-150 µm sized coal on pressure drop characteristics of 53-75 µm sized coal-water slurry at 29, 41, 51 and 61% solid concentration (by weight).

It is observed that pressure drop of 53-75 µm sized coal-water slurry in pipeline is decreases with addition of coarser 106-150 µm sized coal particles. Since the addition of coarser particles improves the effective packing arrangement within the coal particles which leads to reduction of the particle-particle friction among the particles of coal in slurry suspension during transportation further lead to decrease in pressure drop. Similar observations are also made by investigators (Seshadri et al. 2008; Chandel et al. 2009). It is seen from Figure 5.4 that at 29% solid concentration, pressure drop of 53-75 µm sized coal-water slurry is decreased by 27.20 and 25.90% with 20 and 30% addition of 106-150 µm sized coal particles at flow velocity of 2 ms^{-1}, as shown in Figure 5.4. However, value of pressure drop is increased by 6.55% with 40% addition of 106-150 µm sized coal particles. The percentage reduction in pressure drop is observed as 26.62 and 21.54% with 20 and 30% addition of 106-150 µm coal particles in 53-75 µm sized particles of coal. Further 40% addition leads to increase the pressure drop as 5.99% at flow velocity of 5 ms^{-1}.

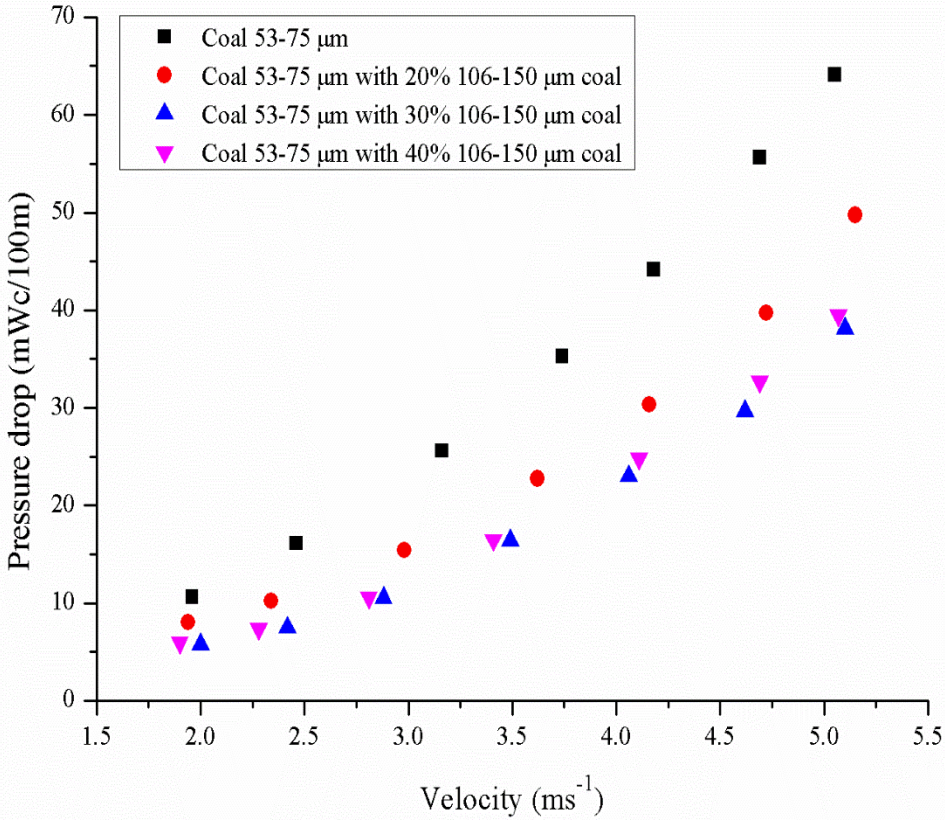

Figure 5.4: Pressure drop characteristics of 53-75 µm sized coal-water with addition of 106-150 µm sized coal at 29% solid concentration

Pressure drop of 53-75 µm sized coal with 20, 30 and 40% addition of 106-150 µm sized coal for 41% solid concentration is shown in Figure 5.5. At 41% solid concentration with 5 ms^{-1} flow velocity, pressure drop decreases as 22.88 and 22.50% with 20 and 30% addition whereas 4.51% increase with 40% addition of 106-150 µm sized coal particles in 53-75 µm sized coal-water slurry.

Similar trend of pressure drop is observed at 51 and 61% solid concentrations of coal-water slurry as represented in Figure 5.6-5.7. At 51% solid concentration with 5 m s^{-1} flow velocity, pressure drop is decreased by 21.10 and 23.43% with 20 and 30% addition while 6.81% of pressure drop is increases with 40% addition of 106-150 µm sized coal particles. The pressure drop is increased by 19.91 and 23.60% with 20 and 30% addition whereas 5.35% with 40% addition of 106-150 µm sized coal particles with 5 m s^{-1} flow velocity at 61% solid concentration (by weight).

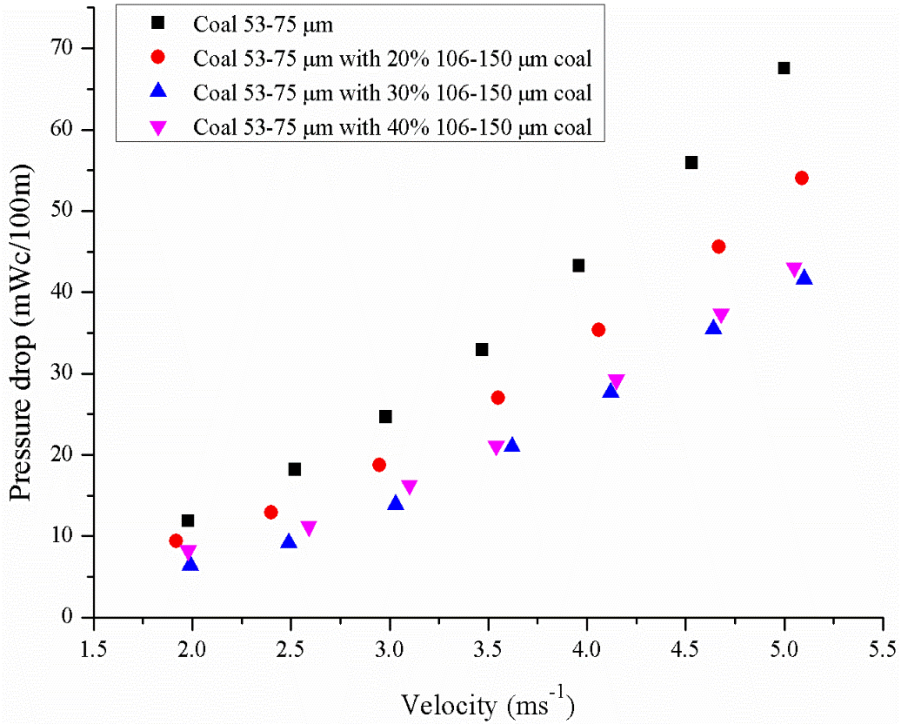

Figure 5.5: Pressure drop characteristics of 53-75 µm sized coal-water with addition of 106-150 µm sized coal at 41% solid concentration

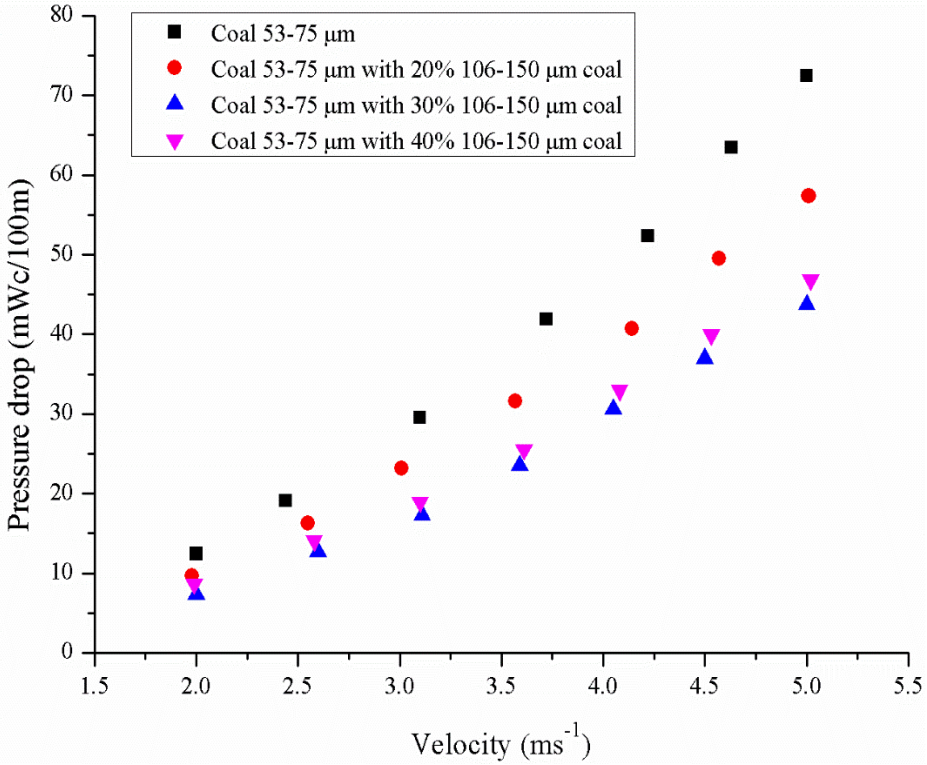

Figure 5.6: Pressure drop characteristics of 53-75 µm sized coal-water with addition of 106-150 µm sized coal at 51% solid concentration

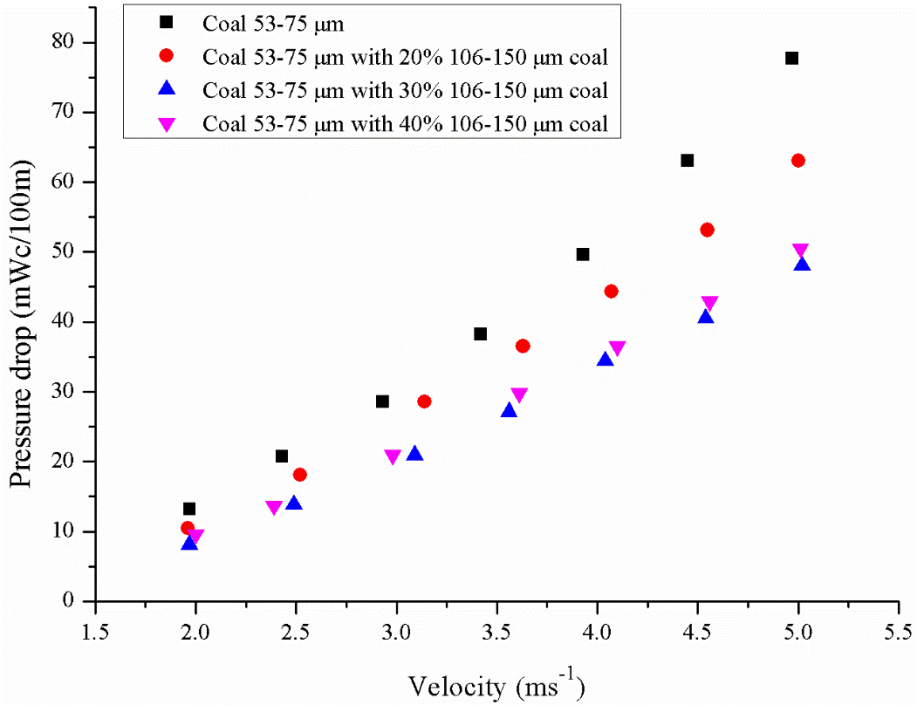

Figure 5.7: Pressure drop characteristics of 53-75 µm sized coal-water with addition of 106-150 µm sized coal at 61% solid concentration

5.6.3 Pressure drop characteristics of 53-75 µm sized coal-water slurry with addition of 150-250 µm sized coal

The pressure drop experimentation during the transport of coal-water slurry is extended to investigate the effect on pressure drop characteristics of coal-water slurry by blending 150-250 µm sized coal particles with 53-75 µm sized coal particles. The solid concentrations of 29, 41, 51 and 61% (by weight) is prepared by adding the 20, 30 and 40% of the 150-250 µm sized coal particles with remaining percentage of 53-75 µm sized coal particles. Figure 5.8-5.11 shows the effect of addition of 150-250 µm sized coal on pressure drop characteristics of 53-75 µm sized coal-water slurry at 29, 41, 51 and 61% solid concentration (by weight).

It is observed that pressure drop of 53-75 µm sized coal-water slurry in pipeline is decreases with addition of coarser 150-250 µm sized coal particles. At 29% solid concentration, pressure drop of 53-75 µm sized coal-water slurry decreased as 44.70 and 46.56% with 20 and 30% addition of 150-250 µm sized coal particles at flow velocity of 2 ms^{-1}, which is shown in Figure 5.8. However, value of pressure drop is decreased by 7.98% with 40% addition of 150-250 µm sized coal particles. Similarly the percentage reduction in pressure drop for 29% solid concentration and 5 ms^{-1} velocity of flow is

observed as 36.52 and 20.44% with 20 and 30% addition of 150-250 µm coal particles in 53-75 µm sized particles of coal. Further 40% addition leads to increase the pressure drop as 7.95% flow velocity of 5 ms^{-1}.

Pressure drop of 53-75 µm sized coal with 20, 30 and 40% addition of 106-150 µm sized coal for 41% solid concentration is shown in Figure 5.9. It is observed that at 5 ms^{-1} flow velocity 22.88 and 22.50% reduction is found in pressure drop with 20 and 30% addition respectively and 4.51% increase in pressure drop with 40% addition of 150-250 µm sized coal. Similar trend in pressure drop is observed for 51 and 61% solid concentrations are represented in Figure 5.10-5.11. At 51% solid concentration with 5 ms^{-1} flow velocity, pressure drop is decreased by 32.07 and 20.39% with 20 and 30% addition while 8.37% of pressure drop is increases with 40% addition of 106-150 µm sized coal particles. The pressure drop is increased by 30.15 and 20.19% with 20 and 30% addition whereas 6.84% with 40% addition of 106-150 µm sized coal particles with 5 m s^{-1} flow velocity at 61% solid concentration (by weight).

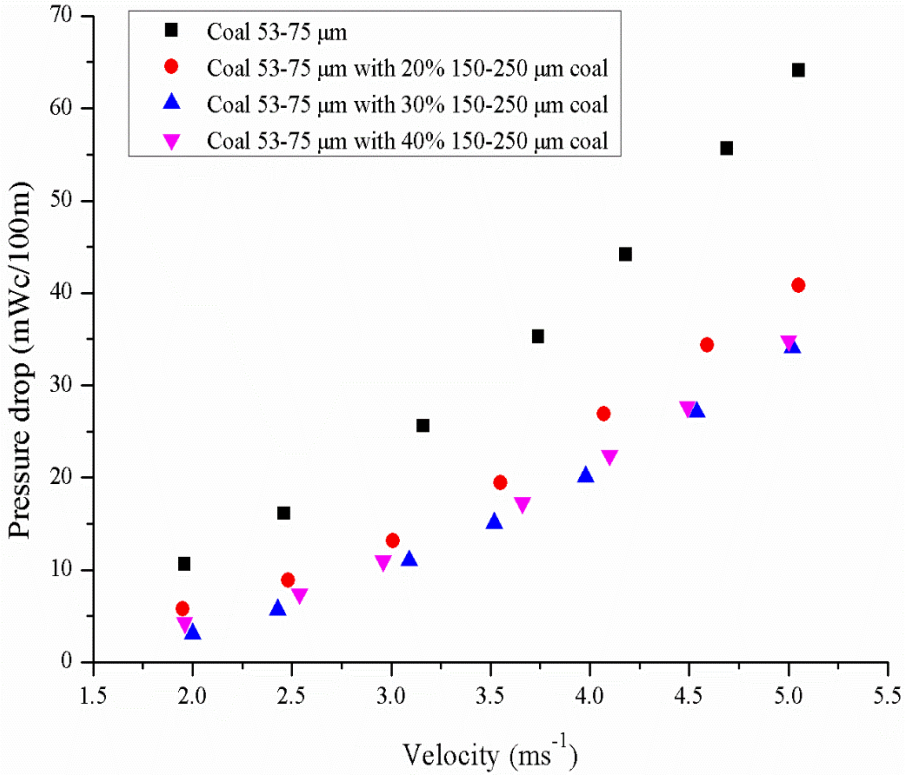

Figure 5.8: Pressure drop characteristics of 53-75 µm sized coal-water with addition of 150-250 µm sized coal at 29% solid concentration

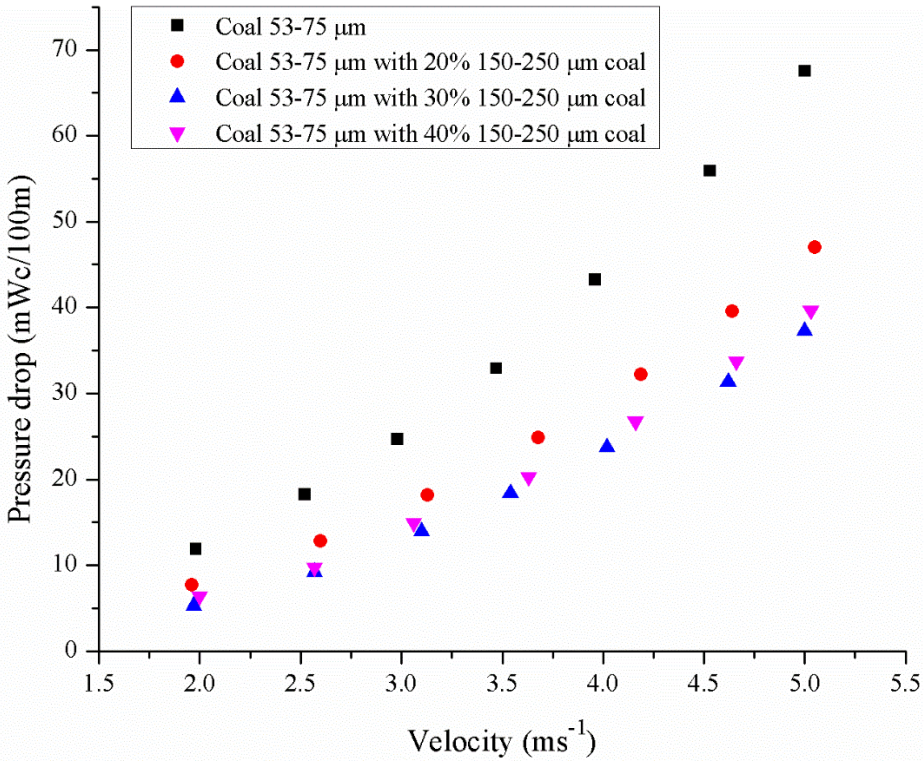

Figure 5.9: Pressure drop characteristics of 53-75 µm sized coal-water with addition of 150-250 µm sized coal at 41% solid concentration

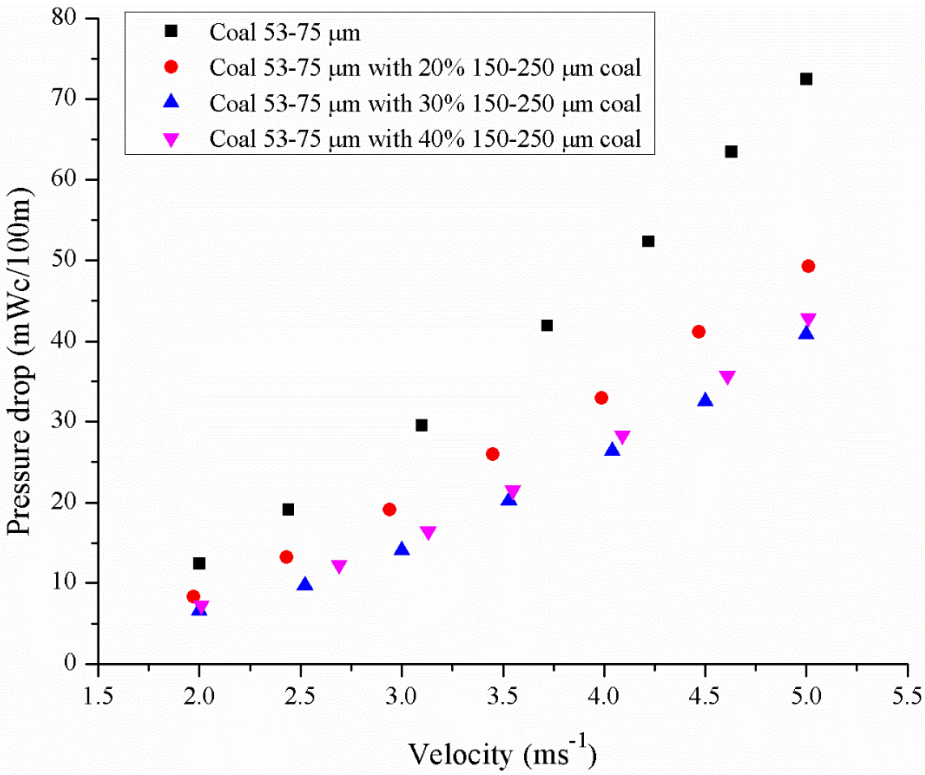

Figure 5.10: Pressure drop characteristics of 53-75 µm sized coal-water with addition of 150-250 µm sized coal at 51% solid concentration

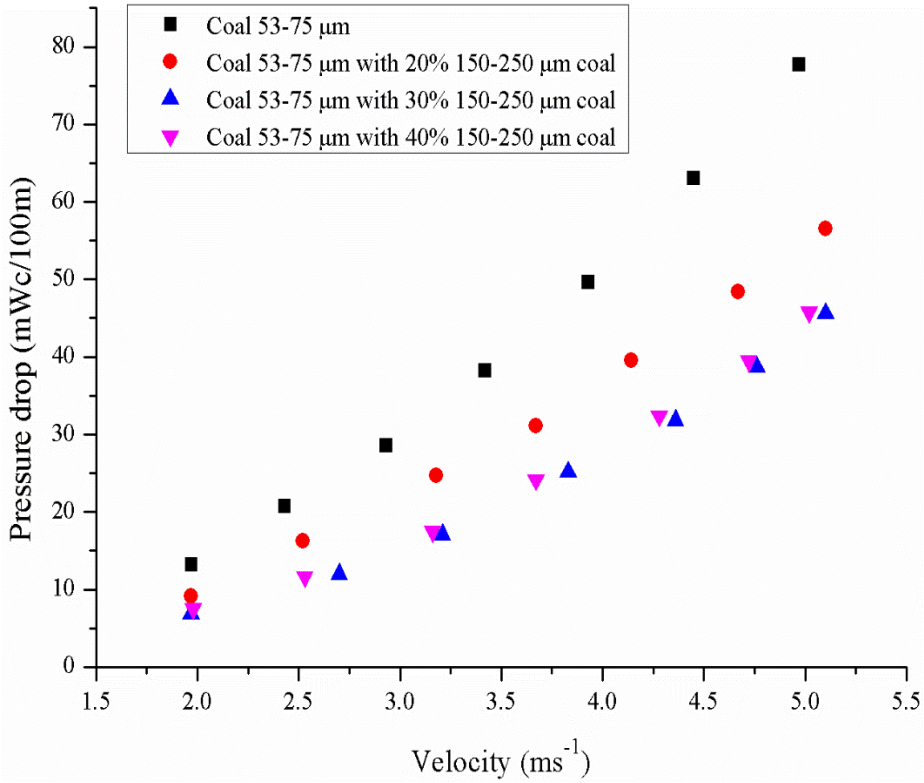

Figure 5.11: Pressure drop characteristics of 53-75 µm sized coal-water with addition of 150-250 µm sized coal at 61% solid concentration

From the results data, it can be concluded that the maximum percentage reduction in pressure drop is observed with 30% addition of coarser coal particles in finer coal particles. It is also found that addition of 150-250 µm sized coal particles shows more reduction in pressure drop as compared to 106-150 µm sized coal particles in 53-75 µm coal-water slurry.

5.7 PRESSURE DROP CHARACTERISTICS OF FLY ASH SLURRY

The pressure drop of fly ash slurry is measured with and without addition of bottom ash at different solid concentrations and flow velocities. Bottom ash is added as an additive with fly ash slurry in the percentage of 10, 20, and 30% (by weight). During the experimentation, the solid concentration of fly ash is taken as 29, 40, 51 and 61% (by weight) and flow velocity varies in the range of 2-5 ms^{-1}.

5.7.1 Pressure drop characteristics of fly ash slurry

The extensive experimentation is carried out to determine the pressure drop in horizontal slurry pipeline for the flow of fly ash slurry at different solid concentrations 29, 41, 51 and

61% (by weight). The pressure drop is measured in terms of meter of water column /100 m pipeline.

The variation in pressure drop in pipeline for fly ash slurry with flow velocity at solid concentration is shown in Figure 5.12. The variation of pressure drop in the slurry pipeline for fly ash slurry with solid concentration and flow velocity is follows the similar trend as coal-water slurry. The pressure drop increases with increase in solid concentration and flow velocity. At flow velocity of 2 ms^{-1}, the pressure drop increases about 13.23, 14.63 and 11.60% respectively with increase in solid concentration from 29-41, 41-51 and 51-61% (by weight) while 10.27, 12.27 and 9.58% increases at flow velocity of 5 ms^{-1}. The pressure drop at solid concentration of 29% (by weight) increased about 88.83, 79.82 and 52.53% with increase in flow velocity from 2-3, 3-4 and 4-5 ms^{-1} respectively however 83.15, 72.91 and 53.15% increase is observed at 61% of solid concentration. Similar observations are made by researchers (Verma et al. 2006; Chandel et al. 2009; Senapati et al. 2015) for the flow of coal ash slurry.

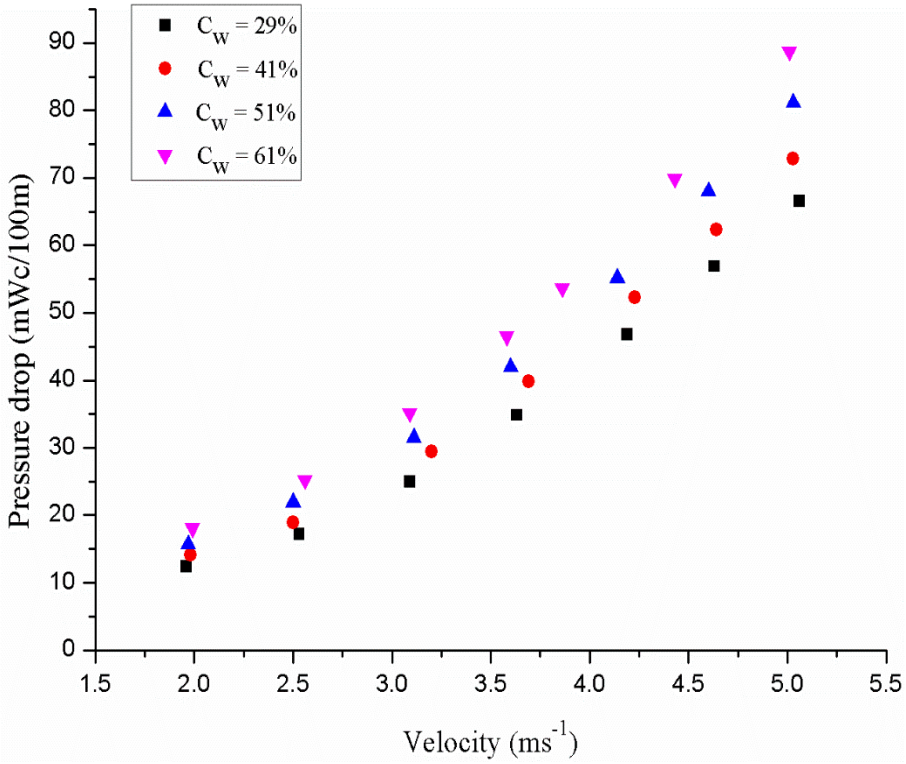

Figure 5.12: Pressure drop characteristics of fly ash slurry at different solid concentrations

5.7.2 Pressure drop characteristics of fly ash slurry with addition of bottom ash

Extensive experimentation is performed to investigate the effect of addition of bottom ash particles on pressure drop characteristics of fly ash slurry. Bottom ash is added in the fly ash in the proportion of 10, 20 and 30% (by weight). During the experimentation, solid concentrations of fly ash are taken as 29, 41, 51 and 61% (by weight) for flow velocity range of 2-5 ms^{-1}.

The variation in pressure drop of fly ash slurry with and without addition of bottom ash for flow velocity at different solid concentrations is shown in Figure 5.13-5.16. Pressure drop characteristic of fly ash slurry at 29% solid concentration (by weight) is represented in Figure 5.13. At flow velocity of 2 ms^{-1}, pressure drop is decreases as 9.51, 15.50 and 9.74% respectively with 10, 20, and 30% addition of bottom ash in fly ash slurry. However, 6.12, 11.54 and 7.13% decreases with 5 ms^{-1} flow velocity.

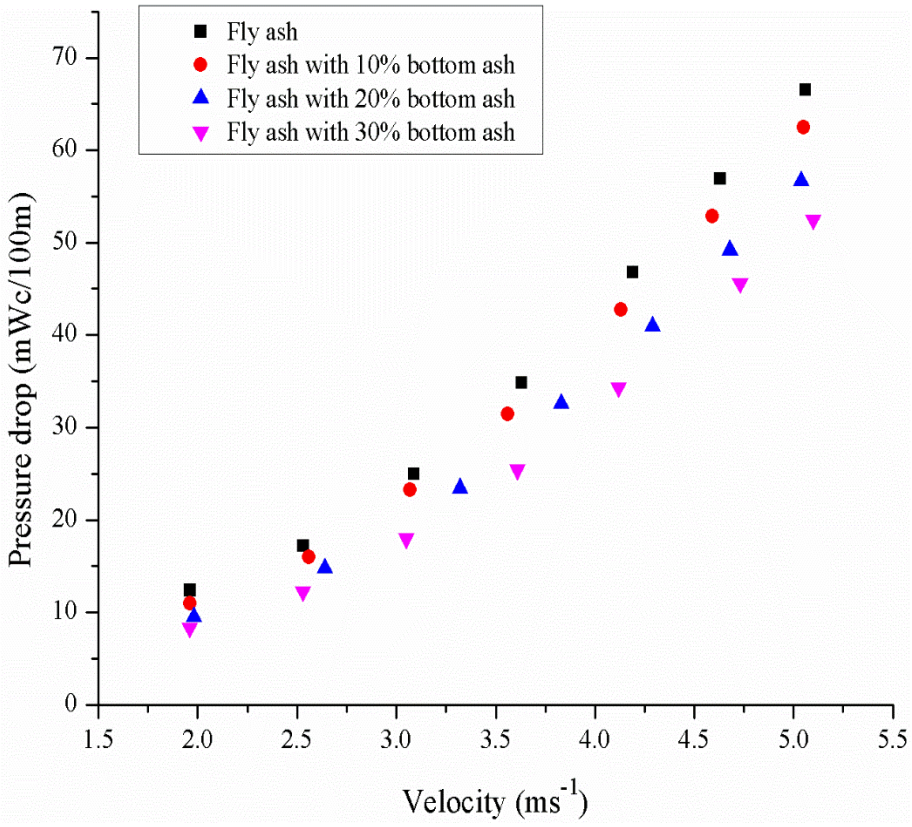

Figure 5.13: Pressure drop characteristics of fly ash slurry with addition of bottom ash at 29% solid concentration

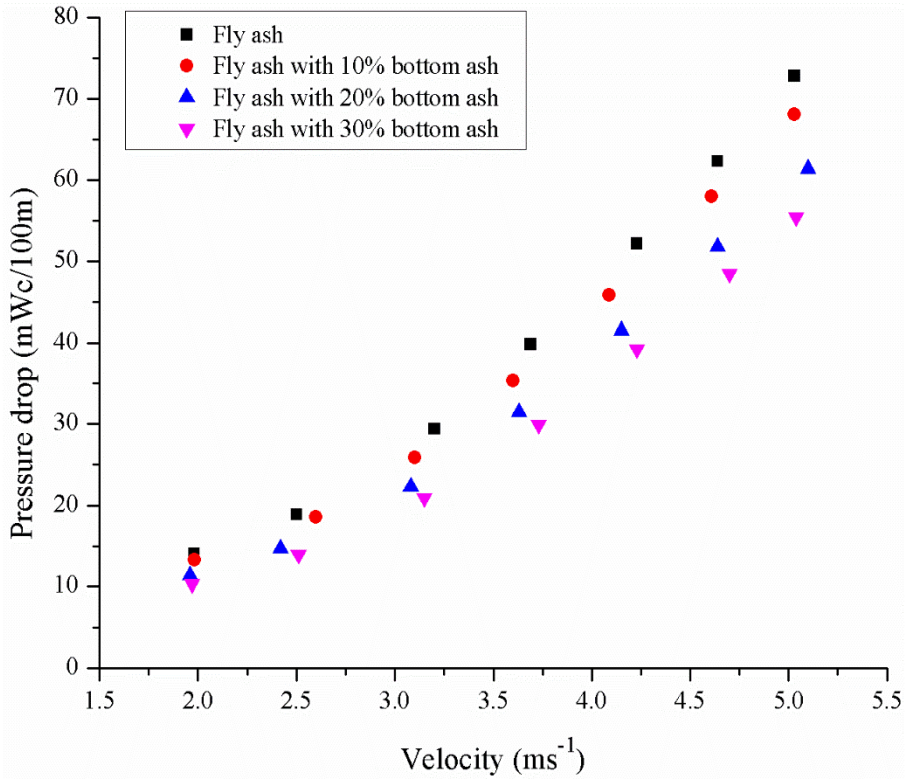

Figure 5.14: Pressure drop characteristics of fly ash slurry with addition of bottom ash at 41% solid concentration

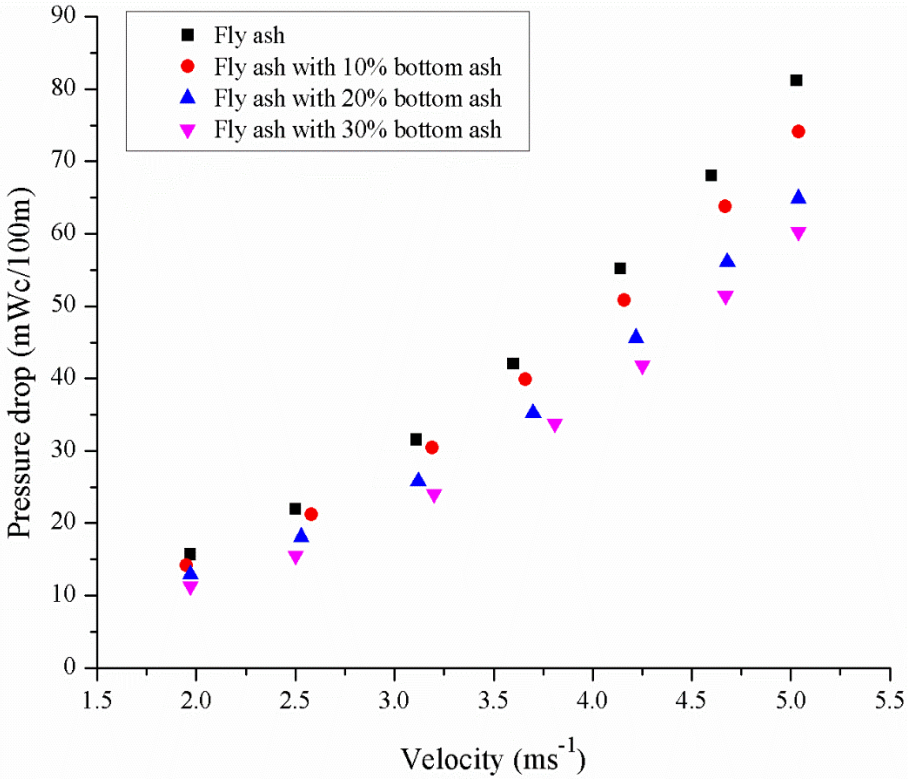

Figure 5.15: Pressure drop characteristics of fly ash slurry with addition of bottom ash at 51% solid concentration

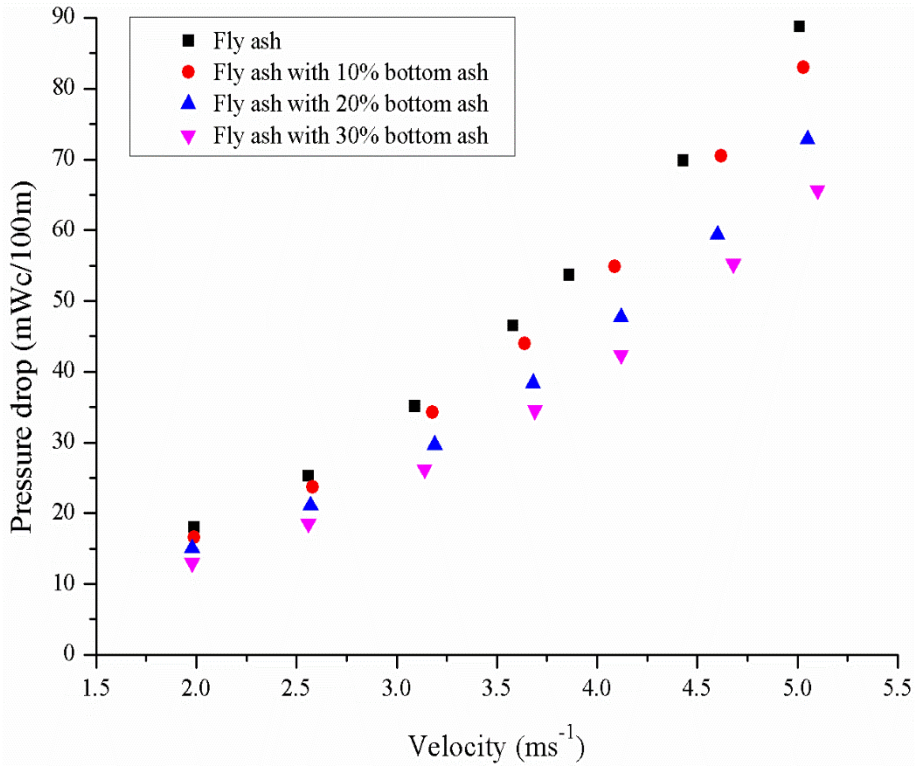

Figure 5.16: Pressure drop characteristics of fly ash slurry with addition of bottom ash at 61% solid concentration

Similar trend in pressure drop is observed for 41, 51 and 61% solid concentrations are represented in Figure 5.14-5.16. At 41% solid concentration and 5 ms^{-1} flow velocity, pressure drop is reduced as 6.62, 11.95 & 7.54% respectively with 10, 20 & 30% addition of bottom ash while 9.39, 12.52 & 7.39% for 51% solid concentration. However, the pressure drop is decreased as 7.18, 13.68 & 9.91% at 61% solid concentration.

From results data, it can be concluded that bottom ash addition improves the flow behaviour which results in reduction of pressure drop of fly ash slurry. The effect of addition of bottom ash is pronounced more at higher solid concentrations of fly ash slurry. The maximum reduction in pressure drop is observed with 20% addition of bottom ash at different solid concentrations.

5.8 CONCLUDING REMARKS

In the present chapter, the Pressure drop characteristics during the transportation of coal and fly ash slurry in a pipeline are determined experimentally for different concentrations and flow velocities. Also the pressure drop characteristics of coal-water slurry have been

conducted by adding the various percentages of coarser coal particles with finer coal particles. Similarly the pressure drop characteristics during the transportation of fly ash slurry have been studied by adding the various percentages of bottom ash in fly ash. Following conclusions are drawn from the results obtained:

- Pressure drop characteristic of both coal-water and fly ash slurry flow in horizontal pipeline is the function for solid concentration and flow velocity.
- Addition of coarser particles of coal in finer particulate coal-water slurry significantly reduces the pressure drop. The maximum reduction in pressure drop is observed with 30% addition of coarser particles in finer coal particles.
- The addition of 150-250 μm sized coal particles shows more reduction in pressure drop as compared to 106-150 μm sized coal particles in 53-75 μm coal-water slurry.
- The addition of bottom ash particles reduces the pressure drop of fly ash slurry in pipeline. Maximum reduction in pressure drop is observed with 20% addition of bottom ash.

CHAPTER 6

NUMERICAL EVALUTION OF PRESSURE DROP CHARACTERISTICS IN SLURRY PIPLINE

6.1 INTRODUCTION

The pressure drop characteristic of slurry flow in pipeline is very complex. The experimental evaluation of pressure drop characteristics in slurry pipeline is costly and time consuming. During the last few years, design and performance analysis of flow in slurry pipelines have experienced great progress with the availability of less expensive high performance computers and user friendly computational fluid dynamics (CFD) software's. The numerical simulation can provide information about the fluid flow characteristics inside the slurry pipline, and thus helps the design engineer to optimize the design of a particular slurry transportation system. This will reduce the cost and time of trial-and-error process of fabricating and testing of the prototype/ model. For this reason, CFD simulation is being used by many piping designers to estimate the head loss and flow field analysis. It is also feasible to visualize the flow in the pipeline by changing the various dependent parameters and provides the valuable information for pipeline design. The pressure drop characteristics of coal and coal fly ash slurry are determined experimentally which is explained in Chapter 5. Now-a-days user friendly commercial computational fluid dynamics code like FLUENT, CFX, and COMSOL etc. are available which can be used directly for simulation purpose.

All CFD codes contain three main components:

a. A **pre-processor** which is used for modeling of the components. It includes geometry generation, mesh generation and the boundary conditions.
b. A **flow solver** which is used to solve the governing equations of the fluid flow. Three methods are used to solve the problem.
    - Finite difference method
    - Finite element method
    - Finite volume method

A **post-processor** which is used for obtaining the results in data format, graphical form, vector plots etc.

6.2 GOVERNING EQUATIONS

Fluid flows are governed by the following three fundamental principles:

- Conservation of mass
- Conservation of momentum
- Conservation of energy

6.2.1 Conservation of Mass Equation

The equation for conservation of mass is written as follows:

$$\frac{\partial \rho}{\partial t} + .\nabla(\rho \vec{V}) = S_m \tag{6.1}$$

The equation is valid for incompressible as well as compressible flows. The source (S_m) is the mass addition in the continuous phase from the dispersed second phase.

For steady state incompressible fluid flow the continuity equation is given by:

$$\rho(\nabla \vec{V}) = 0$$

Where, $\nabla = \frac{\partial}{\partial x_i}\hat{i} + \frac{\partial}{\partial x_i}\hat{j} + \frac{\partial}{\partial x_i}\hat{k}$ and $V = u_i\hat{i} + u_j\hat{j} + u_k\hat{k}$

6.2.2 Conservation of Momentum Equation

Conservation of momentum equation is described as:

$$\frac{\partial}{\partial t}(\rho \vec{V}) + \nabla.(\rho \vec{V}\vec{V}) = -\nabla p + \nabla(\bar{\bar{\tau}}) + \rho\vec{g} + \vec{F} \tag{6.2}$$

Where,

The stress tensor $\bar{\bar{\tau}}$ is given as:

$$\bar{\bar{\tau}} = \mu[(\nabla \vec{V} + \nabla \vec{V}^T)] = -\frac{2}{3}\nabla.\vec{V}I \tag{6.3}$$

For steady state incompressible fluid flow, the momentum conservation equation is given by

$$\nabla.(\rho \vec{V}\vec{V}) = -\nabla p + \nabla.(\bar{\bar{\tau}}) + \rho\vec{g} + \vec{F}$$

6.2.3 Conservation of Energy Equation

$$\frac{\partial}{\partial t}(\rho_i) + \nabla.(\rho_i v) = -p\nabla.v + \nabla.(k\nabla T) + \varphi + S \quad (6.4)$$

6.3 TURBULENCE MODELS

Turbulence is characterized by fluctuations in the velocity flow field. Turbulence occurs when the inertia forces in the liquid dominant the viscous forces. In turbulent flow, the point velocity is divided in two components, one component is the time-averaged component$\bar{u}_i$ which is independent of time and other component is the fluctuating component (u_i'). Whose sum aggregate over a lay time period is zero.

$$u_i = \bar{u}_i + u_i' \quad (6.5)$$

The fluctuating quantities mix with the transport quantities like solid concentration, momentum and energy and produce the fluctuation in transported quantities. The amount of fluctuation may be small scale but have high frequency; they are very expensive to solve computationally in engineering calculation. The instantaneous governing equations can be assemble with time-averaged equations, or manipulated to minimize the small scale. Modified sets of governing equations can be solved numerically. Hoverer, modified governing equation contains additional parameters and turbulence models, are needed to obtain these variable. There is no single turbulence modeling scheme which is accepted to solve all types of the problems. The selection of the turbulence modeling scheme depends on the flow behaviour, type of the problem, level of the accuracy, computational resources and time of the simulation process.

6.3.1 Standard k-ε Model

Standard k-ε model works on the basis of transport equation of dissipation rate which comes out from physical reasoning and turbulence kinetic energy derived from the exact equation. The dissipation rate is generally denoted by symbol ε and turbulence kinetic energy is denoted by *k*. The k-ε model is solved by accounting the assumption that the nature of fluid flow is turbulent and bears negligible influence of molecular viscosity

The turbulence kinetic energy and rate of dissipation is obtained from the following equations:

$$\frac{\partial}{\partial t}(\rho k)+\frac{\partial}{\partial x_i}(\rho k u_i)=\frac{\partial}{\partial x_j}\left[\left(\mu+\frac{\mu_t}{\sigma_k}\right)\frac{\partial k}{\partial x_j}\right]+G_k+G_b-\rho\varepsilon-Y_M+S_k \qquad (6.6)$$

and

$$\frac{\partial}{\partial t}(\rho\varepsilon)+\frac{\partial}{\partial x_i}(\rho\varepsilon u_i)=\frac{\partial}{\partial x_j}\left[\left(\mu+\frac{\mu_t}{\sigma_\varepsilon}\right)\frac{\partial \varepsilon}{\partial x_j}\right]+C_{1\varepsilon}\frac{\varepsilon}{k}(G_k+C_{3\varepsilon}G_b)-C_{2\varepsilon}\rho\frac{\varepsilon^2}{k}+S_\varepsilon \qquad (6.7)$$

$$\mu_t=\rho C_\mu\frac{k^2}{\varepsilon} \qquad (6.8)$$

In these equations, G_k represents the generation of turbulence kinetic energy due to the mean velocity gradients. G_b is the generation of turbulence kinetic energy due to buoyancy. Y_M represents the contribution of the fluctuating dilatation in compressible turbulence to the overall dissipation rate. $C_{1\varepsilon}$, $C_{2\varepsilon}$ and $C_{3\varepsilon}$ are constants σ_k and σ_ε are the turbulent Prandtl numbers for k and ε, respectively. S_k and S_ε are user defined sources terms.

For standard k-ε model, value of constant used is:

$C_{1\varepsilon}$=1.44, $C_{2\varepsilon}$= 1.92, C_μ = 0.09, σ_k = 1.0 and σ_ε= 1.3.

6.3.2 RNG k-ε Model

The k-ε RNG model is derived from Navier-Stokes equation with the help of mathematical technique namely Renormalization group methods (RNG). Many terms of k-ε RNG model are similar to k-ε standard model whereas k-ε RNG model includes few additional terms which refine its accuracy. Accuracy of RNG model is improved in terms of strained flows and swirling flows. These features make the RNG model more accurate and reliable for a wider class of flows than the standard & model. The transport equations of k-ε RNG model are given below:

$$\frac{\partial}{\partial t}(\rho k)+\frac{\partial}{\partial x_i}(\rho k u_i)=\frac{\partial}{\partial x_j}\left(\alpha_k\mu_{eff}\frac{\partial k}{\partial x_j}\right)+G_k+G_b-\rho\varepsilon-Y_M+S_k \qquad (6.9)$$

and

$$\frac{\partial}{\partial t}(\rho\varepsilon)+\frac{\partial}{\partial x_i}(\rho\varepsilon u_i)=\frac{\partial}{\partial x_j}\left(\alpha_\varepsilon\mu_{eff}\frac{\partial \varepsilon}{\partial x_j}\right)+C_{1\varepsilon}\frac{\varepsilon}{k}(G_k+C_{3\varepsilon}G_b)-C_{2\varepsilon}\rho\frac{\varepsilon^2}{k}-R_\varepsilon+S_\varepsilon \qquad (6.10)$$

α_k and α_ε are the inverse effective Prandtl numbers for for *k* and ε, respectively. The model constant values are:

$C_{1\varepsilon}$=1.42, $C_{2\varepsilon}$= 1.68

6.3.3 Realizable k-ε Model

The Realizable k-ε model is quite different from k-ε standard model. The term 'realizable' denotes the reliability of constraints on the Reynolds stresses, consistent with the physics of turbulent flows. The Realizable k-ε model includes two different terms like alternative formulation for the turbulent viscosity and a modified transport equation for the dissipation rate. The transport equations for Realizable k-ε model are given as:

$$\frac{\partial}{\partial t}(\rho k)+\frac{\partial}{\partial x_i}(\rho k u_j)=\frac{\partial}{\partial x_j}\left[\left(\mu+\frac{\mu_t}{\sigma_k}\right)\frac{\partial k}{\partial x_j}\right]+G_k+G_b-\rho\varepsilon-Y_M+S_k \qquad (6.11)$$

and

$$\frac{\partial}{\partial t}(\rho \varepsilon)+\frac{\partial}{\partial x_i}(\rho \varepsilon u_j)=\frac{\partial}{\partial x_j}\left[\left(\mu+\frac{\mu_t}{\sigma_k}\right)\frac{\partial \varepsilon}{\partial x_j}\right]+\rho C_1 S\varepsilon-\rho C_2\frac{\varepsilon^2}{k+\sqrt{\nu\varepsilon}}+C_{1\varepsilon}\frac{\varepsilon}{k}C_{3\varepsilon}G_b+S_\varepsilon \qquad (6.12)$$

Where

$$C_1=\max\left[0.43,\frac{\eta}{\eta+5}\right],\eta=S\frac{k}{\varepsilon},S=\sqrt{2S_{ij}S_{ij}}$$

C_2 *and* $C_{1\varepsilon}$, are constants. The model constant values are:

$C_{1\varepsilon}$=1.44, $C_{2\varepsilon}$= 1.9, σ_k = 1.0 and σ_ε= 1.2.

6.3.4 *k*-ω Model

The *k*-ω model is a two-way transport model which solves the kinetic energy and turbulent frequency of particles. The turbulent frequency is denoted by symbol ω. This model is applicable to solve the fluid flow at low Reynolds number such as near wall region. This model does not contain the complex and non-linear damping functions. Turbulence kinetic energy and turbulent frequency relation is given as:

$$\frac{\partial}{\partial t}(\rho k)+\frac{\partial}{\partial x_i}(\rho k u_i)=\frac{\partial}{\partial x_j}\left(I_k\frac{\partial k}{\partial x_j}\right)+G_k-Y_k+S_k \tag{6.13}$$

and

$$\frac{\partial}{\partial t}(\rho \omega)+\frac{\partial}{\partial x_i}(\rho \omega u_i)=\frac{\partial}{\partial x_j}\left(I_\omega\frac{\partial \omega}{\partial x_j}\right)+G_\omega-Y_\omega+S_\omega \tag{6.14}$$

In these equations, G_k represents the generation of turbulence kinetic energy due to the mean velocity gradients. G_ω is the generation of ωI_k and I_ω represents the effective diffusivity of k and ω due to turbulence. S_k and S_ε are user defined sources terms.

6.3.5 SST k–ω Turbulence Model

The term 'SST' denotes the shear-stress transport. Mentor (1994) developed SST k–ω model by solving the standard k–ω and standard k–ε model which capable to accurate formulation of turbulence flow in pipeline. 6.3.1 SST k–ω Turbulence Model is effective in solving the equations near wall region at higher accuracy. This model is applicable over a wide range of flows (e.g., transonic shock waves, airfoils, adverse pressure gradient flows). The transport equations are given below:

$$\frac{\partial}{\partial t}(\rho k)+\frac{\partial}{\partial x_i}(\rho k u_i)=\frac{\partial}{\partial x_j}\left(I_k\frac{\partial k}{\partial x_j}\right)+G_k-Y_k+S_k \tag{6.15}$$

and

$$\frac{\partial}{\partial t}(\rho \omega)+\frac{\partial}{\partial x_i}(\rho \omega u_i)=\frac{\partial}{\partial x_j}\left(I_\omega\frac{\partial \omega}{\partial x_j}\right)+G_\omega-Y_\omega+D_\omega+S_\omega \tag{6.16}$$

In these equations, G_k represents the generation of turbulence kinetic energy due to the mean velocity gradients. G_ω represents the generation of ω, calculated as described for standard k-ω model. I_k and I_ω represent the effective diffusivity of k and ω, respectively. Y_k and Y_ω represents the dissipation of k and ω due to turbulence. D_ω represents the cross-diffusion term. S_k and S_ε are user defined sources terms.

6.4 MULTIPHASE FLOW MODEL

The multiphase flow model is used for the simulation of the multiphase flow problem like solid-liquid, liquid-vapour, solid-vapour etc. The multiphase flow model is designed with local variables of each individual phases. The multiphase flow problems are solved by the following two approaches:

- Euler-Lagrange approach
- Euler-Euler approach

In Euler-Lagrange approach, liquid phase acts as a continuous phase. Eulerian framework consists of additional coupling terms which are used to solve the mass and momentum equations with by utilizing Time averaged Navier-Stokes equations. Lagrangian framework is used to solve the dispersed phase by tracking the several particles together such as bubbles, drops, solid particles. The dispersed phase can exchange conservation of mass, momentum and energy with the liquid phase either by one-way or two-way coupling. The two frameworks are coupled through interaction forces applied by mechanism of coupling between continuous and dispersed phase. This makes Eulerian-Lagrangian approach appropiate for simulation of the small volume dispersed phase problems like simulation of fuel combustion, spray dryers and particle-laden flow etc.

Eulerian-Eulerian approach is based on the principle of interpenetrating continuum and RANS form of the mass & momentum equations are solved for both the faces. This approach uses the concept of volume fraction which assumes that volume fraction is a function of time and space and the addition of both is equal to 1. Conservation equations provide the empirical relationship which is solved for each phase by a number of equations having similar structure. Euler-Euler multiphase approach is sub-divided into three different models:

- Volume of fraction method (VOF)
- Mixture model
- Eulerian model

VOF model is utilized for separation flows in which continuous phase flow form as distinct interface with dispersed phase. In the VOF model, volume fraction of distinct phases is tracked throughout the entire computational domain and the momentum equations are shared by distinct phases. Mixture model is used for simulation of two of

more phases (liquid or particulate) moving at different velocities. Mixture multiphase models are used for modelling of homogenous two phase flow with very strong coupling. In this model, the mixture momentum equations are solved for each phase moving at prescribed relative velocity. The mixture model is used to simulate the sedimentation, cyclone separators, bubbly flows etc. Eulerian model is one of the most complex models among the other available models. Eulerian model solves the set of mass and momentum equations for both phases. The Eulerian model is used for the simulation of multiphase flow problems like simulation of bubble columns, risers, particle suspension, and fluidized bed etc.

6.4.1 Eulerian Model

In Eulerian model, slurry flow comprises of two separate phase namely bulk solid (b) and continuum (c) phases. The solid concentrations of bulk solid and continuum phases are $\alpha_b$and α_c respectively. The solid concentration of solid phase of coal (α_b) is considered as deciding factor for the selection of multiphase approach. The hypothetical assumption indicate that each phase of suspension individually satisfy laws of conservation of mass and momentum. Following governing equations involve in multiphase model are given below:

Continuity Equation

The continuity equation for bulk solid phase (b) used to evaluate the weight percentage of continuum phase (c) is given by:

$$\nabla.(\alpha_b \rho_b \vec{v}_b) = 0 \tag{6.17}$$

Momentum Equations

The momentum equation for bulk solid and continuum phases are given as equation (6.18) and (6.19).

For fluid phase

$$\nabla.(\alpha_c \rho_c \vec{v}_c \vec{v}_c) = -\alpha_c \nabla P + \nabla.(\overline{\overline{\tau_c}} + \overline{\overline{\tau_{tc}}}) + \alpha_c \rho_c \vec{g} + K_{bc}(\vec{v}_b - \vec{v}_c) + C_{vm}\alpha_b \rho_c (\vec{v}_b.\nabla \vec{v}_b - \vec{v}_c.\nabla \vec{v}_c) + C_l \alpha_b \rho_c (\vec{v}_c - \vec{v}_b) \times (\nabla \times \vec{v}_c) \tag{6.18}$$

The term $C_{vm}\alpha_b\rho_c(\vec{v}_c.\nabla\vec{v}_c - \vec{v}_b.\nabla\vec{v}_b)$ is the virtual mass force in which C_{vm} (virtual mass force coefficient) = 0.5.

For solid phase

$$\nabla.(\alpha_b\rho_b\vec{v}_b\vec{v}_b) = -\alpha_b\nabla P - \nabla P_b + \nabla.(\bar{\bar{\tau}}_b + \overline{\overline{\tau_{tc}}}) + \alpha_b\rho_b\vec{g} + K_{bc}(\vec{v}_b - \vec{v}_c) + C_{vm}\alpha_b\rho_c(\vec{v}_c.\nabla\vec{v}_c - \vec{v}_b.\nabla\vec{v}_b) + C_l\alpha_b\rho_c(\vec{v}_b - \vec{v}_c)\times(\nabla\times\vec{v}_c) \quad (6.19)$$

Where, $K_{bc}(\vec{v}_b - \vec{v}_c)$ is the drag force arises due to velocity difference between solid and liquid phases. The value K_{bc}represents the inter-phase drag coefficient and $C_l\alpha_b\rho_c(\vec{v}_b - \vec{v}_c)\times(\nabla\times\vec{v}_c)$ is the lift force in which C_l (lift coefficient) = 0.5.
$P_b$is the solid pressure as given by:

$$P_b = a_b\rho_b\theta_b + 2\rho_b(1+e_{bb})\alpha_b^2.g_{o,bb}.\theta_b \quad (6.20)$$

In equation (6.21), radial distribution function ($g_{o.bb}$) evaluates the probability between collision of particles which is given below:

$$g_{o.bb} = \left[1 - \left(\frac{\alpha_b}{\alpha_{b,max}}\right)^{1/3}\right]^{-1} \quad (6.21)$$

In equation (6.18) and (6.19) symbol, $\overline{\overline{\tau_{tc}}}$ is the Reynolds stress tensor, whereas $\bar{\bar{\tau}}_b$ is viscous stress tensor for bulk solid and $\bar{\bar{\tau}}_c$ is for continuum, are stated as below:

$$\overline{\overline{\tau_{t,c}}} = -\frac{2}{3}(\rho_c k_c + \rho_c\mu_{t,c}\nabla\vec{U}_c)\bar{\bar{I}} + \rho_c\mu_{t,c}(\nabla\vec{U}_c + \nabla\vec{U}_c^{tr}) \quad (6.22)$$

$$\bar{\bar{\tau}}_b = a_b\mu_b\left(\nabla\vec{v}_b + \nabla\vec{v}_b^{tr}\right) + a_b\left(\lambda_b - \frac{2}{3}\mu_b\right)\nabla\vec{v}_b\bar{\bar{I}} \quad (6.23)$$

$$\bar{\bar{\tau}}_c = a_c\mu_c\left(\nabla\vec{v}_c + \nabla\vec{\vartheta}_c^{tr}\right) \quad (6.24)$$

Bulk viscosity (λ_b) of solid phase given below:

$$\lambda_b = \frac{4}{3}a_b\rho_b d_b g_{o.bb}(1+e_{bb})\left(\frac{\theta_b}{\pi}\right)^{\frac{1}{2}} \quad (6.25)$$

6.5 MODELING OF SLURRY PIPELINE

Commercial computational fluid dynamics tool ANSYS R15.0 Design Modeler (DM) is used to model the slurry pipeline. The diameter and length of pipe are taken as 50 mm and 3 m respectively. Length of the pipe is large enough, so that the flow is fully developed. The schematic diagram of slurry pipeline is represented in Figure 6.1. The material of pipeline is assumed as mild steel of specific density of 7850 kg/m^3. Multiphase Eulerian model is used to determine the flow characteristics of mixture in pipeline. SST k-ω turbulent modelling scheme is selected for simulation of solid-liquid flow in pipeline (Rawat et al. 2016).

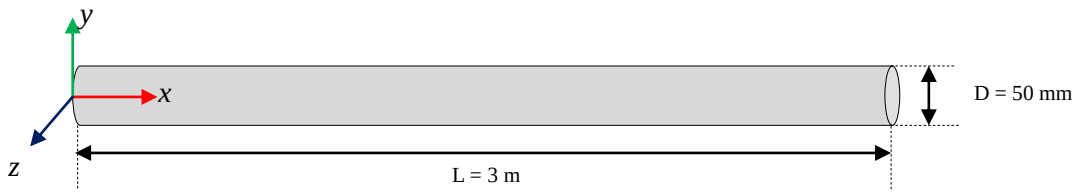

Figure 6.1: Schematic diagram of slurry pipeline

6.5.1 Boundary Conditions

The boundary conditions are applied at inlet, outlet and wall of pipe. The volume fraction and solid concentration of the solid and liquid phase is applied as Inlet boundary conditions. Pressure boundary condition is applied at outlet of pipeline. No slip condition is applied at wall of pipeline. The roughness constant of pipe wall is taken as 0.5 during the CFD simulation (Dewan, 2011). First order scheme is used for pressure correction as well as for solving of momentum, turbulent kinetic energy, and turbulence dissipation rate. 3D segregated solver is used for simulation of coal-water suspension. The pressure velocity coupling is done by using SIMPLE scheme. In order to achieve better convergence, under relaxation factors are applied for momentum, pressure, kinetic energy and dissipation rate as 0.7, 0.3, 0.8 and 0.8 respectively. Numerical simulations are performed on windows based Intel® Core™ i7-6700 machine having 3.41 GHz processing unit with 8 GB RAM and convergence criteria of solution parameter is set to 10^{-4} .

6.5.2 Grid independency test

Grid of tetrahedral-cooper type mesh is used to compute the pressure drop within solution domain as shown in Figure 6.2. Grid independency tests are performed to analyse the effect of total elements in mesh. Meshing of pipeline is done by ANSYS 15.0 Design Modeler (DM) with five different cell sizes. Total number of elements for 4, 5, 6, 7 and 8 mm cell size are found as 549665, 281749, 163622, 103759 and 70844 respectively. The details of mesh quality for different mesh sizes are given in Table 6.1. The value of skewness for all the mesh sizes lies between 0-0.25 which shows the optimal mesh with excellent domain. Also, the orthogonaltiy index is approaches to 1 i.e. 0.86 which indicates that mesh is of good quality.

Table 6.1: Mesh quality of pipe with different mesh sizes.

Mesh size	4	5	6	7	8
Skewness	0.218	0.217	0.217	0.22	0.221
Orthogonality index	0.86	0.86	0.86	0.856	0.858

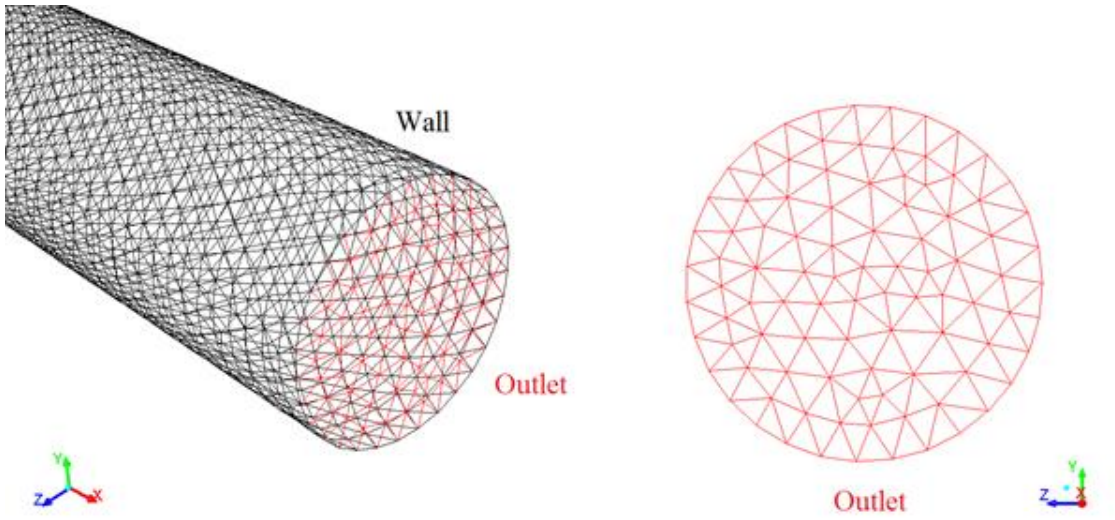

Figure 6.2: Grid of tetrahedral-cooper type mesh

Numerical simulations are performed by using the velocity inlet, pressure outlet and No slip wall boundary conditions. The grid independency test is performed for 59 µm weighted mean particle size of coal with 30% (by weight) solid of coal-water slurry. The solid concentration is taken as 2 ms^{-1}. Pressure drop variation with different meshes of different number of cells is shown in Figure 6.3. It is observed from Figure 6.3 that value

of pressure drop becomes independent after 281749 grid size. Roache (1997) proposed the grid convergence index model to check the grid convergence. According to Roache (1997), grid convergence index (GCI) is the measure of quantitative error associated with mesh which is represented below:

$$\mathrm{GCI}^{12} = 3\frac{{e_a}^{12}}{r^p - 1} \tag{6.39}$$

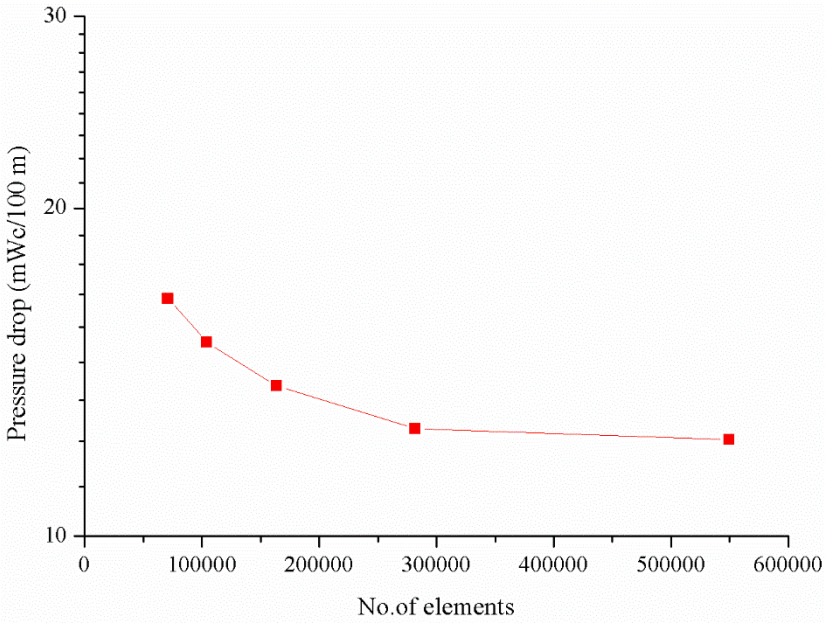

Figure 6.3: Variation of pressure drop with number of elements

Where, constant value '3' represents value of safety factor, the value of factor 'p' is taken as 2, $r = (N_1/N_2)^{1/3}$ and e_a= relative error associated with two grid size $\left|\frac{f_1 - f_2}{f_1}\right|$. The values f_1 and f_2 represents the pressure drop on two different grid sizes. GCI is used to measures the difference between CFD simulated values of pressure for two different grids spacing in present study. GCI test is performed for four different levels of mesh sizes. Figure 6.4 shows the GCI values of between different levels.

The value of pressure drop decreases with increase in number of elements. The GCI value is found as 0.958 and pressure drop is increasing from 15.07 to 16.53 mWc/100m for level 4-5. For level 3-4, 2-3 and 1-2, the value of GCI is found as 0.818, 0.654 and 0.11 and pressure drop increases 12.74 to15.07, 12.55to 12.74 and 12.27to 12.55 mWc/100m respectively. The minimum GCI value is found at level 1-2 is 0.11 which deviates lesser as

compared to value 0.65 at level 2-3. So, mesh size with cell size 5 mm contributes minimum error between different grid mesh sizes and also shows minimum deviation in pressure drop.

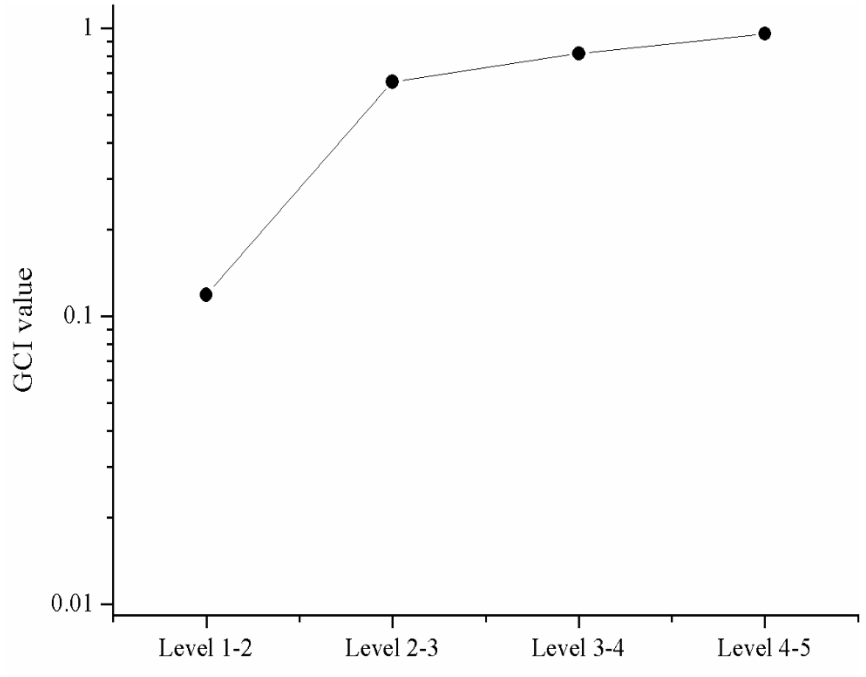

Figure 6.4: Variation of GCI index with cell size for different meshes

6.5.3 Turbulence model for prediction of pressure drop in slurry pipeline

Numerical simulations are performed by using different turbulence models to calculate the pressure drop in slurry pipeline for the flow of coal-water slurry. Numerical simulations are carried out on 50 mm diameter pipe. The solid concentration of slurry is taken as 61% (by weight) with 59 μm weighted mean particle size for different flow velocities ranges between 2-5 ms^{-1}. Numerical simulations are performed to compare the pressure drop in pipeline with Realizable k-ε, RNG *k-ε*, Standard *k-ε*, SST *k-ω* and Standard *k-ω* different turbulence modelling schemes. Figure 6.5 shows the comparison of present numerical simulation results with the experiment results. Maximum deviation in pressure drop for Realizable k-ε, RNG *k-ε*, Standard *k-ε*, SST *k-ω* and Standard *k-ω* turbulence models is observed as 10.07, 11.40, 13.37, 10.07, 5.25 and 7.90% respectively. Simulation results of SST k-ω model shows minimum deviation and establish close agreement with experimental data and lies in 7.90% deviation. SST k-ω model showed better results as compared to other models. So in the present work, the numerical simulations are performed on 50 mm pipe by using SST *k-ω* turbulence model for coal-water slurry

suspension with different flow velocities ranges between 2-5 ms^{-1} at solid concentrations ranges between 30-60% (by weight).

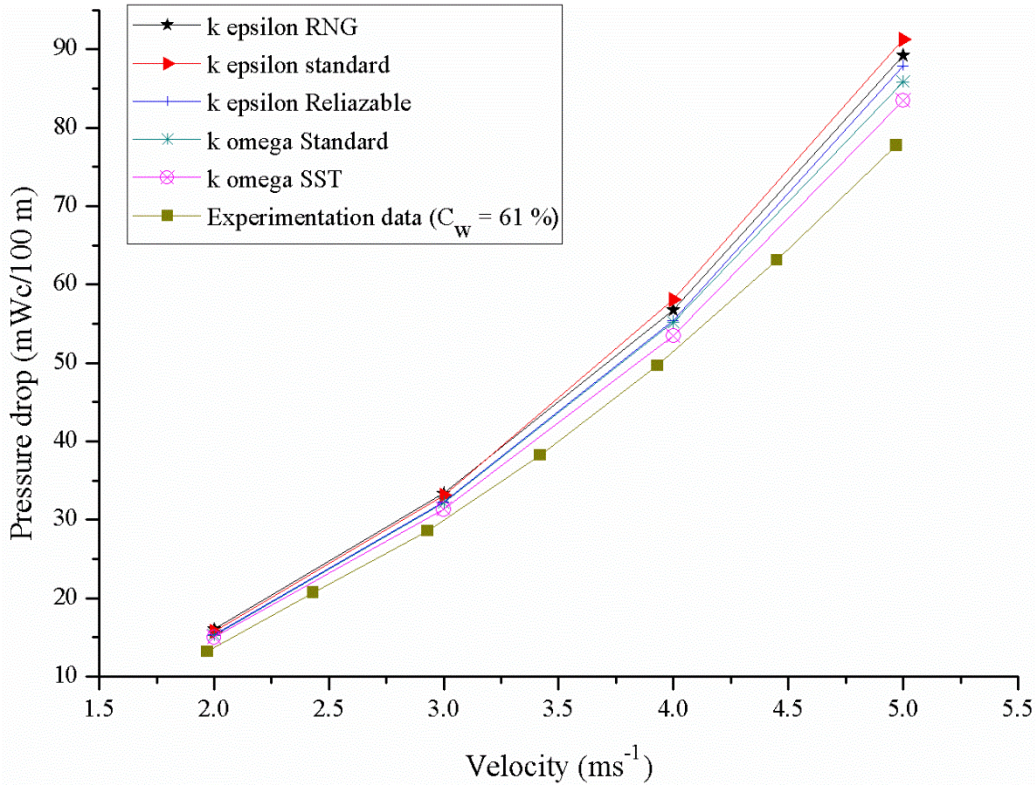

Figure 6.5: Validation of numerical simulation with experimentation

6.6 PREDICTION OF PRESSURE DROP CHARACTERISTICS OF COAL-WATER SLURRY IN SLURRY PIPELINE

SST k-ω model is used for the numerical simulation of solid-liquid flow through the pipeline. Water is taken as primary phase whereas solid is taken as secondary phase. The coal particles of 53-75 µm size are taken as solid. The pressure drop characteristics of coal-water slurry in pipeline are numerically predicted for solid concentration (C_w) of 30, 40, 50 and 60% (by weight) at flow velocity ranging from 2-5 ms^{-1}. Flow becomes fully developed after 0.5 m distance from inlet of pipe. The pressure drop is calculated in 1 m from pipe outlet and volume fraction distributions of coal particles are observed at pipe outlet (Kaushal et al. 2012).

6.6.1 Pressure drop characteristics of coal-water slurry

The variations of pressure drop in slurry pipeline are calculated in the terms of mWc/100m (meter of water column per meter) with flow velocity at different solid concentrations is

shown in Figure 6.6. It is observed that pressure drop increases with increases flow velocity at all solid concentrations of coal-water slurry. As the flow velocity of particles increases, the kinetic energy of particles also increases which tends to increase the impact forces and localized attacks on pipe wall that results in higher pressure drop. Similar phenomenon is experimentally observed by researchers (Chandel et al. 2009; Senapati et al. 2010) with fly ash slurry.

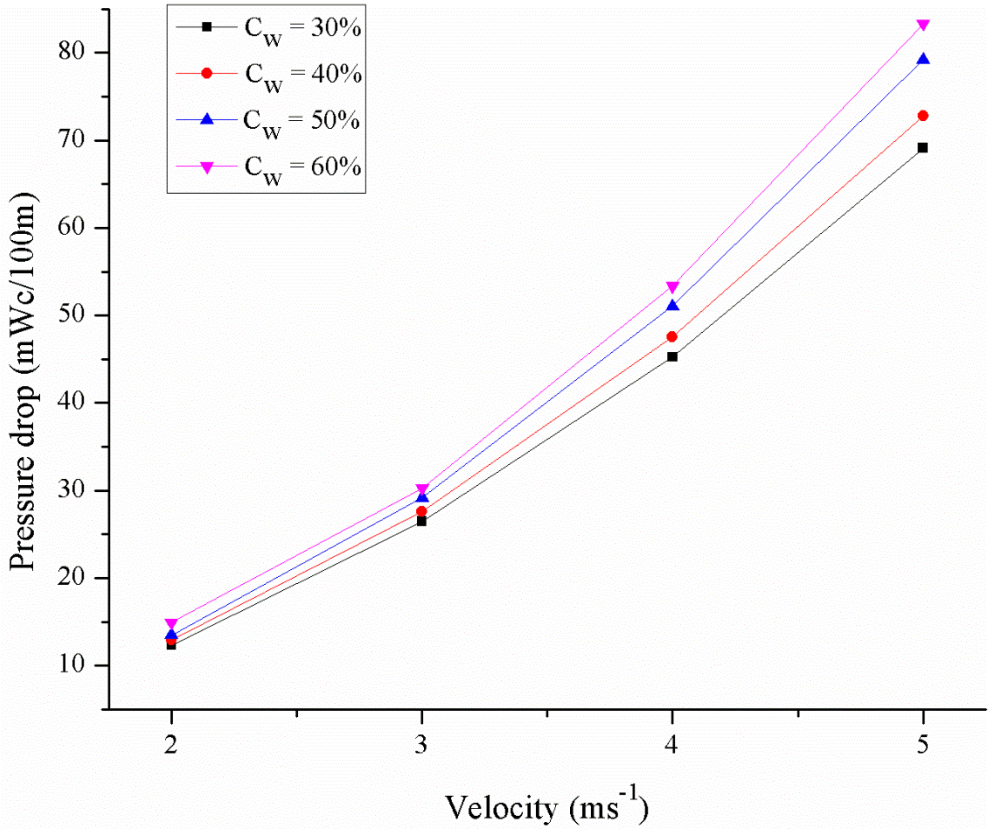

Figure 6.6: Pressure drop characteristics of coal-water slurry at different solid concentrations

The gradual increase of pressure drop continues up to flow velocity of 3 ms^{-1} and further increase in flow velocity leads to lower the increase in pressure drop. At 30% solid concentration (by weight), pressure drop is increase as 53.38, 41.46 and 34.57% with increase in flow velocity from 2-3, 3- 4 and 4-5 ms^{-1} respectively whereas at 60% solid concentration, 52.26, 41.44 and 35.97% increase in pressure drop is observed. It seems that minimum pressure drop in pipeline is 12.34 mWc/100m at 30% solid concentration (by weight) with flow velocity of 2 ms^{-1} whereas maximum pressure drop is observed as 83.33 mWc/100m at solid concentration of 60% (by weight) with flow velocity of 5 ms^{-1}.

It is also observed that at a specific flow velocity, pressure drop increases with the increase in solid concentration. This is due to the fact that increase in solid concentration results in steep increase in density and viscosity of the slurry suspension. Similar type of phenomenon is observed by investigators (Verma et al. 2006; Seshadri et al. 2008; Kumar et al. 2017).

6.6.2 Volume fraction distribution of coal-water slurry

The volume fraction distribution contours in vertical plane of pipe outlet at different flow velocities 2-5 ms^{-1} with solid concentration 30% (by weight) is shown in Figure 6.7. From Figure 6.7(a), higher settling region is observed at lower portion of pipe wall due to action of gravity whereas lean concentration region is visible on the upper portion of pipe at 2 ms^{-1} solid concentration. At 5 ms^{-1} solid concentration, settling region at the lower portion and lean concentration region situated at upper portion of pipe reduces, as shown in Figure 6.7(d). Higher volume fraction zone is represented by red colour. Higher volume fraction zone exits at lower solid concentration i.e. 2 ms^{-1} which occupies large area. It is also noticed that the volume fraction zone shifts away from surrounding wall with increase in flow velocity.

Similar trend of change in volume fraction distribution observed at 40, 50 and 60% solid concentration at different velocities are shown in Figures 6.8-6.10 respectively. From Figure 6.8-6.10, the magnitude of volume fraction distribution increases with increase in solid concentration. Maximum magnitude of volume fraction at pipe outlet is found as 0.261, 0.334, 0.399 and 0.458 respectively at 30, 40, 50 and 60% solid concentration (by weight) at solid concentration of 2 ms^{-1}. From volume fraction distribution results, it can be concluded that the lean concentration region and settling region reduces with the increase in flow velocity at the upper and lower portion of the pipe due to homogenous mixing of slurry.

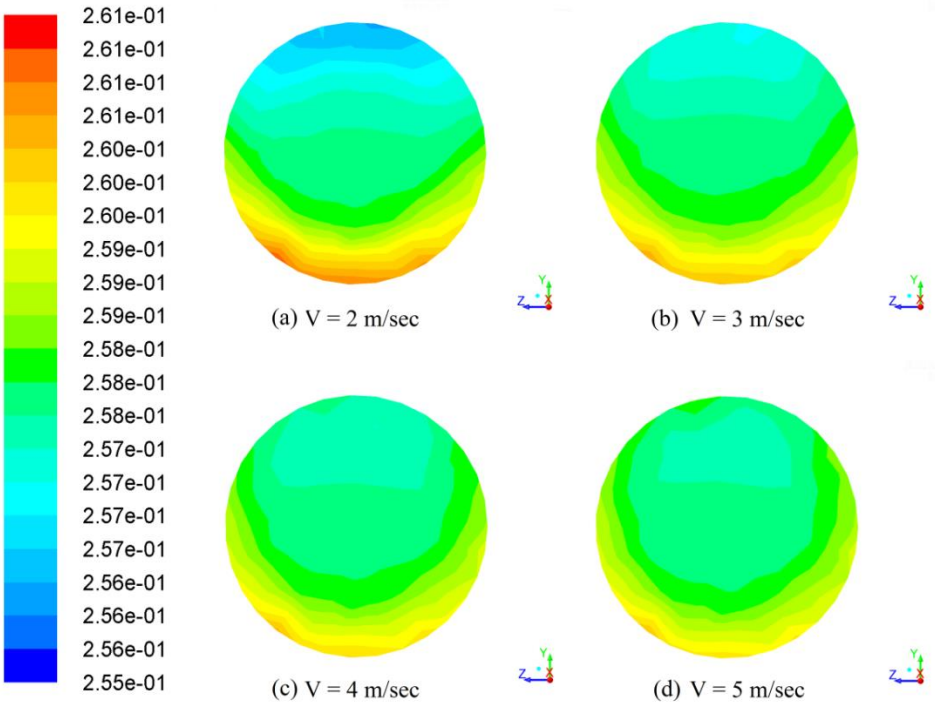

Figure 6.7: Volume fraction contours of coal-water slurry at 30% solid concentration

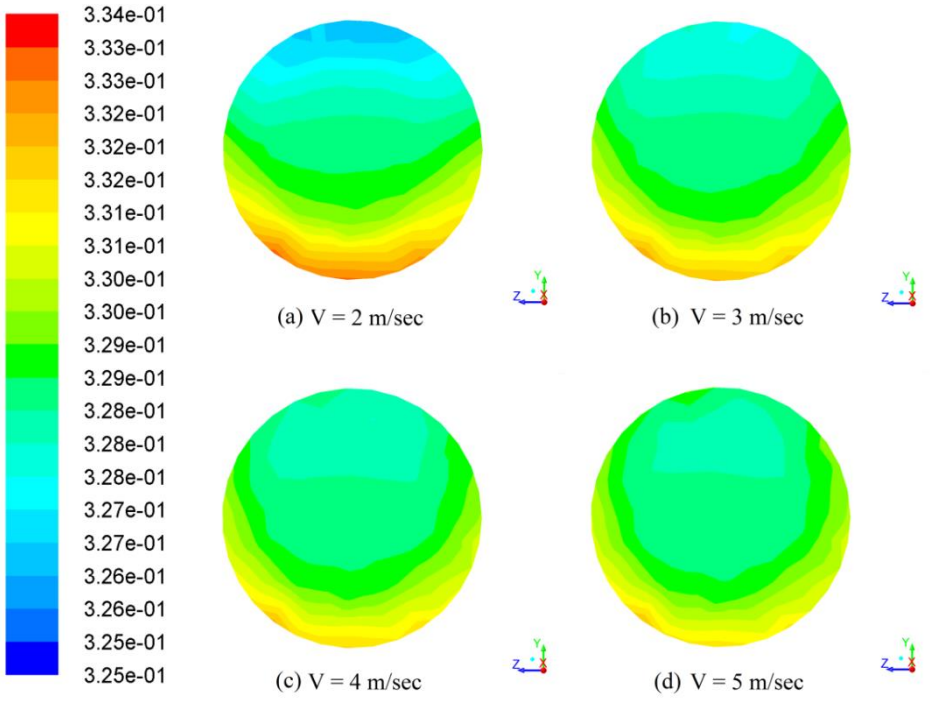

Figure 6.8: Volume fraction contour of coal-water slurry at 40% solid concentration

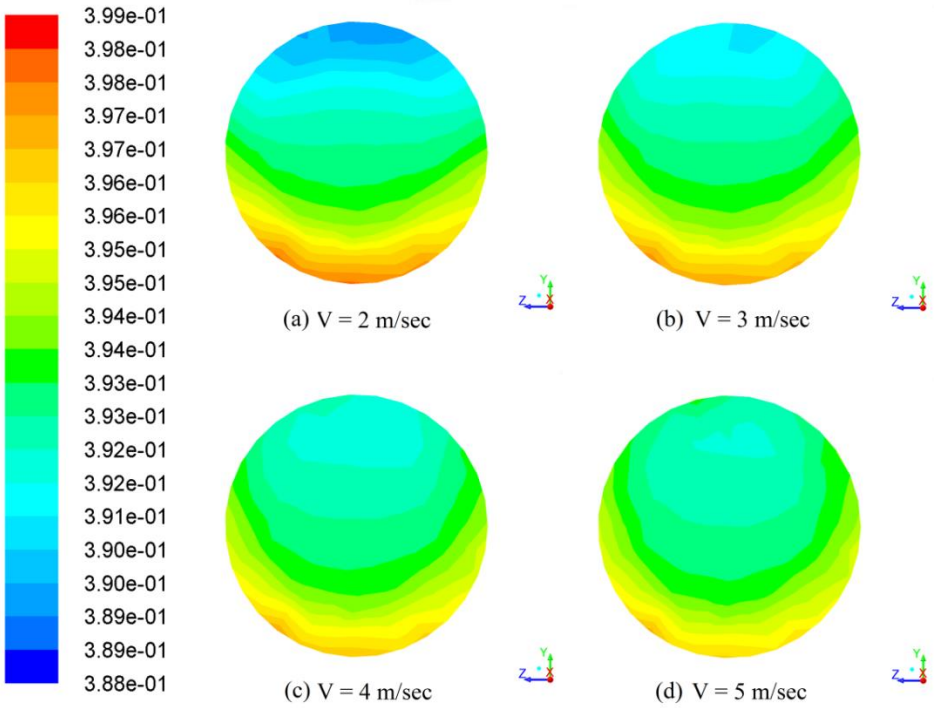

Figure 6.9 : Volume fraction contours of coal-water slurry at 50% solid concentration

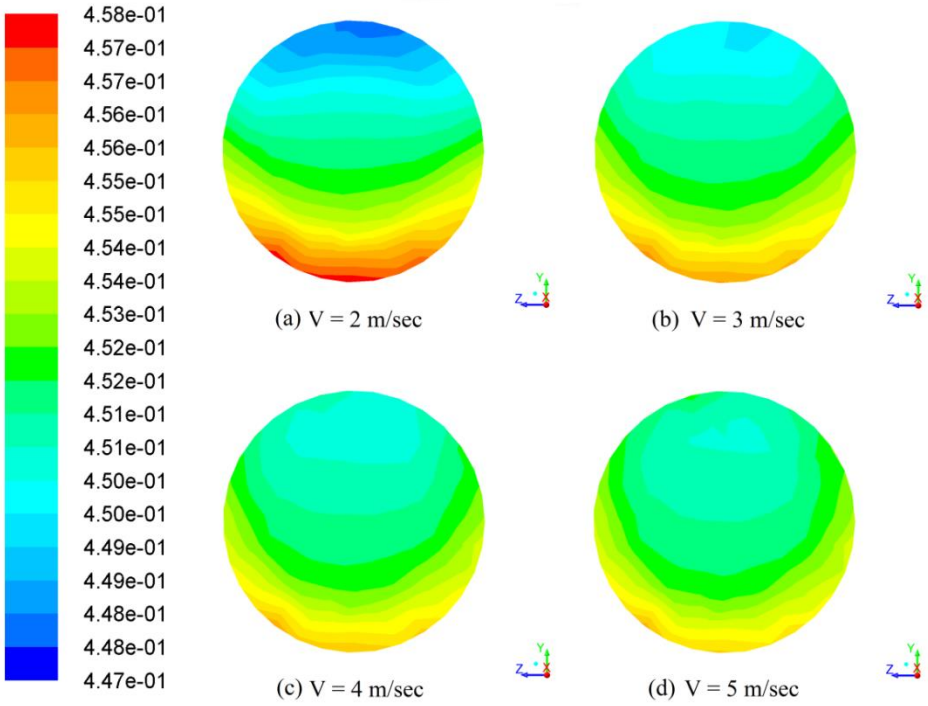

Figure 6.10: Volume fraction contours of coal-water slurry at 60% solid concentration

6.6.3 Effect of particle size on pressure drop characteristics of coal-water slurry

Pressure drop characteristics in slurry pipeline is also numerically evaluated for the flow of coal-water slurry at 59,109, 159 and 209 µm sized coal particle of having 30-60% solid concentration (by weight) with 2-5 ms^{-1} flow velocity. The effect of particle size is investigated on pressure drop characteristics and concentration distribution.

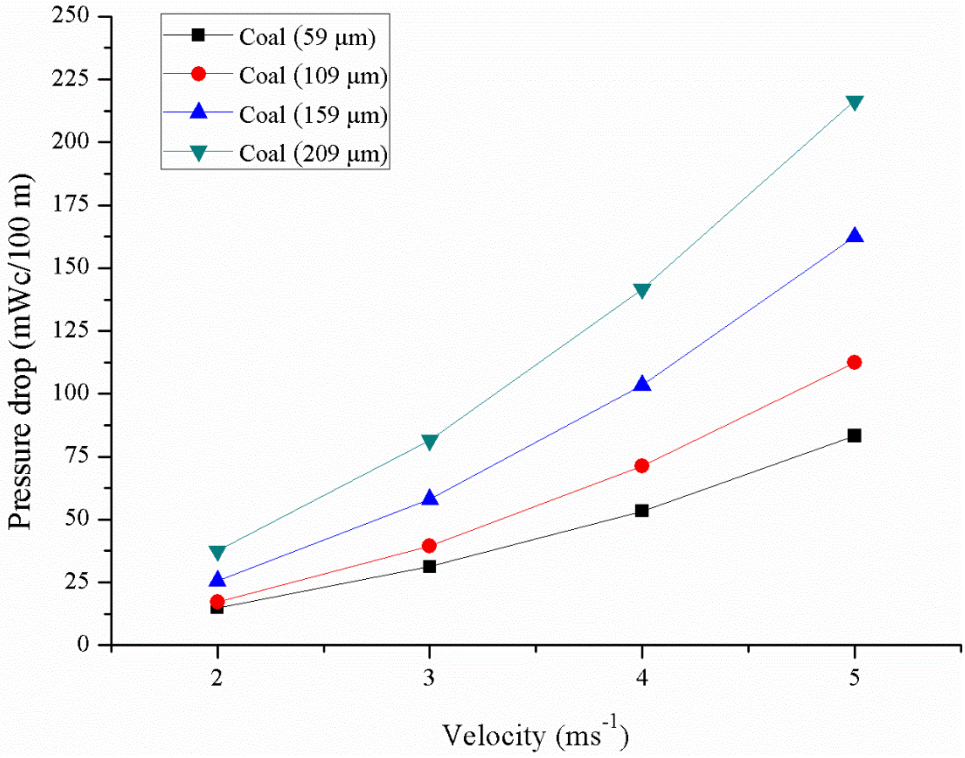

Figure 6.11: Effect of particle size on pressure drop characteristics of coal-water slurry at 60% solid concentration

The variation of pressure drop characteristics of pipeline with particle size at different flow velocities 2-5 ms^{-1} at solid concentration 60% (by weight) is shown in Figure 6.11. It is observed that the pressure drop increases with increase in particle size at all velocities. The coarser coal particles (209 µm) show higher value of pressure drop as compared to other particle. Coarser coal particles are having more impact on pipe wall as compare to finer coal particles which results in higher pressure drop. At 5 ms^{-1} solid concentration, increase in pressure drop is observed as 25.89, 30.82 and 24.92% for particle size range 59-109, 109-159 and 159-209 µm respectively. Minimum pressure drop in slurry pipeline is found as 14.92 mWc/100 m for 59 µm coal at 2 ms^{-1} flow velocity whereas maximum pressure drop is found as 216.48 mWc/100 m for 209 µm coal at 5 ms^{-1} flow velocity. It is also found that pressure drop increase marginally with increase in particle size at 2 ms^{-1}

flow velocity with 60% solid concentration (by weight) whereas steep increase in pressure drop is observed at 5 ms^{-1} flow velocity.

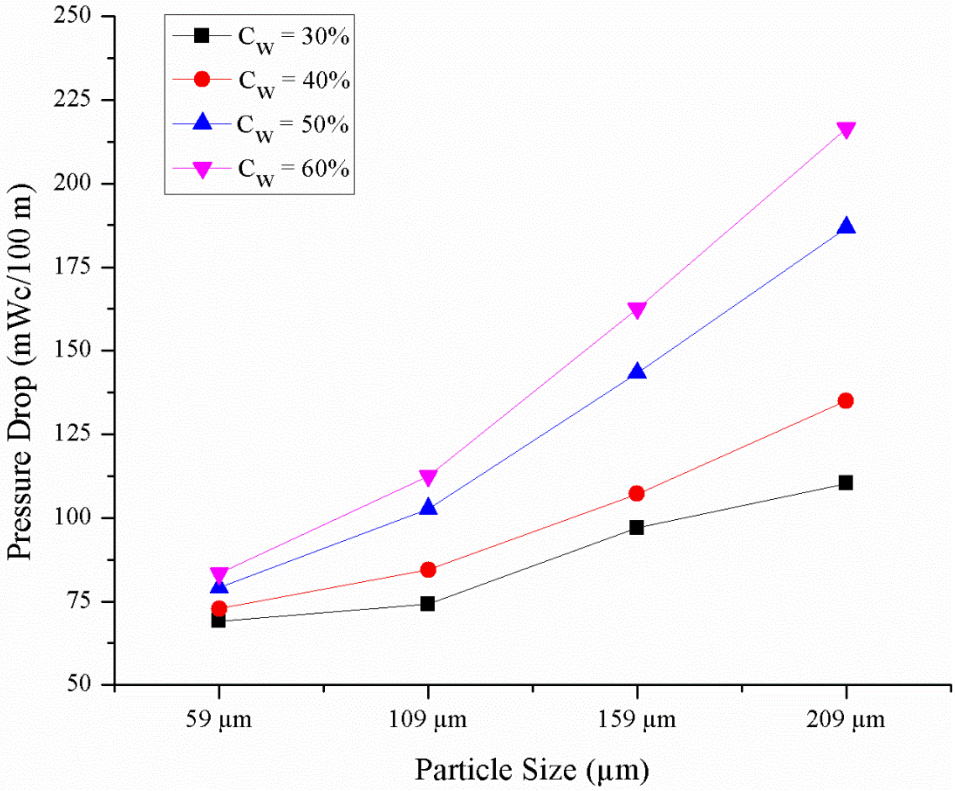

Figure 6.12: Effect of particle size on pressure drop characteristics of coal-water slurry at 5 ms^{-1} flow velocity

The variation of pressure drop characteristics in pipeline with particle size at different solid concentration in the range of 30-60% by weight) for flow velocity 5 ms^{-1} is shown in Figure 6.12. It is found that the pressure drop in slurry pipeline increase as 18.26, 27.77 and 13.71% with increase in solid concentration range from 30-40, 40-50 and 50-60% (by weight) for 209 µm sized coal whereas 5.04, 8.07 and 4.99% increase for 59 µm sized coal. The coarser particle sized coal show higher rate of increase in pressure drop as compared to finer particle sized coal with the increase in solid concentration. It seems that maximum pressure drop in pipeline is 216.48 mWc/100m at 60% solid concentration (by weight) for 209 µm sized coal whereas minimum pressure drop is observed as 69.11 mWc/100m at 60% (by weight) solid concentration for 59 µm sized coal.

6.6.4 Effect of particle size on volume fraction distribution of coal-water slurry

The effect of particle size on volume fraction distribution in vertical plane of pipe outlet is evaluated with 30% solid concentration (by weight) for 2-5 ms^{-1} flow velocity, as shown in Figure 6.13-6.16. The higher concentration region at pipe outlet varies is represented by red colour whereas lower concentration region is denoted by blue colour respectively. From Figure 6.13, magnitude of volume fraction increases with the increase in particle size. The magnitude of settling decreases from lower-to-upper direction on vertical central axis of pipe. The area of settling and lean concentration region for 209 µm sized coal is found larger compared to 59-159 µm sized coal. For 59 µm sized coal, the settling concentration exists nearby wall at pipe outlet whereas it shifts towards the centre of the pipe with increase in particle size up to 209 µm sized coal. From Figures 6.13 -6.16, the increase in settling is found as 1.52, 5.35 and 12.21% respectively with increase in particle size range from 59-109, 109-159 and 159-209 µm at 2 ms^{-1} solid concentration whereas 0.76, 1.17 and 2.89% at 5 ms^{-1} solid concentration. It seems that fine coal particles shows more settling as compare larger sized coal particles.

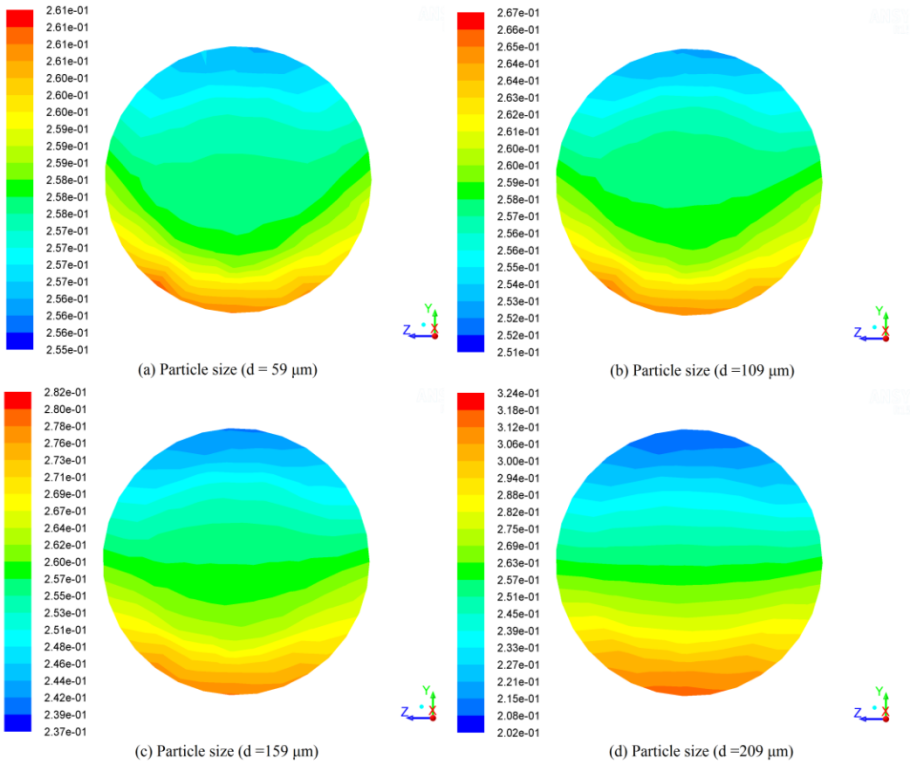

Figure 6.13: Effect of particle size on volume fraction contours of coal-water slurry at 30% solid concentration with flow velocity 2 ms^{-1}

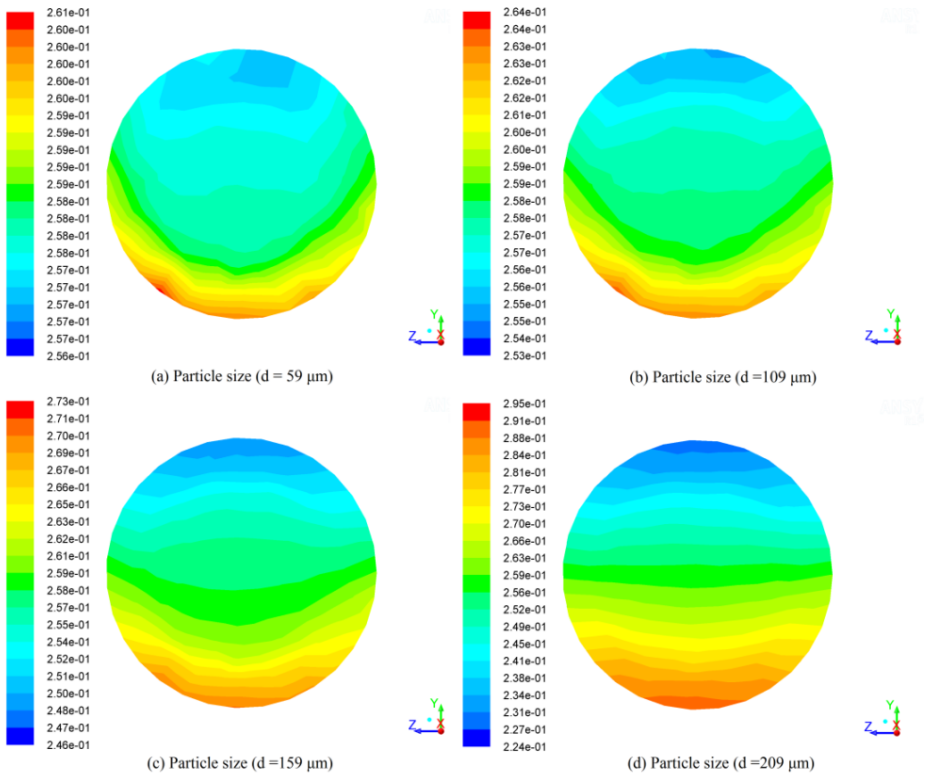

Figure 6.14: Effect of particle size on volume fraction contours of coal-water slurry at 30% solid concentration with flow velocity 3 ms^{-1}

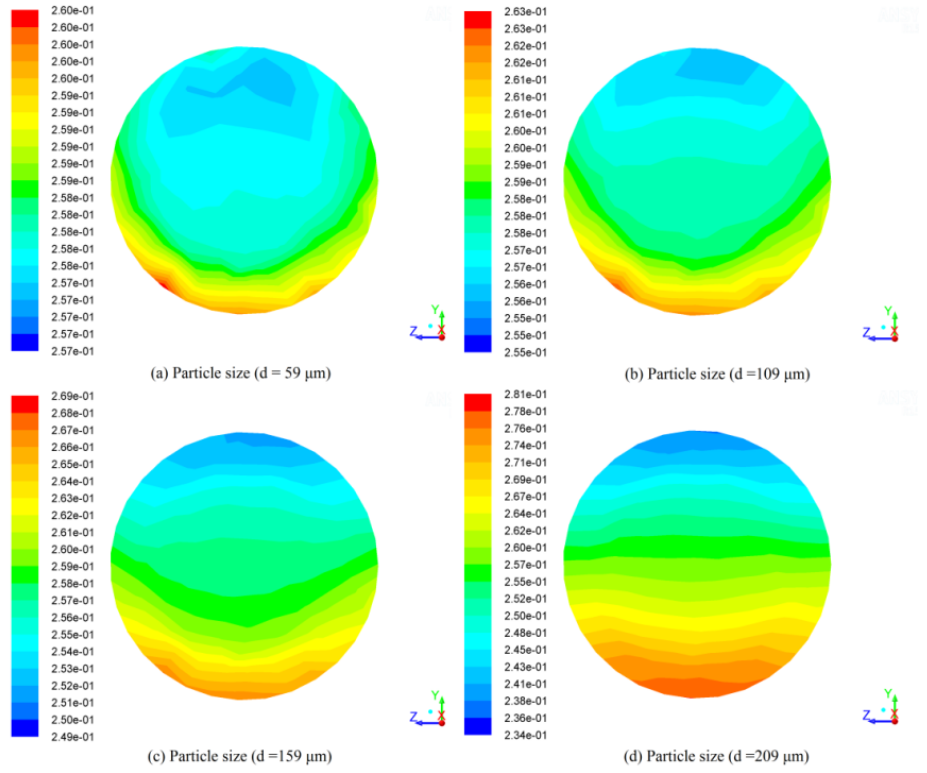

Figure 6.15: Effect of particle size on volume fraction contours of coal-water slurry at 30% solid concentration with flow velocity 4 ms^{-1}

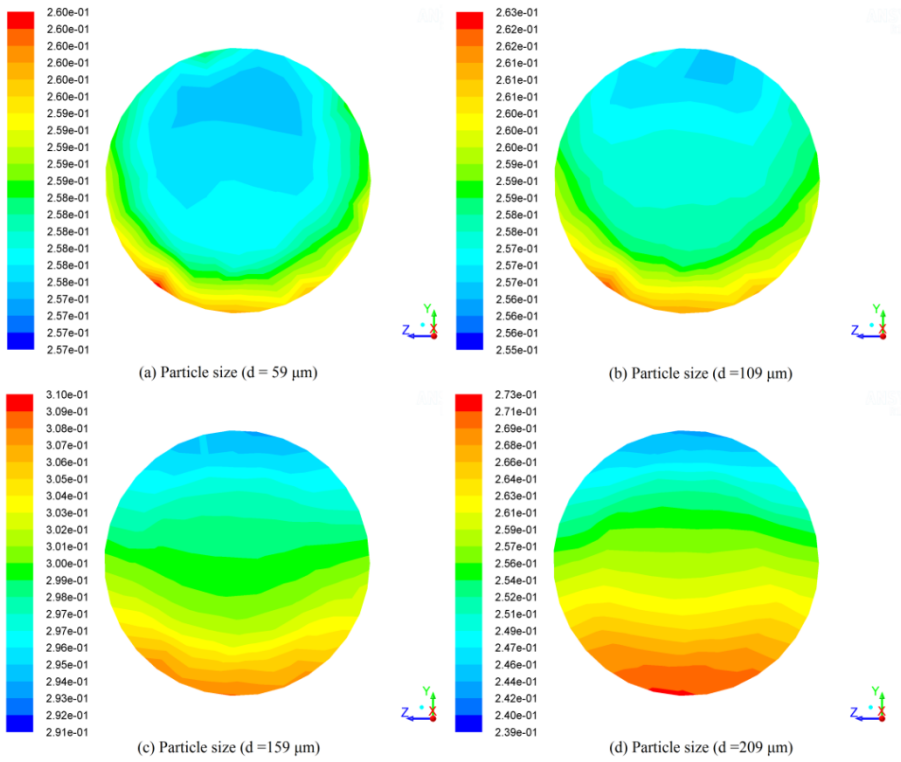

Figure 6.16: Effect of particle size on volume fraction contours of coal-water slurry at 30% solid concentration with flow velocity 5 ms^{-1}

The volume fraction distributions contours in vertical plane of pipe outlet having solid concentration for 60% (by weight) at 2-5 ms^{-1} flow velocity are shown in Figure 6.19-6.22. For 59 µm sized coal, decrease in settling is observed as 0.34, 0.08 and 0.08% respectively with increase in flow velocity from 2-3, 3-4 and 4-5 ms^{-1} whereas 9.58, 3.78 and 2.85% with 209 µm sized coal. The settling region is shifted towards the centre of the pipe with increase in particle size which is pronounced more at higher solid concentrations. Similar trend of settling is observed for all volume fraction distributions with solid concentration range of 30-60% (by weight). The settling region and lean concentration region at pipe outlet reduces with increase in flow velocity from 2-5 ms^{-1}. It is noticed that the concentration zone shifts away from wall surrounding towards the centre of the pipe. The magnitude of higher concentration settled zone increases with increase in solid concentration. From simulation results, area occupied by higher efflux concentration zone is found to be increased with increase in solid concentration. This happens due to increase in density of coal-water slurry with the increase in solid concentration.

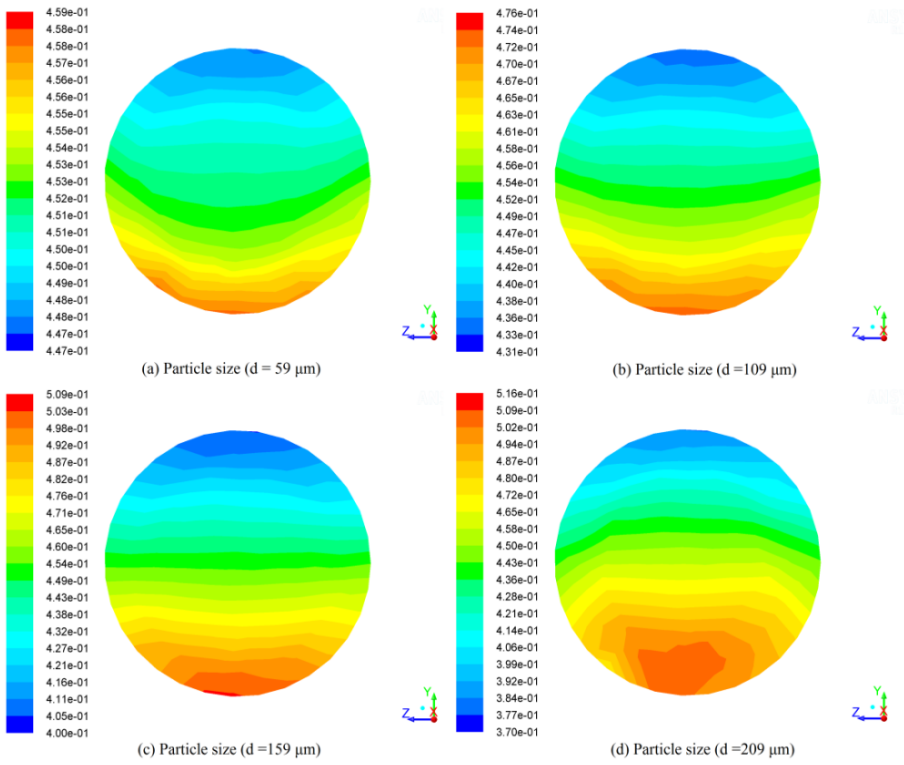

Figure 6.17: Effect of particle size on volume fraction contours of coal-water slurry at 60% solid concentration with flow velocity 2 ms^{-1}

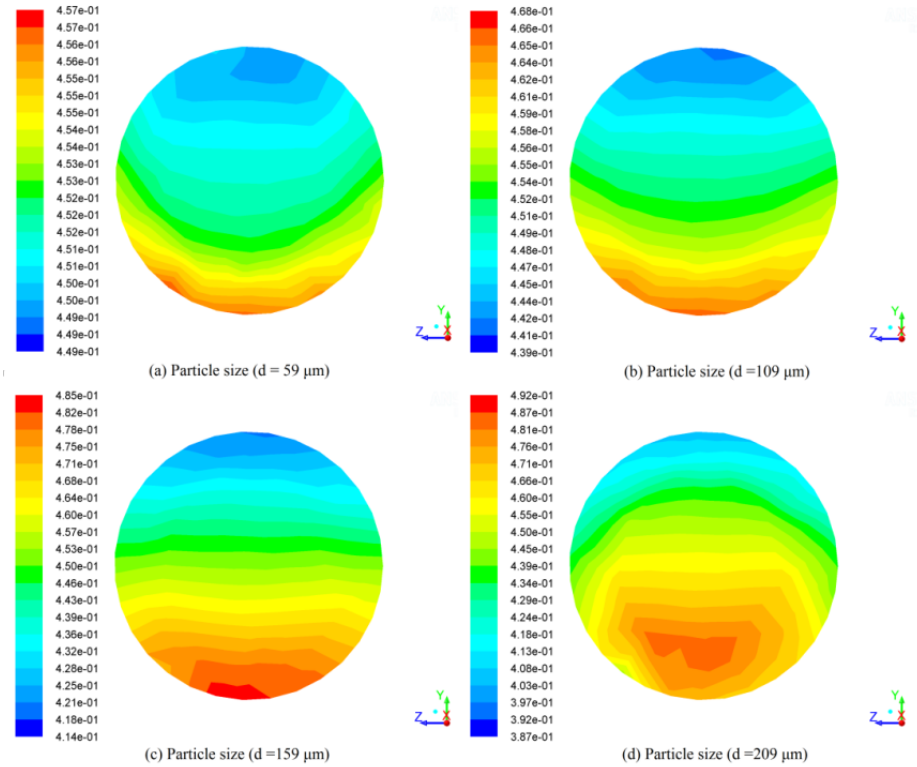

Figure 6.18: Effect of particle size on volume fraction contours of coal-water slurry at 60% solid concentration with flow velocity 3 ms^{-1}

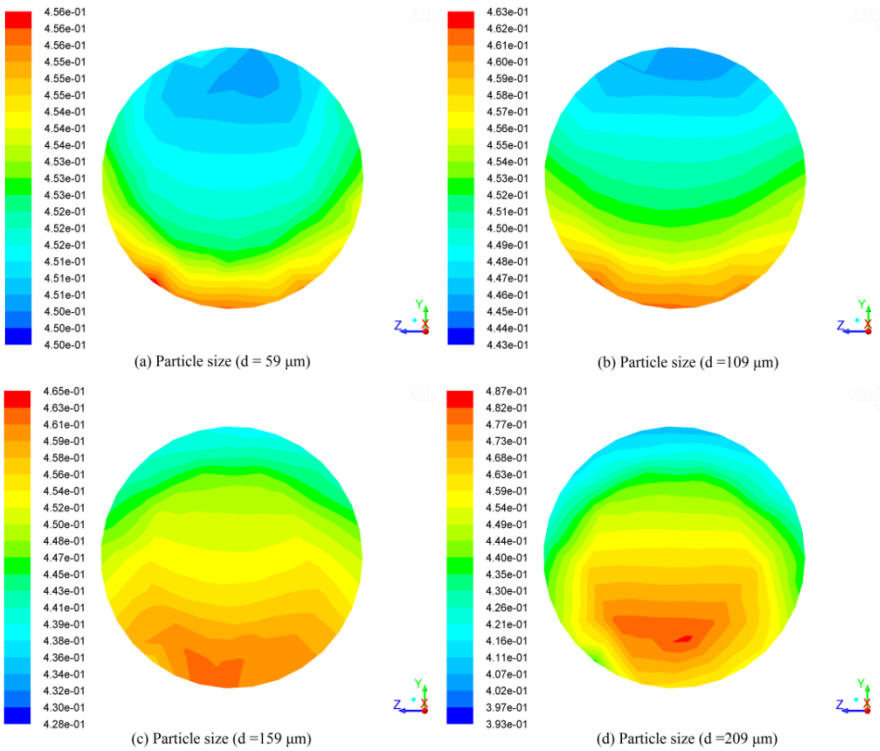

Figure 6.19: Effect of particle size on volume fraction contours of coal-water slurry at 60% solid concentration with flow velocity 4 ms^{-1}

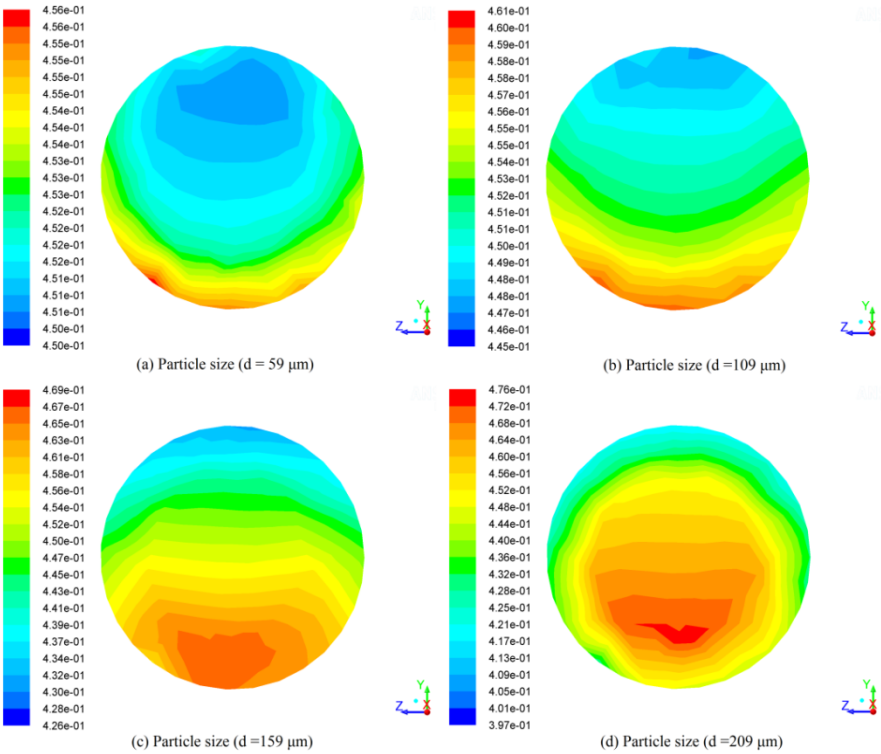

Figure 6.20: Effect of particle size on volume fraction contours of coal-water slurry at 60% solid concentration with flow velocity 5 ms^{-1}

6.7 CONCLUDING REMARKS

In the present chapter, the pressure drop characteristics for the flow coal-water slurry is numerically determined with CFD code FLUENT for different particle sizes at different concentrations and flow velocities. Following conclusions are drawn from the results obtained:

- SST k-ω model showed better results as compared to other models. Simulation results of SST k-ω model shows minimum deviation and establish close agreement with experimental data.
- Pressure drop increases with increase in particle size at all velocities. The coarser coal particles (209 µm) show higher value of pressure drop as compared to finer coal (59 µm) particles. Coarser coal particles are having more impact on pipe wall as compare to finer coal particles which results in higher pressure drop.
- Magnitude of higher concentration settled zone increases with increase in solid concentration. This happens due to increase in density of coal-water slurry with the increase in solid concentration.
- Magnitude of volume fraction increases with the increase in particle size. The settling region is shifted towards the centre of the pipe with increase in particle size which is pronounced more at higher solid concentrations.

CHAPTER 7
OPTIMIZATION OF PRESSURE DROP PARAMETERS USING TAGUCHI METHOD

7.1 INTRODUCTION

The rheological characteristics of the coal and coal ash slurry suspension are analyzed in Chapter 4. The effect of influencing parameters like solid concentration, particle size and flow velocity on the pressure drop characteristics are studied experimentally in chapter 5 and numerically in chapter 6. Experimental and numerical study shows that flow velocity, solid concentration and particle size are the influencing parameters of pressure drop characteristics. So, it is necessary to identify the most sensitive influencing parameter of pressure drop characteristics. In this chapter, the various influencing parameters of pressure drop are optimized by using Taguchi method. L_{16} (4^2) orthogonal array is used to determine the S/N ratios. Lower-the-better rule is used to characterize the S/N ratios. Pressure drop is determined by performing the experiments at different solid concentration with different velocities ranges between 2-5 ms^{-1} by using pilot plant test loop. The experiments are performed with 53-75μm coal, coal bimodal (with addition of 106-150 and 150-250μm) and fly ash (with and without addition of bottom ash). In present work, an attempt has been made to optimize the influencing parameters of pressure drop in slurry pipeline.

7.2 DESIGN OF EXPERIMENTS

Experiments are designed by using Taguchi's experimental design (Taguchi 1990) for determination of optimum pressure drop in terms of mWc/100 m i.e. meter of water column per 100 meter. The different input parameters varied at different levels for different cases are represented in Table 7.1. L_{16} (4^2) array is used for three input parameters and each of parameter has four levels. Pressure drop is considered as an output or response parameter. L_{16} (4^2) array represents the minimum number of experiments performed by the Taguchi's experimental design to find out the most influencing parameter during pressure drop experimentation.

Table 7.1: Variable parameters for pressure drop experiments

Experiment Cases	Factors	Levels			
		I	II	III	IV
Common for all cases	Velocity (ms^{-1})	2	3	4	5
	Concentration (%)	29	41	51	61
Case 1	Addition of 106-150 µm range (%)	0	20	30	40
Case 2	Addition of 150-250 µm range (%)	0	20	30	40
Case 3	Addition of Bottom ash (%)	0	10	20	30

Experimentation is conducted in three different cases. In all the three cases, two influence parameters namely flow velocity and solid concentration are taken same whereas the third influencing parameter i.e. particle size is varied. First and second case is carried out for coal and third case is conducted for fly ash. The influence of addition of 106-150 and 150-250 µm particle size on pressure drop of 53-75 µm sized coal is analysed in first and second case respectively. In third case, the bottom ash is added in the fly ash and its influence on pressure drop is tested. Lower-the-better quality rule is chosen to optimize the various pressure drop influencing parameters. Signal-to-noise ratio is used to measure the quality characteristics in which signal indicates the output characteristic and noise indicates the value of undesirable attributes.

7.3 SIGNAL-TO-NOISE RATIO

The experimental interpretations are transformed in terms of signal-to-noise (S/N) ratios. The S/N ratios are obtained using MINITAB 16 software package. The S/N ratio depends upon the performance characteristics of experimental design. The most influencing parameter can be determined from the difference between S/N ratios. The lower-the-better quality rule for calculating the S/N ratio is given as:

$$S/N = -10 \times \log\left[\frac{1}{n}\sum y_i^{\,2}\right] \tag{7.1}$$

Where, y_i is the pressure drop observations and n is the total observations.

Table 7.2: $L_{16}(4^2)$ orthogonal array with different S/N ratios for 53-75 µm sized coal-water slurry with addition of 106-150 and 150-250 µm sized coal

S. No.	Flow Velocity (ms^{-1})	Solid concentration (by weight)	Addition of 106-150 um sized coal			Addition of 150-250 um sized coal		
			Composition (%)	Pressure drop (mWc/100m)	S/N ratio (dB)	Composition (%)	Pressure drop (mWc/100m)	S/N ratio (dB)
1	2	29	0	11.03	-20.8515	0	11.03	-20.8515
2	2	41	20	9.92	-19.9302	20	8.07	-18.1375
3	2	51	30	7.54	-17.5474	30	6.64	-16.4434
4	2	61	40	8.99	-19.0752	40	7.93	-17.9855
5	3	29	20	15.63	-23.8792	20	13.07	-22.3255
6	3	41	0	25.04	-27.9727	0	25.04	-27.9727
7	3	51	40	17.09	-24.6548	40	15.27	-23.6768
8	3	61	30	19.92	-25.9858	30	14.98	-23.5102
9	4	29	30	22.57	-27.0706	30	20.03	-26.0336
10	4	41	40	27.41	-28.7582	40	24.96	-27.9449
11	4	51	0	47.73	-33.5758	0	47.73	-33.5758
12	4	61	20	43.23	-32.7157	20	37.02	-31.3687
13	5	29	40	38.6	-31.7317	40	34.49	-30.7539
14	5	41	30	40.36	-32.119	30	35.18	-30.9259
15	5	51	20	57.18	-35.1449	20	49.23	-33.8446
16	5	61	0	78.15	-37.8586	0	78.15	-37.8586

Table 7.3: L_{16} (4^2) orthogonal array with different S/N ratios for fly ash with bottom ash addition

S. No.	Flow Velocity (ms^{-1})	Solid concentration (by weight)	Addition of bottom ash		
			Composition (%)	Pressure drop (mWc/100m)	S/N ratio (dB)
1	2	29	0	12.62	-22.02
2	2	41	10	13.4	-22.54
3	2	51	20	12.20	-21.73
4	2	61	30	13.33	-22.50
5	3	29	10	22.01	-26.85
6	3	41	0	25.98	-28.30
7	3	51	30	22.13	-26.90
8	3	61	20	31.01	-29.83
9	4	29	20	35.56	-31.02
10	4	41	30	34.94	-30.87
11	4	51	0	51.89	-34.30
12	4	61	10	52.94	-34.47
13	5	29	30	50.41	-34.05
14	5	41	30	59.26	-35.45
15	5	51	10	73.31	-37.30
16	5	61	0	88.66	-38.95

L_{16} (4^2) orthogonal array is used to determine the S/N ratio for various input parameters at different levels is for case 1-2 and 3, as mentioned in Table 7.2-7.3. The overall mean of S/N ratios for case 1, 2 and 3 is found as -1.71, -1.65 and -1.86 dB respectively. The values of rank and delta are generated on the basis of smaller-the-better characteristic of S/N ratios. The response table of different S/N ratio for pressure drop with addition of 106-150 µm sized coal in 53-106 µm coal-water slurry is summarized in Table 7.4. Table 7.4 indicates that value of delta for flow velocity is highest among the other influencing parameters. The value of delta for flow velocity for case 1, 2 and 3 is found as 14.86, 14.99 and 9.10 respectively. The value delta is the sum of the difference between the S/N ratio values at all four levels. The highest value of delta for flow velocity shows that the rank of factor namely velocity is highest among all other factors.

Table 7.4. Response of Signal-to-noise ratio of 53-75 µm sized coal-water slurry with addition of 106-150 µm sized coal

Level	Velocity (ms^{-1})	Solid Concentration	Addition of 106-150 µm
1	-19.35	-25.88	-30.06
2	-25.62	-27.20	-27.92
3	-30.53	-27.73	-25.68
4	-34.21	-28.91	-26.05
Delta	14.86	3.03	4.38
Rank	1	3	2

Table 7.5. Response of Signal-to-noise ratio of 53-75 µm sized coal-water slurry with addition of 150-250 µm sized coal

Level	Velocity (ms^{-1})	Solid Concentration	Addition of 150-250 µm
1	-18.35	-24.99	-30.06
2	-24.37	-26.25	-26.42
3	-29.73	-26.89	-24.23
4	-33.35	-27.68	-25.09
Delta	14.99	2.69	5.84
Rank	1	3	2

Table 7.6. Response table for Signal-to-noise ratio of fly ash slurry with addition of coal bottom ash

Level	Velocity (ms^{-1})	Solid Concentration	Addition of coal bottom ash
1	-22.20	-28.49	-30.89
2	-27.97	-29.29	-30.29
3	-32.67	-30.20	-29.65
4	-36.44	-31.44	-28.58
Delta	14.10	2.95	2.31
Rank	1	2	3

The effect of S/N ratios of pressure drop for different cases is shown in Figure 7.1-7.3. At flow velocity of 2 ms^{-1} with 51% solid concentration, minimum pressure drop is observed as 7.54 mWc/100m with 30% addition of 106-150 µm sized coal in 53-75 µm sized coal-water slurry whereas 6.64 mWc/100m for 150-250 µm sized coal. The S/N ratios are observed as -17.58 and-16.44 dB for case 1 and 2 respectively with minimum pressure drop. However, maximum pressure drop occurred as 78.15 mWc/100m at 5 ms^{-1} and solid concentration of 61% without addition coarser particles size range (106-150 and 150-250 µm) with lowest S/N ratio of -37.86 dB.

Figure 7.3 represents the mean effect plot for fly ash with addition of bottom ash. It is found that minimum pressure drop is observed as 12.20 mWc/100m at flow velocity of 2 ms^{-1} with 29% solid concentration with 30% addition of bottom ash. S/N ratio is observed as -21.73 dB at minimum value of pressure drop. However, maximum pressure drop occurred as 88.66 mWc/100m at velocity of 5 ms^{-1} and concentration of 61% with the addition of 0% concentration of bottom ash with highest S/N ratio of -38.95 dB.

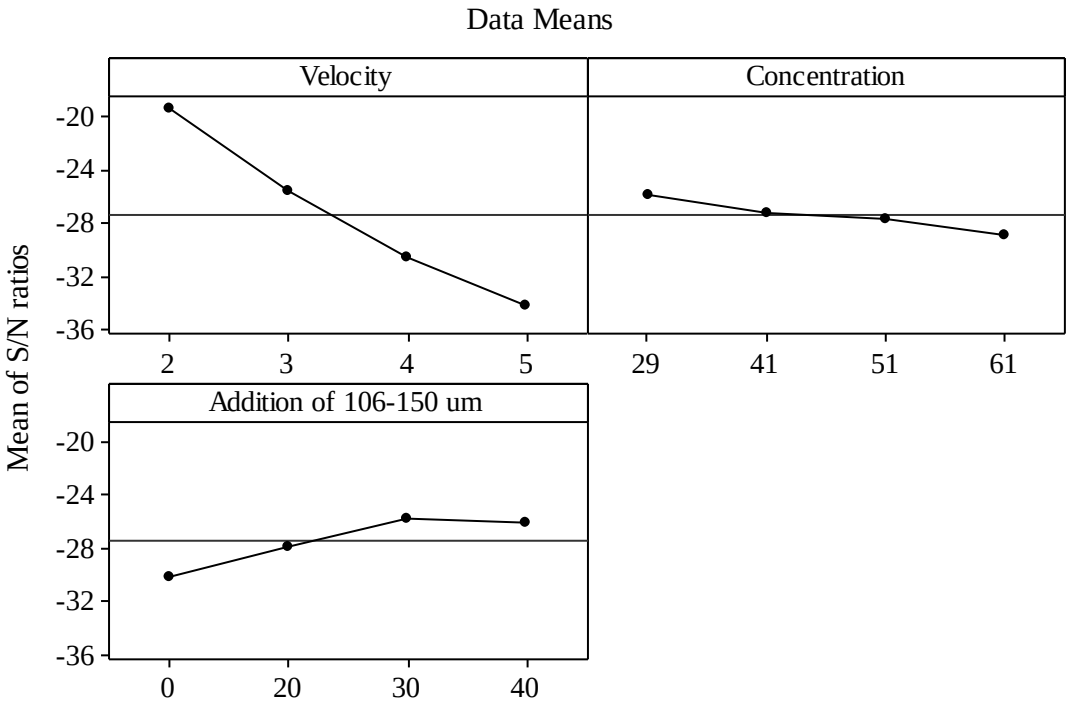

Figure 7.1. Main effect plot of S/N ratios for pressure drop of 53-75 µm sized coal-water slurry with addition of 106-150 µm sized coal

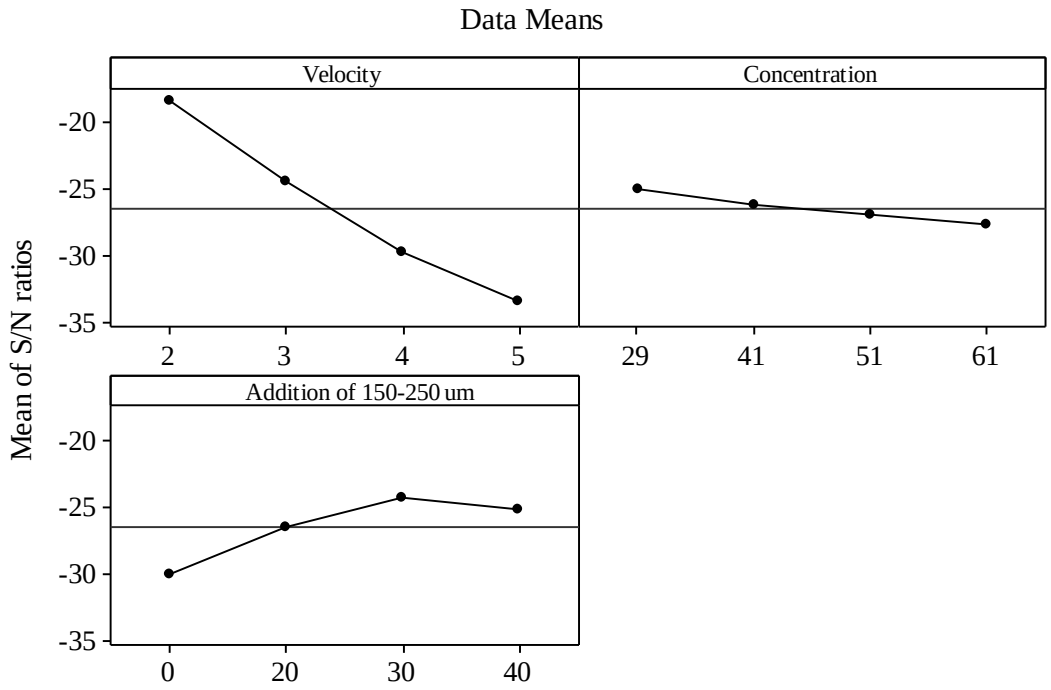

Figure 7.2. Main effect plot of S/N ratios for pressure drop of 53-75 µm sized coal-water slurry with addition of 150-250 µm sized coal

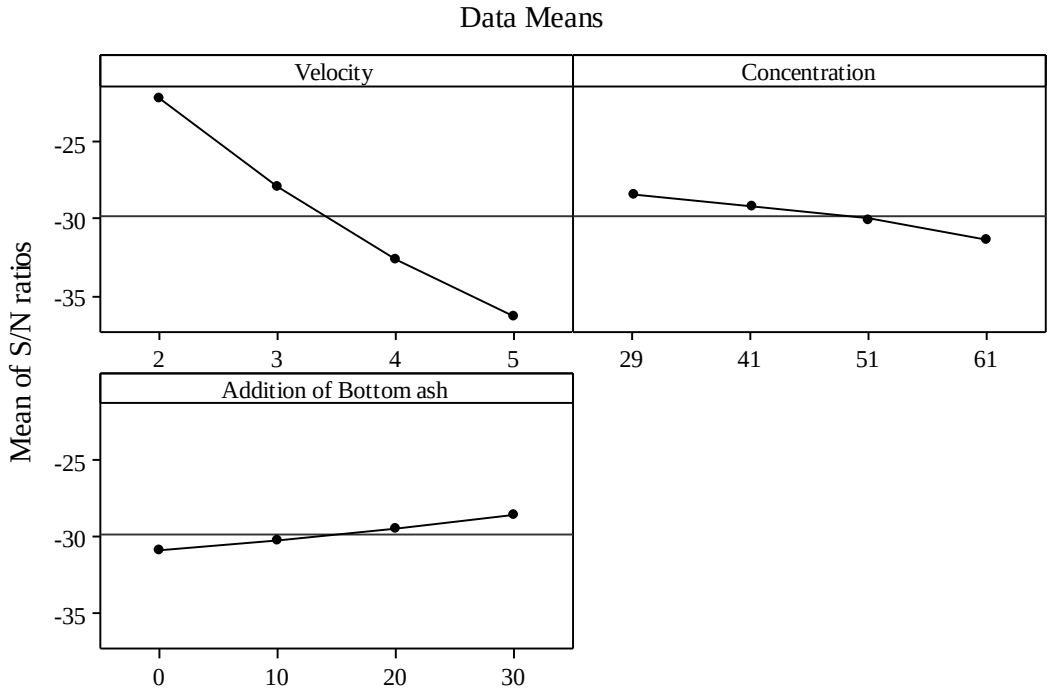

Figure 7.3 Main effect plot of S/N ratios for pressure drop of fly ash slurry with addition of bottom ash

7.3.1 Interaction of influencing parameters of pressure drop

The interaction of different input parameters on response parameter (Pressure drop) for with 53-75 µm sized coal-water slurry with addition of 106-150 and 150-250 µm sized coal is shown in Figure 7.4-7.5. From Figure 7.4(a), it is found that two lines are non-parallel to each other which indicate the existence of interaction between flow velocity & solid concentration. Figure 7.4(b) indicates that one line is non-parallel to respective lines which indicate that the existence of interaction between velocity & addition of coarser particle size range (106-150 µm). It seems that significant pressure drop occurred with change in flow velocity with solid concentration and addition of coarser particle size. However, Figure 7.4(c) shows all the lines are intersecting each other which indicate the significant interaction between flow velocity and addition of coarser 106-150 µm sized coal particles. Similar type of trend is observed in Figure 7.5 with the addition of 150-250 µm sized coal.

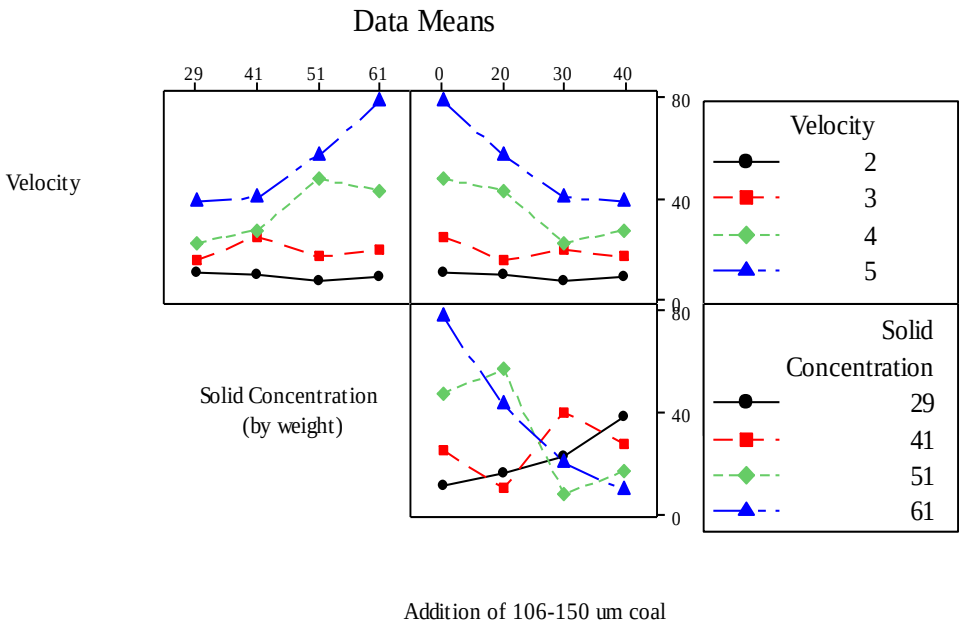

Figure 7.4: Interaction plots of pressure drop for 53-75 µm sized coal-water slurry with addition of 106-150 µm sized coal

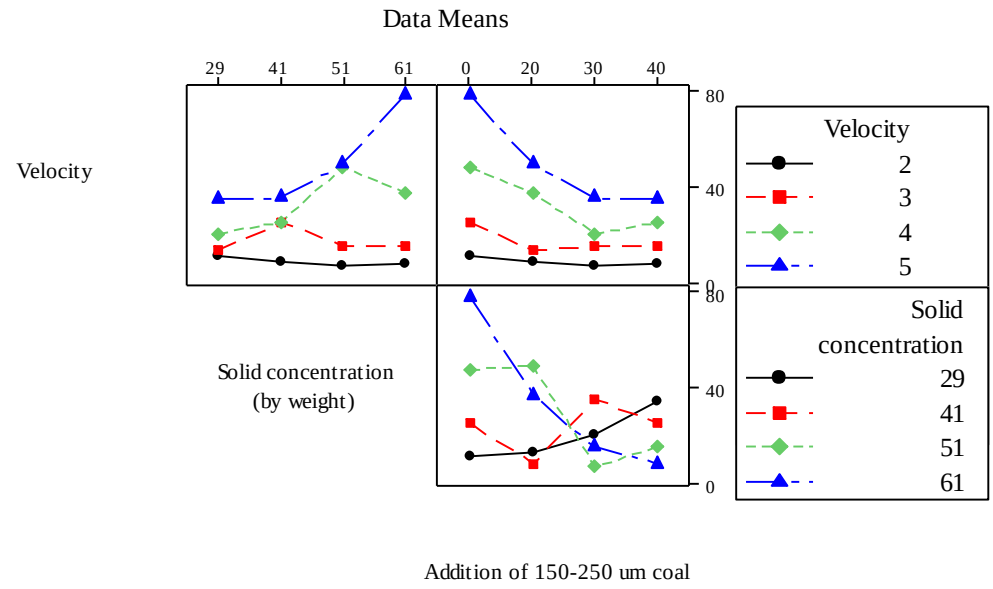

Figure 7.5: Interaction plots of pressure drop for 53-75 µm sized coal-water slurry with addition of 150-250 µm sized coal

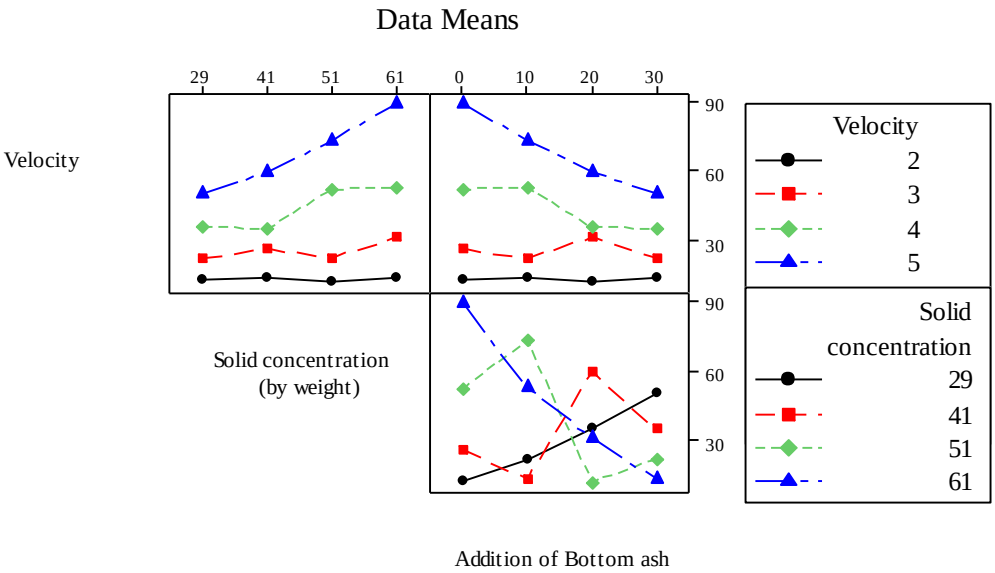

Figure 7.6: Interaction plots of pressure drop for fly ash slurry with addition of bottom ash

Figure 7.6 represents the interaction plot for fly ash with the addition of bottom ash. From Figure 7.6(a & b), it is found that all the lines are parallel to each other which indicate the absence of interaction between flow velocity & solid concentration and flow velocity & addition of bottom ash. From Figure 7.6(d), it seems that all the lines are intersecting each other which represent the strong interaction between all the input parameters.

7.3.2 Interaction between influencing parameters for response parameter

Contour plots of pressure drop against velocity and solid concentration

Contour plots indicating ranges of pressure drop against velocity and solid concentration (by weight) for coal and fly ash slurry, as shown in Figure 7.7. From Figure 7.7(a) & (b), it was observed that pressure drop was less than 10 mWc/100m while the flow velocity was less than 2.6 ms^{-1}.

For the addition of 106-150 µm sized coal in 53-75 µm sized coal, the pressure drop was found in between range 10-20 mWc/100m while the solid concentration lies in range 30-60% (by weight) at velocity of 2.5 to 3.6 ms^{-1}. For the addition of 150-250 µm sized coal in 53-75 µm sized coal, the pressure drop was found in between range 10-20 mWc/100m while the solid concentration lies in range 30-60% (by weight) at velocity of 2.5 to 4.1 ms^{-1}.

(a)

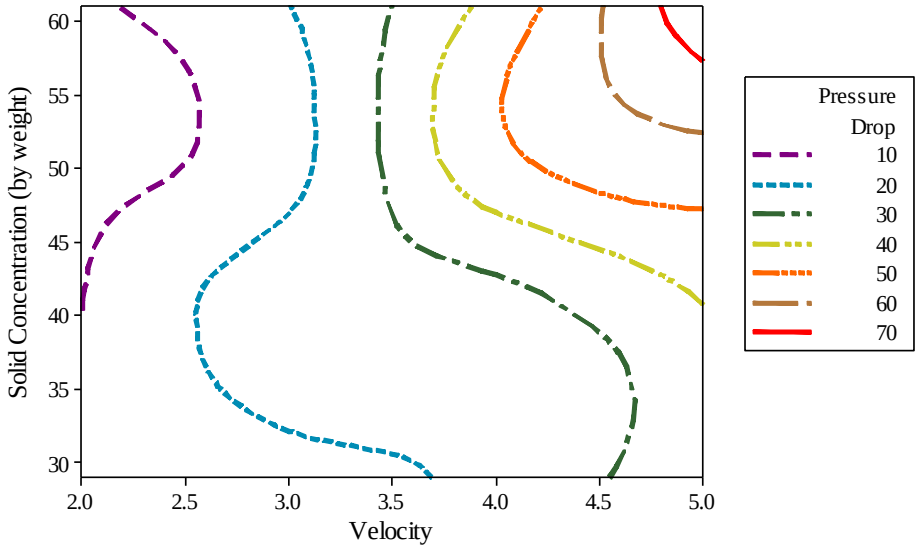

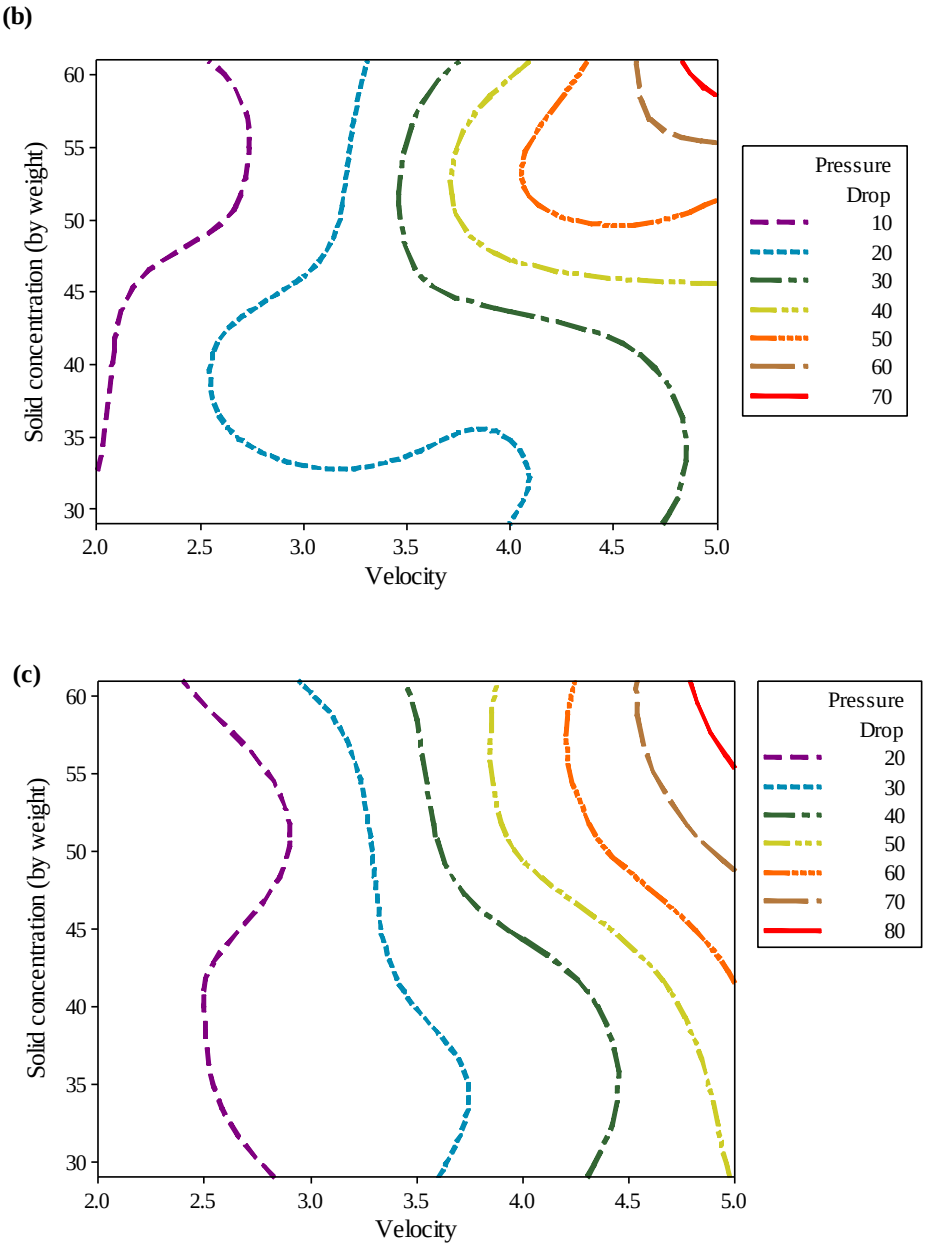

Figure 7.7: Contours of pressure drop against velocity and solid concentration (by weight) addition of (a) 106-150 µm sized coal in 53-75 µm sized coal (b) 150-250 µm sized coal in 53-75 µm sized coal (c) bottom ash in fly ash

From Figure 7.7(c), it is observed that pressure drop lies in the range 10-20 mWc/100m while velocity varies in range 2.4 to 3.0 ms^{-1}. Pressure drop was found above 70 mWc/100m for the addition of 106-150 µm and 150-250 µm sized in 53-75 µm sized coal while solid concentration was found in between range 55-60% (by weight) at velocity of 4.8 to 5.0 ms^{-1}.

For the addition of bottom ash in fly ash, the pressure drop above 80 mWc/100m while solid concentration was found in between range 55-60% (by weight) at velocity of 4.8 to 5.0 ms^{-1}.

Contour plots of pressure drop against velocity and addition of particles

Contour plots indicating ranges of pressure drop against (a) velocity, addition of 106-150 µm sized coal in 53-75 µm sized coal (b) velocity, addition of 150-250 µm sized coal in 53-75 µm sized coal (c) velocity, addition of bottom ash in fly ash fly ash slurries, as shown in Figure 7.8. From Figure 7.8(a-b), it was observed that pressure drop was less than 10 mWc/100m while the flow velocity was less than 2.6 ms^{-1} for 10-40% addition of 106-150 and 150-250 µm µm sized coal in 53-75 µm sized coal.

The pressure drop was found below 20 mWc/100m while the velocity lies between 2-2.75 ms^{-1} upto 40% addition of bottom ash in fly ash slurry, as shown in Figure 7.8(c). Similarly, the pressure drop ranges against addition of addition of 106-150 and 150-250 µm sized coal in 53-75 µm sized coal & additives bottom ash fly ash slurry at different velocities is shown in Figure 7.8.

(a)

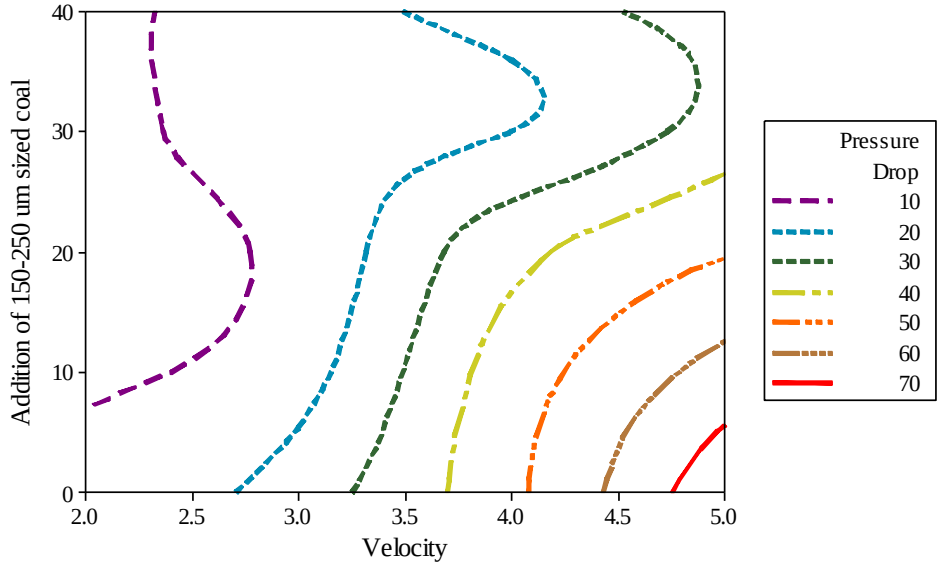

(b)

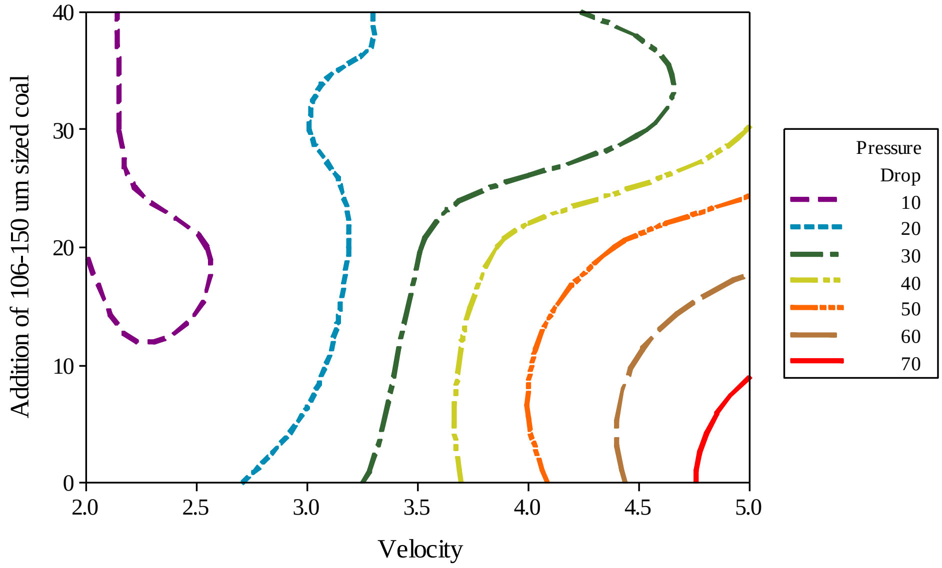

(c)

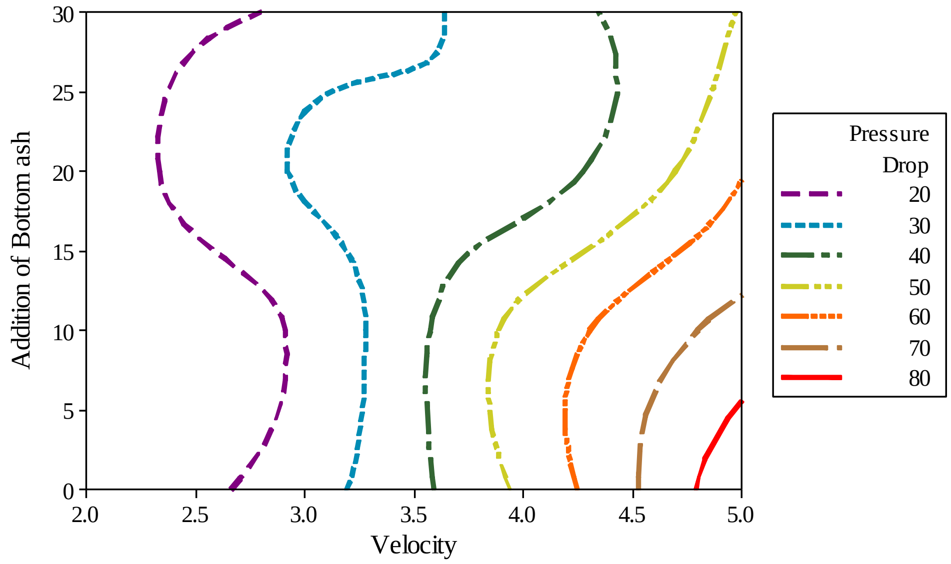

Figure 7.8: Contours of pressure drop against velocity and addition of (a) 106-150 µm sized coal in 53-75 µm sized coal (b) 150-250 µm sized coal in 53-75 µm sized coal (c) bottom ash in fly ash fly ash slurry

7.3.3 Analysis of pressure drop data

Analysis of variance is carried out from probability distribution plots. The confidential interval of 0.05 is taken into account. Figure 7.9 and 7.10 represent the probability plots for coal with addition of 106-150 and 150-250 µm sized coal. The p-value is found as 0.156 and 0.163 respectively for addition of 106-150 and 150-250 µm sized coal which indicates the non-linear augmentation of pressure drop.

Figure 7.11 represents the probability plots of pressure drop for the flow of fly ash with addition of bottom ash. The p-value is found as 0.161 for pressure drop from analysis of variance. Result data shows a normal distribution of residuals (errors).

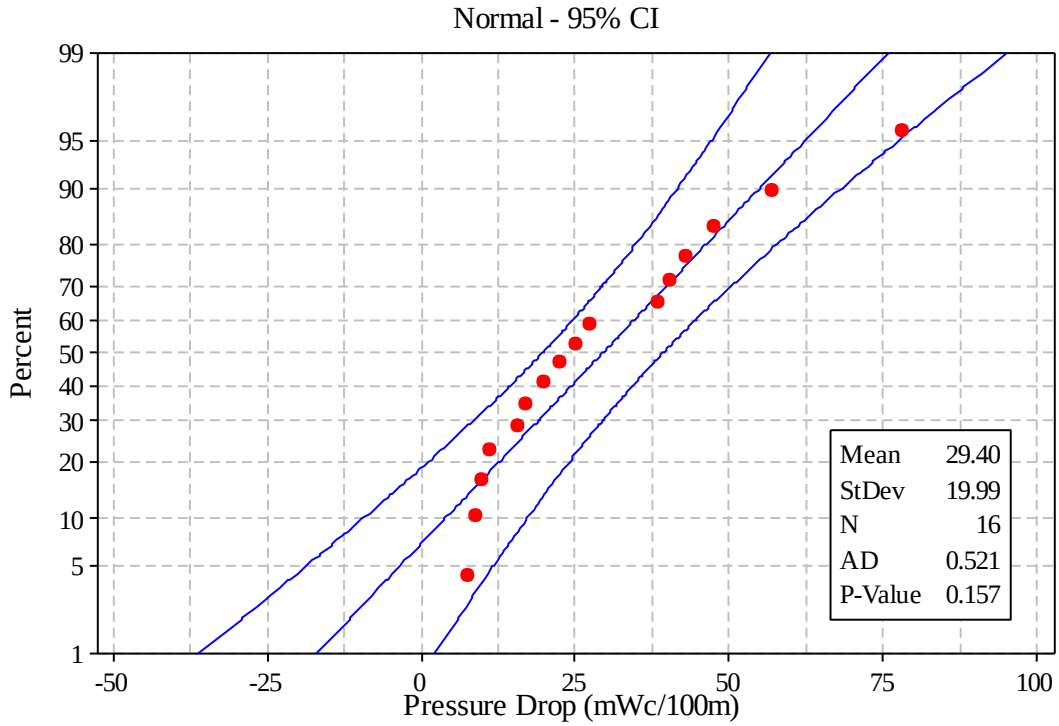

Figure 7.9: Probability plot for pressure drop of 53-75 µm sized coal-water slurry with addition of 106-150 µm sized coal

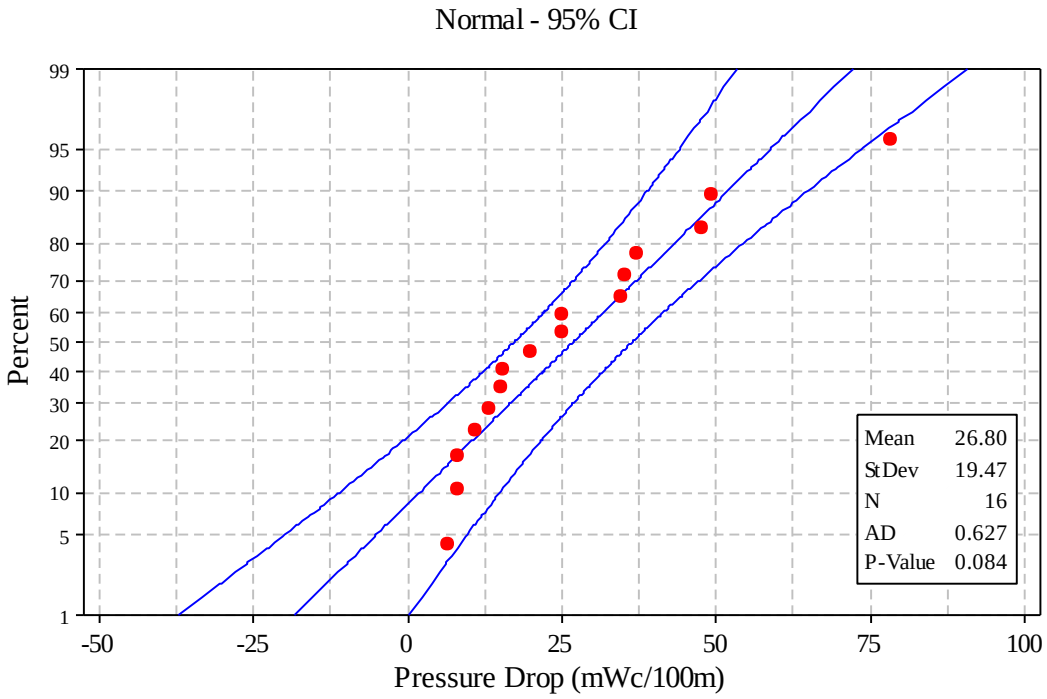

Figure 7.10: Probability plot pressure drop of 53-75 µm sized coal-water slurry with addition of 150-250 µm sized coal

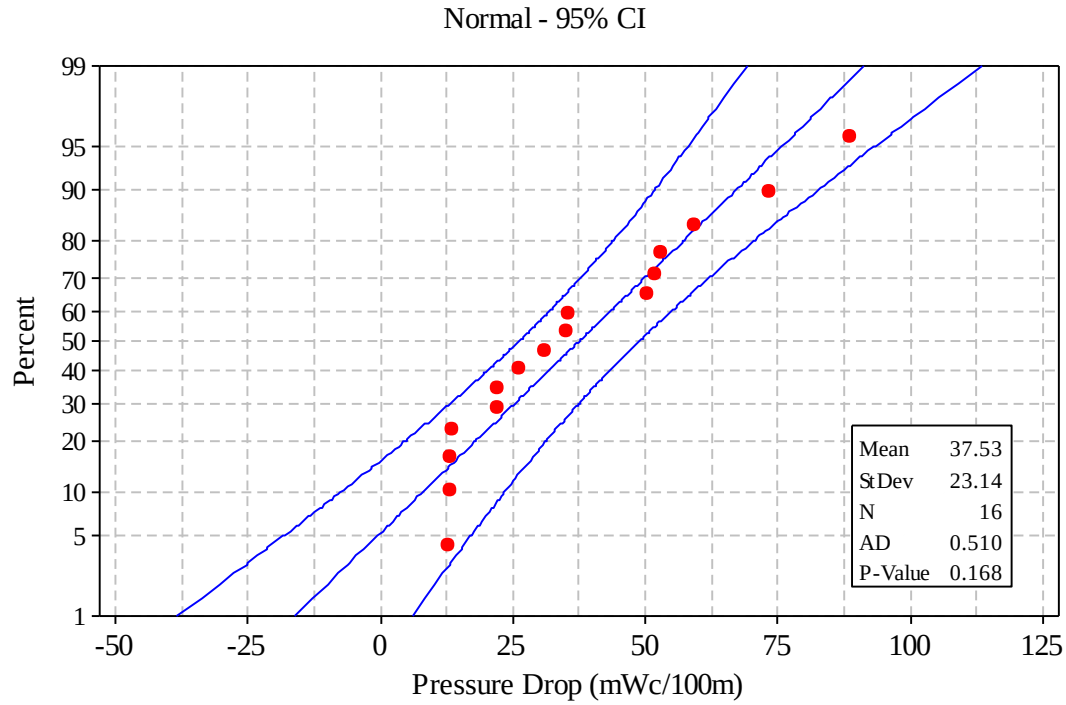

Figure 7.11: Probability plot for pressure drop of fly ash slurry with addition of bottom ash

7.4 CONCLUDING REMARKS

Taguchi's experimental design is used to optimize the influencing parameters like flow velocity, solid concentration, addition of additive and particle size. Pressure drop characteristic during the transportation of slurry in pipeline with influence of different parameters are analyzed. The following conclusions are drawn on the basis of present investigation:

- Taguchi's approach is successful to predict the pressure drop experimentation for influence of different parameters varying at different levels.
- Interaction between all the input parameters is found significant due to intersection of lines each other.
- The response of flow velocity is ranked as 1 which implicates towards most dominated parameter.
- Pressure drop shows a normal distribution of residuals (errors) and lies in 5% confidential interval.

CHAPTER 8

CONCLUSIONS AND FUTURE SCOPE

8.1 CONCLUSIONS

This chapter includes the conclusions based on the results presented in the previous chapters. The pressure drop characteristics for handling multiparticulate coal and coal ash slurry suspension have been evaluated with different solid concentration and flow velocity.

Following conclusions have been drawn on the basis of present study:

- The finer coal particles show maximum settled concentration as compared to the coarser coal particles. Similar trend of static settled concentration is observed with fly and bottom. The coarser irregular shape of particles of bottom ash leads to lower static settled concentration whereas the fine spherical shape of particles of fly ash leads to higher static settled concentration.
- The rheological behavior of the coal-water slurry is shows Newtonian behaviour up to 30% solid concentration and above depicts pseduplastcis flow characteristics.
- Fly ash slurry suspensions show Newtonian behaviour up to 30% solid concentration (by weight) beyond it follows Bingham fluid flow characteristics.
- The apparent viscosity of 53-75 μm particle sized coal –water slurry reduces with addition of 106-150 and 150-250 μm sized coarser coal particles. Optimum reduction in apparent viscosity is found with 30% addition of coarser particles. Coal particles of 150-250 μm size shows more reduction in apparent viscosity of 53-75 μm particle sized coal –water slurry as compared to 106-150 μm sized coal particles.
- The addition of bottom ash in fly ash also reduces the apparent viscosity of fly ash slurry. The maximum apparent viscosity reduction of fly ash suspension is found with 20% addition of bottom ash whereas marginal reduction in apparent viscosity is observed with addition of 10 and 30%. Addition of bottom ash suspension also reduces rheological parameters and results in substantial saving in the energy consumption.
- The pressure drop experiments shows that a substantial reduction in pressure drop can be achieved through addition of coarser particles in the finer particles. The maximum

reduction in pressure drop of 53-75 μm particle sized coal-water slurry is observed with 30% addition of 150-250 μm sized coal particles.

- Pressure drop of fly ash slurry in horizontal pipeline show maximum reduction with 20% addition of bottom ash.
- SST k-ω model showed better results as compared to other models. Simulation results of SST k-ω model shows minimum deviation and establish close agreement with experimental data.
- Numerical simulation results show that the pressure drop in pipeline increases non-linearly with increase in flow velocity, solid concentration and particle size. Particle size was found more dominant factor as compared to the influx velocity and concentration for Pressure drop in pipeline. Fine particles settled more as compare to larger size particles. Settling concentration slightly increases with increase in particle size.
- Taguchi's approach is successful to predict the pressure drop experimentation for influence of different parameters varying at different levels. Flow velocity is found most significant parameter followed by solid concentration and addition of additive composition.

8.2 FUTURE SCOPE

The further work needs to be carried for better understanding of the flow mechanism of highly concentrated slurry through pipes. Some probable work that could be done in coming future by researchers is listed below:

- To study detailed flow field analysis of the solid-liquid flow through slurry pipeline using sophisticated instrument like laser Doppler velocimeter (LDV) etc.
- To study the performance characteristics of progressive cavity screw pump with solid materials of different properties so as to establish the relationship between particle size distribution and head-to-efficiency ratio of screw pump.
- To study the shut-down/re-start characteristics of the slurry pipeline and pump at higher concentration.
- To study the wear characteristics of different pump and piping materials with help of erosion wear tester.
- To investigate the performance of the slurry suspension at high concentration with addition of different suitable additives.

REFERENCES

American Public Health Association (APHA). 1995. *Standard methods for examination of water and wastewater 19th Ed*. Washington, DC: American Public Health Association.

Ahmad, M. Singh, S.N. and Seshadri, V. 1995. Pressure drop in a long radius 90º horizontal bend for the flow of multi sized heterogeneous slurries, *International Journal of Multiphase Flow*, 2(2): 329-334.

Aktas, Z. and Woodburn, E.T. 2000. Effect of addition of surface active agent on the viscosity of a high concentration slurry of a low rank British coal in water. *Fuel Processing Technology*, 62: 1–15.

Assefa K.M. and Kaushal, D.R. 2015. A new model for the Viscosity of Highly Concentrated Multi-sized Particulate Bingham Slurries, *Particulate Science and Technology*, 35(1): 77-85.

Aude, T.C. Thompson, T.L. and Wasp, E.J. 1974. Economics of slurry pipeline system, 3rd International Conference on the Hydraulic transport of Solids in Pipe,Golden, Color., USA, 2-13.

Aude, T.C. Thompson, T.L. and Wasp, E.J. 1975. Slurry pipe line system oil and gas, Journal of Pipelines, 66-73.

Baba, A. Gurdal G. and Sengunalp, F. 2010. Leaching characteristics of fly ash from fluidized bed combustion thermal power plant: Case study: Çan (Çanakkale-Turkey), *Fuel Processing Technology*, 91: 1073-1080.

Babcock, H. A. 1971. Heterogeneous flow of heterogeneous solids. *Advances in Solid Liquid Flow in Pipes and its Application*, Pergamon Press, Oxford, 125-148.

Bandhyopadhyay, T.K. and Das, S.K. 2013. Non-Newtonian and Gas-non-Newtonian Liquid Flow through Elbows -CFD Analysis, *Journal of Applied Fluid Mechanics*, 6(1): 131-141.

Bbraganca, S.R. Goncalves, M.R.F. Bergmann, C.P. and Rubio, J. 2009. Coal ash transportation as paste like highly loaded pulps in Brazil: characterization and main features, *International Journal of Coal Preparation and Utilization*, 29: 203-215.

Biswas, A. Gandhi, B.K. Singh, S. N. and Seshadri, V. 2000. Characteristics of coal ash and their role in hydraulic design of ash disposal pipelines, *Indian Journal of Engineering and Material Science*, 7: 1-7.

Blissett, R. and Rowson, N. 2012. A review of the multi-component utilisation of coal fly ash, *Fuel*, 97: 1–23.

Boylu, F. Dincer, H. and Atesok, G., 2004. Effect of Coal Particle Size Distribution, Volume Fraction and Rank on the Rheology of Coal-Water Slurries, *Fuel Processing Technology*, 85: 241–250.

Bunn, T.F. and Chambers, A.J. 1993. Experiences with dense phase hydraulic conveying of vales point fly ash, *International Journal of Powder Handling and Processing*, 5(1): 35-44.

Buranasrisak, P. and Narasingha, M.H. 2012. Effects of Particle Size Distribution and Packing Characteristics on the Preparation of Highly-Loaded Coal-Water Slurry, *International Journal of Chemical Engineering and Applications*, 3: 31-35.

Carleton, A.J. French, R.J. James, J.G. Broad, B.A. and Streat, M. 1978. Hydraulic transport of large particles using conventional and high concentration conveying, *Proceedings, 5th International Conference on the Hydraulic Transport of Solids in Pipes*, Hanover: 15-28.

Chandel, S., V. Seshadri and S.N. Singh. 2009. Effect of Additive on Pressure Drop and Rheological Characteristics of Fly Ash Slurry at High Concentration, *Particulate Science and Technology*, 27(3): 271–284.

Chandel, S. Singh S.N. and Seshadri, V. 2010. Transportation of High Concentration Coal Ash Slurries through Pipelines, *International Archieve of Applied Sciences and Technology*, 1(1): 1-9.

Chen L. Duan Y. Liu M. and Zhao C. 2010. Slip flow of coal water slurries in pipelines, *Fuel*, 89: 1119–1126.

Cheng, D.C.H. 1980. Viscosity-concentration equations and flow curves for suspensions, *Chemical & Industrial*, 1: 403-406.

Chen, L. Duan, Y. Pu, W. and Zhao, C. 2009. CFD Simulation of Coal-Water Slurry Flowing in Horizontal Pipeline, *Korean Journal of Chemical Engineering*, 26(4): 1144-1154

Chhabra, R.P. and Richardson, J.F. 1983. Hydraulic transport of coarse gravel particles in a smooth horizontal pipe, *Chemical Engineering Residual Design*, 61: 313-317.

Convery, M. Downing, L. Yin, C.Y. Goh, B.M. and Sharifah, A.S.A.K. 2010. Characterization of glass-ceramics produced from vitrification of class f Malaysian coal fly ash, *International Journal of Mechanical and Materials Engineering*, 5(1): 1-4.

Csizmadia, P. and Hos C. 2013. Predicting the friction factor in straight pipes in the case of Bingham plastic and the power-law fluids by means of measurements and CFD simulation, *Chemical Engineering*, 57/1(2): 79–83.

Das, D. 2008. Effect of organized assemblies. part 4 formulation of highly concentrated coal-water slurry using a natural surfactant, *Energy & Fuels*, 22: 1865–1872.

Darby, R. and Melson, J. 1981. How to predict the friction factor for the flow of Bingham plastics, *Chemical Engineering Journal*, 88(26): 59-61.

Dewan, A. 2011. Tackling turbulent flows in engineering, *Springer Science & Business Media*, London.

Eesa, M. and Barigou, M. 2009. CFD Investigation of the Pipe Transport of Coarse Solids in Laminar Power Law Fluids, *Chemical Engineering Science*, 64: 322-333.

Einstein, A. 1956. Investigation on the theory of the Brownian movement, *Dover Publications*, New York.

Ekambara, K. Sanders, R.S. Nandakumar, K. and Masliyah J.H. 2009. Hydrodynamic Simulation of Horizontal Slurry Pipeline Flow Using Ansys-Cfx, *Industrial & Engineering Chemical Residue*, 48, 8159-8171.

Gahlot, V.K. Seshadri, V. and Malhotra, R.C. 1988. A method for the experimental determination of the rheological parameters of multi-sized course particulate slurries, *International symposium on hydraulic transportation of coal and other minerals*, IIT Delhi, 283-295.

Gahlot, V.K. Seshadri, V. and Malhotra, R.C. 1992. Effect of Density, Size Distribution, and Concentration of Solid on the Characteristics of Centrifugal Pumps, *Journal of Fluid Engineeing*, 114(3): 386-389.

Gandhi, B.K. Singh, S.N. and Seshadri, V. 1998. Predictions of performance characteristics slurry pump handling clear liquid, *Indian Journal of Engineering & Materials Sciences*, 5: 91-96.

Gandhi, B.K. Singh, S.N. and Seshadri, V. 2001. Performance characteristics of centrifugal slurry pumps, *Transaction actions of ASME, Journal of Fluid Engineering*, 123:271-280.

Gay, E.C. Nelson, F.A. and Armstrong, W.P. 1969. Flow properties of suspensions with solid concentration, *American Institute of Chemical Engineers Journal*, 15(6): 815.

Ghanta, K.C. and Purohit, N.K. 2002. Effect of particle size distribution (psd) on the viscosity of suspension of bi-dispersed particles, *Proceedings Hydro transport 15*, Cranfield, Bedfort, England, 299-313.

Gillies R.G. and Shook C.A. 1994. Concentration Distributions of Sand Slurries in Horizontal Pipe Flow, *Particulate Science and Technology*, 12(1): 45-69.

Gillies R.G. Shook C.A. and Xu J. 2004. Modelling Heterogeneous Slurry Flows at High Velocities, *The Canadian Journal of Chemical Engineering*, 82: 1060-1065.

Gopaliya M.K. and Kaushal D.R. 2014. Analysis of Effect of Grain Size on Various Parameters of Slurry Flow through Pipeline Using CFD. *Particulate Science and Technology*, 33:4, 369-384.

Gupta, R. Singh, S.N. and Sehadri, V. 1995. Prediction of uneven wear in a slurry pipeline on the basis of measurements in a pot tester, *Wear,* 184: 169-178.

Gurses, A. Açıkyıldız, M. Dogar, C. Karaca, S. and Bayrak, R. 2006. An investigation on effects of various parameters on viscosities of coal-water mixture prepared with Erzurum-Aşkale lignite coal, *Fuel Processing Technology,* 87: 821-827.

Hasan, A.R. Baria, D.N. and Rao, A.V. 1986. Rheological behaviour of low-rank coal water slurries, *Chemical Engineering Communications,* 46: 227-240.

Heywood, N.I. Mehta, K.B. Poplar, D. and Moore, C.D. 1993. Assesment of the flow characteristics of pulverised fuel ash slurries at higher concentration. *12th International conference on slurry handling and pipeline transport*, Hydrotransport-12, Belgium,

Hossain, A. Naser, J. and Imteaz, J.N. 2011. CFD Investigation of Particle Deposition in a Horizontal Looped Turbulent Pipe Flow, *Environmental Modeling & Assessment*, 16: 359-367.

IS 10500. 2009. Draft Indian Standard Drinking Water-Specification, *New Delhi: Bureau of Indian standards.*

Iyer, R. S., and Scott, J. A. 2001. Power station fly ash: A review of value-added utilization outside of the construction industry, *Resourses Conservation Recycle*, 31:293–300.

Kaushal D.R. and Tomita Y. 2002. An improved method of predicting pressure drop along slurry pipeline. *Particulate Science and Technology*. 20: 305-324.

Kaushal, D.R. Sato, K. Toyota, T. Funatsu, K. Tomita, Y. 2005. Effect of Particle Size Distribution on Pressure Drop and Concentration Profile in Pipeline Flow of Highly Concentrated Slurry, *International Journal of Multiphase Flow*, 31: 809-823.

Kaushal, D.R. Thinglas, T. Tomita, Y. Kuchii, S. and Tsukamoto, H. 2012. CFD Modeling for Pipeline Flow of Fine Particles at High Concentration, *International Journal of Multiphase Flow*, 43: 85-100.

Kaushal D.R. and Tomita Y. 2013a. Prediction of concentration distribution in pipeline flow of highly concentrated slurry, *Particulate Science and Technology*, 31: 28-34.

Kaushal, D.R. Kumar, A. Tomita, Y. Kuchii, S. and Tsukamoto, H. 2013b. Flow of Mono-Disperesed Particles Through Horizontal Bend, *International Journal of Multiphase Flow*, 52, 71-91.

Krampa-Morlu, F.N. Bergstrom, D.J. Bugg, J.D. Sanders, R.S. and Schaan, J., 2004. Numerical simulation of dense coarse particle slurry flows in a vertical pipe, *In: 5th International Conference on Multiphase flow*, Yokohama, Japan.

Kumar U. Gandhi B.K. Singh S.N. Seshadri V. and Gupta V.K. 2000. Performance characteristics of demonstration unit for transportation of solid-liquid flow at high concentration setup at NCPP, Dadri, *Proceedings International Seminar on Material handling Systems Indian Institute of Plant Engineers*, November16-18, New Delhi: 126-136.

Kumar, U., Mishra, R., Singh, S. and Seshadri, V. 2003. Effect of particle gradation on flow characteristics of ash disposal pipelines, *Powder Technology*, 132 (1): 39-51.

Kumar, S. Mohapatra, S.K. and Gandhi, B.K. 2013. Effect of addition of fly ash and drag reducing on the rheological properties of bottom ash, *International Journal of Mechanical and Materials Engineering*, 8(1): 1-8.

Kumar, S. Mohapatra, S.K. and Gandhi, B.K. 2014. Performance Characteristics of Centrifugaol Slurry Pump with Multi-sized Particulate Bottom and Fly ash Mixtures, *Particulate Science and Technology*, 32, 466-476.

Kumar U. Singh S.N. and Seshadri V. 2015. Experimental Investigation on Pressure Drop Characteristics of Bi-Modal Slurry Flow in a Straight Horizontal Pipe, *International Journal of Scientific & Engineering Research*, 6(11): 153-158.

Kumar K., Kumar. S. Gupta, M. and Garg H.C. 2016. Effect of addition of bottom ash on the rheological properties of fly ash slurry at varying temperature, *Materials Science and Engineering*, doi:10.1088/1757-899X/149/1/012044.

Kumar K., Kumar. S. Gupta, M. and Garg H.C. 2017. Measurement of flow characteristics for multiparticulate bottom ash water suspension with additives, *Journal of Residuals Science & Technology*, 14(1):11-17.

Krieger, I.M. 1968. Shear rate in the couetta viscometer, *Transaction Society of Rheology*, 12: 5-13.

Lahiri, S.K. and Ghanta, K.C. 2010. Slurry Flow Modeling by CFD, *Chemical Industry & Chemical Engineering Quarterly*, 16(4): 295-308.

Landel, R.F. Moser, B.G. and Baumann, A.J. 1965. Rheology of concentrated suspension: effect of surfactant, *4th International Congress on Rheology*, 663-673.

Lazarus, J.H. and Sive, A.W. 1984. A novel balance beam tube viscometer and rheological characteristics of high concentration fly ash slurries, *Ninth International Conference on Hydraulic Transport of Solids in Pipes*, Rome, Italy, 207-226.

Leong, Y.K. Creasy, D.E. Boger, D.V. and Nguyen, Q.D. 1987. Rheology of browncoal-water suspensions, *Rheology Acta*, 26: 291–300.

Li L., Usui H. and Suzuki H. 2002. Study of pipeline transportation of dense fly ash-water slurry, *Coal Preparation*, 22(2): 65-80.

Ling, J. Skudarnov, P.V. Lin, C.X. and Ebadian, M.A. 2003. Numerical investigations of liquid-solid slurry flows in a fully developed turbulent flow region, *International Journal of Heat and Fluid Flow*, 24: 389-398.

Lin, C.X. and Ebadian, M.A. 2008. A numerical study of developing slurry flow in the entrance region of a horizontal pipe, *Computers& Fluids*, 37: 965-974.

Link, J.M. Faddick, R.R. and Lavingia, N.J. 1974. Slurry pipeline economics, *Society of Mining Engineering, AIME Annual meeting*, Dallas Texas.

Logos, C. and Nguyen, Q.C. 1996. Effect of Particle Size on the Flow Properties of a South Australian Coal-Water Slurry, *Powder Technology*, 88: 55-58.

Lorenzi, L.D. and Bevilacqua, P. 2002. The Influence of particle size distribution and nonionic surfactant on the rheology of coal water fuels produced using Iranian and Venezuelan coals, *Coal Preparation.* 22: 249-268.

Lu P. and Zhang M. 2002. Resistance properties of coal–water paste flowing in pipes, *Fuel*, 81: 877-881.

Maclnnes, M.A. 2002. Investigation into effects of slurry thinners on the rheology of chalk slurries, *Proceeding Hydrotransport 15, BHRA Group, Fluid Engineering*, Cranfield, Bedford, England, 375-384.

Mandal, S.S. Ojha, C.S.P. and Bhargava, P. 2005. Wind turbulence modeling at near wall zone using k-e model: A review, *Journal of Wind Engineering*, 2(1): 52-59.

Matousek V. 2009. Predictive model for frictional pressure drop in settling slurry pipe with stationary deposit, *Powder Technology*, 192: 367-374.

Mazumder, Q.H. 2012. CFD Analysis of the Effect of Elbow Radius on Pressure Drop in Multiphase Flow, *Modelling and Simulation in Engineering*, doi:10.1155/2012/125405.

Menter, F.R. 1994. Two-equation eddy-viscosity turbulence models for engineering applications, *American Institute of Aeronautics and Astronautics Journal*, 32(8): 1598-605.

Moreland, C. 1963. Viscosity of suspensions of coal in mineral oil, *Canadian Journal of Chemical Engineering*, 41: 24-28.

Mosa E.S. Saleh A.H.M. Taha T.A. and El-Molla A.M. 2008. Effect of chemical additives on flow characteristics of coal slurries, *Physicochemical Problems of Mineral Processing*, 42: 107-118.

Mishra, R. Singh, S.N. and Seshadri, V. 1998. Improved model for the prediction of pressure drop and velocity field in multi-sized particulate slurry flow through horizontal pipes, *Powder handling & processing*, 10(3): 279-287Mishra, R. Fabien, C. Singh, S. and Seshadri, V. 2001. Holdup in multisized particulate solid-liquid flow through horizontal pipe, *Indian Journal of Engineering & Materials Sciences*, 8: 84-89.

Mishra, S.K. Senapati, P.K. and Panda, D. 2002. Rheological Behavior of Coal-Water Slurry, *Energy Sources, Part A: Recovery, Utilization, and Environmental Effects*, 24: 159-167.

Nabil, T. El-Sawaf, I. and El-Nahhas K. 2013. Computational Fluid Dynamics Simulation of the Solid Liquid Slurry Flow in a Pipeline, *Seventh International Water Technology Conference, IWTC 17*, Istanbul.

Naik, H.K. Mishra, M.K. and Rao K.U.M. 2011.Infkuence of Chemical Regants on Rheological Properties of Fly Ash-Water Slurry at Varing Temprature Enviorment, Coal Combustion and Gasification Products, 3: 83-93.

Nayak, B.D. Mallick, P.K. and Dey, D.N. 1999. Studies on agglomeration of fly ash for refractory applications, *Proceedings of International Symposium on Beneficiation, Agglomeration and Environment*, Bhubaneswar, Jan 20–22, pp. 265–271.

Nguyen, Q.D. Logos, C. and Semmler, T. 1997. Rheological Properties of South Australian Coal-Water Slurries, *Coal Preparation*, 18: 185-199.

Panda, D. and Pradhan, B. 2014. Hydraulic transport of fly ash and fly ash- bottom ash mixtures at high concentrations, *International Journal of Chemical Engineering and Applied Sciences*, 4(1): 1-4.

Pani, G. K. Rath, P. Barik R. and Senapati, P.K. 2015. The effect of selective additives on the rheological behaviour of power plant ash slurry, *Particulate Science and Technology*, 33(4): 418-422.

Parida, A. Panda, D. Mishra, R.N. Senapati, P.K. and Murthy, J.S. 1995. Transportation of fly ash slurry, *Proceeding of workshop on the fly ash management*, Bhubaneswar, 51-63.

Parida, A. Senapati, P.K. and Mishra, B.K. 2006. Slurry pipelines for fly ash-a design method for energy efficient fly ash disposal by hydraulic conveying, *Bulk solids handling*, 26(8): 556-562.

Pavel V. and Zdenek C. 2011. Effect of Particle Size Distribution and Concentration on Flow Behaviour of Dense Slurries. *Particulate Science and Technology*, 29: 53-65.

Praharaj, T. Swain, S.P. Powell, M.A. Hart, B.R. and Tripathy, S. 2002. Delineation of groundwater contamination around an ash pond: Geochemical and GIS approach. *Environmental International*, 27: 631–638.

Rabinovich, E. and Kalman, H. 2011.Threshold velocities of particle-fluid flows in horizontal pipes and ducts: Literature review, *Reviews in Chemical Engineering*, 27(5): 215-239.

Rawat A. Singh S. N. and Seshadri, V. 2016. Computational methodology for determination of head loss in both laminar and turbulent regimes for the flow of high concentration coal ash slurries through pipeline, *Particulate Science and Technology*, 34(3): 289-300.

Reddy, G.V. Mohapatra, S.K. and Sinha, R.K. 1994. Rheological properties of coal oil mixtures: influence of coal properties, *Fuel Science and Technology International*, 12 (9): 1257-1270.

Roache, P.J. 1997. Quantification of uncertainity in computation fluid dynamics, *Annual Review of Fluid Mechanics*, 29: 123–160.

Roh, N. Shin, D.H. Kim, D.C. and Kim, J.D. 1995. Rheological behaviour of coal-water mixtures effects of coal type, loading and particle size, *Fuel*, 74: 1220-1225.

Roscoe, R. 1952. The viscosity of suspension of rigid spheres, *British Journal Applied Physics*, 3: 267-274.

Round, G.F. and Hessari, A.R. 1987. Rheology of coal slurries, pH and size distribution effects, *Particulate and Multiphase Processes*, 3: 329–340.

Rutger, R. 1962. Relative viscosity of concentrated suspensions of rigid spheres in Newtonian fluids, *Rheology, Acta*, 2: 202-209.

Sahoo, B.K. De, S. Carsky, M. and Meikap, B.C. 2010. Enhancement of Rheological Behavior of Indian High Ash Coal-Water Suspension by Using Microwave Pretreatment, *Industrial & Engineering Chemical Research*, 49, 3015–3021.

Schrick, W. Smith, L.G. Hass, D.B. and Husband, W.H.W. 1972. Experimental studies on the hydraulic transport of coal. *Engineering Division of Saskatchewan Research Council*, Canada.

Senapati, P.K. Panda, D. and Parida, A. 2005. Studies on high concentration fly ash-bottom mixture slurry, *Bulk Solid Handling*, 25(6): 386-290.

Senapati, P.K. Das, D. Nayak, A. Mishra, P.K. 2008. Studies on Preparation of Coal Water Slurry Using a Natural Additive, *Energy Sources, Part A: Recovery, Utilization, and Environmental Effects*, 30: 1788-1796.

Senapati, P.K. Mishra, B.K. and Parida, A. 2010. Modeling of viscosity for power plant ash slurry at higher concentrations: Effect of solids volume fraction, particle size and hydrodynamic interactions, *Powder Technology*, 197: 1-8.

Senapati, P.K. Mohapatra, R. Pani, G.K. and Mishra, B.K. 2012. Studies on rheological and leaching characteristics of heavy metals through selective additive in high concentration ash slurry, *Journal of Hazardous Materials*, 229-230: 390– 397.

Senapati, P.K. Mishra, B.K. and Parida, A. 2013. Analysis of friction mechanism and homogeneity of suspended load for high concentration fly ash & bottom ash mixture slurry using rheological and pipeline experimental data, *Powder Technology*, 250: 154-163.

Senapati, P.K. and Mishra, B.K. 2015. Bulk Hydraulic Disposal of Highly Concentrated Fly Ash and Bottom Ash-Water Slurries, *Particulate Science and Technology*, 33(2): 124-131.

Seshadri, V. Singh, S.N. Jain, K.K. and Verma, A.K. 2008**.** Effect of additive on head loss in the high concentration slurry disposal of fly ash, *Journal of Institution of Engineers*, 89: 3-10.

Shao S. Chen X. Liu H. and Wang F. 2012. Preparation of Coal Slurry with Alcohol Fermentation Wastewater, *Energy Sources, Part A: Recovery, Utilization, and Environmental Effects*, Part A, 34, 919–928.

Singh, R.K. Gupta, N.C. and Guha, B.K. 2012, The leaching characteristics of trace elements in coal fly ash and an ash disposal system of thermal power plants, *Energy Sources, Part A: Recovery, Utilization, and Environmental Effects*, 34: 602-608.

Singh, M.K., Ratha, D., Kumar, S. and Kumar, D. 2016. Influence of particle size distribution and temperature on rheological behavior of coal slurry, *International Journal of Coal Preparation and Utilization*, 36: 44-54.

Sive, A.W. and Lazarus, J.H. 1987. Hydraulic transport system design for high concentration fly ash slurries, *Ash a Valuable Resource,* Pretoria, South Africa.

Skudarnov, P.V. Lin, C.X. Ebadian, M.A. 2004. Double-Species Slurry Flow in a Horizontal Pipeline, *Journal of Fluid Engineering*, 126: 125-132.

Slatter P. 2000. The Role of Rheology in the Pipelining of Mineral Slurries, *Mineral Processing and Extractive Metallurgy Review,*20: 281-300.

Slatter P. 2011. The Engineering Hydrodynamics of Viscoplastic Suspensions, Particulate Science and Technology, 29: 139–150.

Taguchi, G. 1990. Introduction to Quality Engineering, *Asian Productivity Organization*, Tokyo.

Thomas, D.G. 1965. Transport characteristics of suspensions, a note on the viscosity of Newtonian suspension of uniform spherical particles, *Journal of Colloid Sci*ence, 20: 267-273.

Tian-ye G.U. Guo-gang W.U. Qi-Hui L.I. and Xian-Liang M.E.N.G. 2008. Blended coals for improved coal water slurries. *Journal of China University of Mining and Technology*, 18(1): 50-54.

Tiwari, K.K. Basu, S.K. Bit, K.C. Banerjee, S. and Mishra, K.K. 2003. High-concentration coal-water slurry from Indian coals using newly developed additives, *Fuel Processing Technology*, 85: 31-42.

Toda, M. and Kuriyami, M. 1988. The influence of particle size distribution of coal on fluidity of coal water mixtures, *Powder Technology*, 55: 241–247.

Tripathy P.S.M. and Mukherjee S.N. 1997. Perspectives on Bulk Use of Fly Ash. CFRI Golden Jubilee Monograph. New Delhi: Allied Publishers Limited, 123.

Turian, R.M. Hsu, F.L. Avramidis, K.S. Sung, D.J. and Allendorfer R.K. 1992. Settling and Rheology of Suspensions of Narrow-Sized Coal Particles, *American Institute of Chemical Engineers Journal,* 38(7): 969-975.

Usui, H. Sano, Y. Sawada, M. and Hongoh, T. 1986. Adjustment of particle size distribution for the preparation of highly loaded coal-water slurries with reduced viscosity, *Society of Chemical Engineers, Japan*, 12: 51–56.

Vlasak P. and Chara Z., 2009. Conveying of solid particles in Newtonian and non-Newtonian carriers, *Particulate Science and Technology*, 27(5), 428-443.

Verma, A.K. Singh S.N. Seshadri V. 2006. Pressure Drop for the Flow of High Concentration Solid-Liquid Mixture Across 90^{o} Horizontal Conventional Circular Pipe Bend, *Indian Journal of Engineering & Material Sciences*, 13: 477-483.

Vlasak, P. and Chara, Z. 2011. Effect of particle size distribution and concentration on flow behavior of dense slurries, *Particulate Science and Technology*, 29(1): 53-65.

Wang, L. and Zeng, F. 1998. Effect of ash in coal on the properties of coal water slurry, *Coal Processing and Comprehensive Utilization*, 3: 18–21.

Ward, A. Bunn, T.F. and Chambers, A.J. 1999. The bays water fly ash transportation system, *Journal of Coal Preparation*, 21: 125-147.

Wasp, E.J. Aude, T.C. Seiter, R.H. and Thompson, T.L. 1968. Hetro-homogeneous solid-liquid flow in turbulent regime, *ASCE Int. Symp, on solid-liquid flow, Univ. of Pennsyluania,* , U.S.A.

Williams, P.S. 1953. Flow of concentrated suspensions, *Journal of Applied Chemistry,* 3: 120-127.

Wilson, K.C. 1982. A dense phase option for coarse coal pipelining, *Journal of Pipelines,* 5: 251-257.

Wu, D. Yang, B. and Liu, Y. 2015. Pressure drop in loop pipe flow of fresh cemented coal gangue-fly ash slurry: Experiment and simulation, *Advanced Powder Technology*. doi: 10.1016/j.apt.2015.03.009.

Yavuz, R. and Kucukbayrak, S. 1998. Effect of particle size distribution on rheology of lignite-water slurry, *Energy Sources*, 20(9): 787–794.

Yong-gang, W. Yan, Y. Xiang-kun, G. and De-ping, X. 2009. Rheological behavior of Shengli coal-solvent slurry at low temperatures and atmospheric pressure, *Mining Science and Technology,* 19: 779–783.

Yuchi, W. Li, B. Li, W. and Chen, H. 2005. Effects of coal characteristics on the properties of coal water slurry, *Coal Preparation,* 25: 239-249.

Zhou, M. Pan, B. Yang, D. Lou, H. and Qiu, X. 2010. Rheological Behavior Investigation of Concentrated Coal-Water Suspension. *Journal of Dispersion Science and Technology*, 31: 838-843.

LIST OF PUBLICATION

PAPERS PUBLISHED

1. Singh, M.K. Ratha, D.N. Kumar, S. and Kumar, D. 2016. Influence of Particle Size Distribution and Temperature on Rheological Behavior of Coal Slurry, *International Journal of Coal Preparation and Utilization*, 36: 44-54. **(SCI indexed).**
2. Singh, M.K. Kumar, S. and Ratha, D.N. 2016. Physio-chemical and leaching characteristics of fly and bottom ash, *Energy Sources, Part A: Recovery, Utilization, and Environmental Effects*, 38(16): 2377-2382. **(SCI indexed).**
3. Singh, M.K. Kumar, S. and Ratha, D.N. 2017. Design of Slurry Transportation Pipeline for the Flow of Muti-Particulate coal ash Suspension. *International Journal of Hydrogen Energy, 42(30): 19135-19138.* **(SCI Indexed)**.
4. Singh, M.K. Kumar, S. and Ratha, D.N. 2016. Computational Analysis on Disposal of Coal Slurry at High Solid Concentrations through Slurry Pipeline, *International Journal of Coal Preparation and Utilization, doi.org/10.1080/19392699.2017.1346632.* **(SCI indexed)**
5. Singh, M.K. Kumar, S. and Ratha, D.N. 2015. Mineral Characterization of Indian Coal, *International Journal of Applied Engineering Research*, 10(78): 131-135. **(Scopus Indexed).**
6. Singh, M.K. Kumar, S. and Ratha, D.N. 2016. Study of Pressure Distribution Inside Slurry Pipeline Using CFD, In: *National Conference on Recent Technological Developments in Mechanical Engineering*, January 22-23, 2016.